DISSERTATION

ESTABLISHING CANINE OSTEOSARCOMA AS A SOLID TUMOR MODEL FOR THE EVALUATION OF B7-H3 CAR T CELL THERAPY

Submitted by

Jennifer Cao

Department of Microbiology, Immunology and Pathology

In partial fulfillment of the requirements

For the Degree of Doctor of Philosophy

Colorado State University

Fort Collins, Colorado

Summer 2023

Doctoral Committee:

Advisor: Steven Dow

Anne Avery
Alan Schenkel
Douglas Thamm

ABSTRACT

ESTABLISHING CANINE OSTEOSARCOMA AS A SOLID TUMOR MODEL FOR THE EVALUATION OF B7-H3 CAR T CELL THERAPY

Osteosarcoma (OS) is a highly aggressive primary bone cancer that mainly affects children and young adults. OS is the third most common childhood cancer, after lymphoma and brain tumors. Major advances in the 1980's in neoadjuvant chemotherapy has increased 5-year survival rates in OS from 30% to 70%. Unfortunately, for patients that do not respond to standard therapy or that have metastatic disease the 5-year survival rate is still 20% with no major improvements in the last 4 decades. Approximately 15-20% of patients have metastatic lesions at the time of diagnosis and 25-30% of all OS patients will develop metastatic disease. For this subset of patients advances in treatment options are desperately needed. OS also occurs in high rates in large breed dogs with an estimated 10,000 cases in dogs per year in the United States compared to 1,000 cases per year in humans. The dog has been a well-established translational model for OS due to the similar clinical presentation, cell origin, histological features, and disease progression between canine and human OS.

Development of chimeric antigen receptor (CAR) T cell therapy has revolutionized the treatment for advanced and relapsed B-cell lymphomas and leukemias. CAR T cell targeting of B cell marker CD19 has shown up to 90% complete remission in patients with advanced B cell leukemia. However, efforts to expand CAR T cell therapy to solid tumor types have not seen the same clinical success as with blood cancers. Major barriers unique to solid tumor CAR T cell therapy are A) selection of tumor associated antigen target, B) CAR T cell trafficking to tumor sites from the circulation and C) immune suppressor cells within the tumor microenvironment (TME).

To develop more effective CAR T cell therapies against solid tumor, we utilized canine OS as a translational animal model. To establish canine osteosarcoma as a platform for evaluating B7-H3 CAR T cell

therapy, first we validated B7-H3 as an antigen target in canine OS. We found differential expression of B7-H3 with high levels of B7-H3 expression on OS cell lines and FFPE biopsies, whereas normal canine tissues were B7-H3 negative or low. Next, we optimized generation of canine B7-H3 CAR T cells from whole blood isolated from tumor bearing dogs to maximize both T cell expansion and CAR transduction efficiency. We also found that the addition of cytokines IL-7 and IL-15 minimize CAR T cell exhaustion due to *ex vivo* activation and expansion. We next determined that canine B7-H3 CAR T cells exerted antigen specific killing and cytokine activity against B7-H3+ canine OS cell lines.

To address issues with CAR T cell trafficking we evaluated the addition of chemokine receptor CXCR2 to B7-H3 CAR T cells. To assess the utility of the B7-H3-CXCR2 CAR we determined that canine OS cell lines secreted high levels of ligand chemokine CXCL8 at baseline. To further evaluate functionality, we evaluated the two CAR constructs in a mouse xenograft model of canine OS. We found that the B7-H3-CXCR2 CAR construct had significantly greater anti-tumoral activity than the single B7-H3 CAR construct in inhibiting tumor growth and achieving complete tumor elimination. Studies were also designed to determine if modifying the TME with combination drugs losartan and propranolol improved CAR T cell activity. This is based on recent successful studies with losartan and propranolol in dogs with OS and glioma. We found that combination losartan and propranolol decreased the population of mouse CD11b+Ly6C^{high} tumor associated macrophages (TAMs) to xenografted canine OS tumors. *In vitro* assays showed that immune suppressive macrophages enhance B7-H3-CXCR2 CAR T cell function when co-cultured, likely through CAR activation by macrophage B7-H3 expression.

Collectively, the results from these studies pave the way for assessing B7-H3-CXCR2 CAR T cells in dogs with metastatic OS. Clinical outcomes in spontaneous OS in dogs will likely give more clinically relevant results serving as a platform for evaluating new CAR T cell therapies and combination therapies with TME modification, radiation, or checkpoint blockade. Success of this work can provide a new adoptive

cell immunotherapy treatment option to patients both canine and human with metastatic osteosarcoma. Additionally, B7-H3-CXCR2 CAR T cells can be applied to other B7-H3 positive CXCL8 secreting tumor types.

ACKNOWLEDGEMENTS

First, I would like to express my gratitude to my mentor Dr. Steve Dow who has guided me through this project and whose eagerness to build collaboration, kind guidance, and passionate dedication to science and built me into a better scientist, researcher, and immunologist. I am very honored to have been a part of your lab and to have had the opportunity to work among the great colleagues here in the immunotherapy research lab and at the Flint animal cancer center. I want to extend thanks specifically to Renata Impastato, Laura Chubb, and Jade Kurihara who have supported me, and my project having spent hours together in the mouse room and in the lab or planning experiments with our white board calendar.

Additionally, I want to acknowledge our collaborators at the University of Colorado, Dr. Mike Verenris and Dr. Jessica Lake. Their extensive knowledge and guidance has been incredibly valuable and essential to my work as well as my growth as a cancer immunologist. I would like to extend my gratitude to my committee Drs. Anne Avery, Doug Thamm and Alan Schenkel for their excellent feedback, kind criticisms and always being genuinely interested and excited in my work and progress as a graduate student. I want to give big, big thanks to the combined DVM/PhD program for the financial support, emotional support, and guidance from Drs. Ed Hoover, Sue VandeWoude, Justin Lee, Dan Regan and Anne Avery and my DVM/PhD classmates. It's been a very long road and there is still more to go but I'm very grateful to have had you all along the way.

Finally, I want to acknowledge my friends and family who have supported me through it all. Biggest thanks to my husband Matt Morris for your endless support and love. Thanks to my wonderful DVM friends and unofficial boba club, Sarah and Aimee for being with me through all the good times, tears and celebrations.

DEDICATION

This dissertation is dedicated to my husband and best favorite person, Matt Morris.

All your support, love, dinners you've made me, hobbies, and unfinished projects we've shared together.

Doing it all with you has been the best part.

TABLE OF CONTENTS

Chapter 1: Introduction

Human Osteosarcoma

Osteosarcoma (OS) is an aggressive primary bone tumor derived from the mesenchymal lineage[1]. OS primarily affects children and young adults being the third most common type of childhood cancer after lymphomas and brain tumors[2] and representing 3-6% of childhood cancers and 1% of adult cancers[3]. Incidence of OS is estimated to be 3.4 cases per million people per year with a bimodal age distribution, peaking at 15-19 years of age and in elderly patients over 65 years of age[3]. OS occurrence in young populations skews towards young males that are 1.4 times more likely to develop OS than young females[4,5]. Although not fully understood, the most common location of occurrence in OS is at the metaphyseal regions of long bones with taller children being more at risk[6]. This indicates that growth and rapid bone production are involved in the development of OS[5].

Primary OS can be categorized by histological features as intramedullary, telangiectatic (having blood filled cysts and multinucleated giant cells), parosteal (having cartilage production, bone production and cells with fibroblastic morphology) or periosteal (showing mature bone and atypical hyaline cartilage)[7]. Intramedullary OS can be further characterized into histological groups osteoblastic (secretion of bone matrix), chondroblastic (secretion of cartilage matrix) or fibroblastic (having collagen secreting spindle cells) with osteoblastic being the most prevalent subcategory[7,8]. Most tumors present with a mixture of histological features. The heterogeneity both within tumors and between individuals is a major characteristic of OS and one of the challenges to developing molecular targeted therapies. A few genes have been found to be prevalent in many OS cases such as TP53, RB, MDM2, ATRX and DLG2 however most OS cases (95%) are sporadic events with no identifiable driver gene mutation[9-15].

OS has a complex immune infiltrate largely comprised of tumor-associated macrophages (TAMs)[16]. Other immune cells found within the tumor microenvironment (TME) include dendritic cells (DCs),

lymphoid cells such as regulatory T cells (T regs), tumor infiltrating lymphocytes (TILs) and myeloid derived suppressor cells (MDSCs)[17]. TAMs within the TME are a heterogenous group in a spectrum of proinflammatory M1 and immune suppressive M2 phenotype[17,18]. In contrast to many other epithelial tumors, increased proportion of TAM infiltrates correlate with increased survival and decreased incidence of metastasis[19]. Clinical trials with macrophage activating agent mifamurtide in combination with standard chemotherapy significantly improved 6-year overall survival rates[20]. A low ratio of CD8+ cytotoxic T cells compared to myeloid cell infiltrates and lack of tumor neoantigens in OS characterize OS as an immunologically "cold" tumor[21]. CD8+ TILs in OS is inversely correlated with rates of metastasis[22]. Additionally, higher ratios of CD8+ TILs to FOXP3+CD4+ T regs correlates with prolonged survival in OS patients[23]. Expression of checkpoint molecule programmed death-ligand 1 (PD-L1) expressed by myeloid cells and tumors cells to suppress anti-tumoral immune response has been associated with poorer 5-year event free survival[24,25]. Expression of PD-1 in OS TILs has low prevalence and so far has not had strong prognostic indicator[26]. Use of inhibitors of PD-L1/PD-1 signaling through monoclonal antibody therapy in OS has not yielded significant benefit or is in early stage clinical trials in combination with other therapies[27,28].

Development of adjuvant chemotherapy in the 1970s increased 5-year survival rates in OS from 20% to 50%[29]. Current therapeutic emphasis for OS is pre-operative chemotherapy to reduce the size of the primary tumor followed by limb sparing surgery with post-surgical adjuvant chemotherapy targeting any residual primary tumor or metastatic lesions[30,31]. The most common combination of agents used in patients with resectable tumors are adjuvant high-dose methotrexate, doxorubicin, and cisplatin[32]. 5-year survival rates for patients with localized OS with current standard of care reaches 80%[33]. Resected tumor specimens are tested for necrosis with various chemotherapeutic drugs and given a Huvos and Rosen score based on percentage of necrosis with good responders having greater than 90% necrosis (grade IV= 100% necrosis, grade III= 99-90% necrosis) and poor responders having less than 90% necrosis (grade II= less

than 90% necrosis, grade I= less than 50% necrosis)[34,35]. This method and scale grading is used to inform post-operative chemotherapy[36].

In contrast to the great achievements in treatment of OS, patients who do not respond to conventional therapy or develop metastatic disease still have very poor prognosis. 30-40% of patients will recur within 2-3 years and approximately 15-20% of patients diagnosed with OS will present with metastatic lesions at time of diagnosis[37,38] with 90% of metastatic lesions appearing in the lungs[37]. For these subsets of patients, the 5-year survival rate is 20% with no improvements made in the past four decades[2]. Lack of progress in improvements to decreasing recurrence, or improving treatments for metastatic patients may be due to OS's rarity and wide variability between patients[39]. New strategies are currently being developed to improve OS treatment including immunotherapy, bone resorption inhibition and targeting receptor tyrosine kinases and intracellular signaling[6].

Canine Osteosarcoma as a translational model for pediatric OS

Pet dogs with spontaneously occurring OS represent a heterogenous group of patients that closely mirror human OS. Canine OS as a translational model for human OS has been well established to help strengthen preclinical research and work done with mouse models[40]. Canine OS as a translational model has many advantages including increased rate of incidence compared to human OS, similar immune landscape, histological characteristics, clinical presentation, and disease progression. While mouse models offer homogenous tumor populations which facilitates the assessment of specific molecular processes with predictable development of primary and metastatic lesions, mouse models do not recapitulate individual and intratumoral heterogeneity. Being immune competent, spontaneous canine OS represents the complex TME which plays a critical part in disease progression and treatment resistance[41]. For these reasons canine OS is especially valuable in the development of immunotherapy.

OS has a higher incidence rate in dogs compared to humans with an estimated 10,000 cases in the United States per year[42] while less than 1,000 people in the United States are affected by OS each year.[33,43] Higher incidence in large and giant breed dogs than small breed dogs also indicates that growth and bone production is involved in the development of OS mirroring the correlation in height to human OS[5,44]. Common sites for primary lesions occur in the distal radius and proximal humerus, areas correlating with maximal skeletal load implicating microtrauma and bone remodeling in OS development[45,46]. Canine OS also has a high rate of metastasis with metastasis to the lungs being the most common presentation (50-84%)[47].

Canine OS is categorized histologically in 6 subtypes: osteoblastic, chondroblastic, fibroblastic, telangiectatic, giant cell-rich and poorly differentiated with osteoblastic being the most common subtype just like in human OS[48-50]. Additionally, like human OS many tumors are heterogenous and contain multiple histologic characteristic[51]. Once diagnosed, the standard of care for dogs with OS is limb amputation followed by chemotherapy. Dogs are much more likely to receive full limb amputation as opposed to limb-sparing procedures that are the standard in human treatment of OS. Combination adjuvant chemotherapy in dogs has not shown significant benefit over carboplatin alone[7] with single agent carboplatin treatment resulting in a lower proportion of adverse events than other treatment protocols[45,52,53]. The median survival time for dogs with OS that receive surgery and chemotherapy is approximately 1 year[52].

Adoptive cell therapy for cancer

Adoptive cell therapy (ACT) is a form of immunotherapy that uses immune cells as a therapeutic product. These Immune cells are often patient derived and modified *ex vivo* and intravenously infused back into a patient to fight disease[54]. The field of immune therapy dates back to the 1950s but has exponentially expanded in the field of cancer in the past three decades[55]. ACT can be classified into three main categories based on the type of immune modification used, 1) ACT with tumor-infiltrating

lymphocytes (TILs), 2) ACT using T cell receptor (TCR) gene therapy, and 3) ACT with chimeric antigen receptor (CAR) modified immune cells[56].

TIL ACT was developed by the Rosenberg group that adoptively transferred TILs in a mouse model of metastatic melanoma which showed an anti-tumoral effect in the recipient mouse[57]. Translation of this therapy into humans involves *ex vivo* expansion of CD3+ TILs from resected patient tumors[54]. Autologous expanded TILs are then reinfused into patients after lymphodepletion[58]. Pre-infusion lymphodepletion was developed for TIL ACT to improve TIL engraftment by establishing "physical space" decreasing the competition for T cell homeostatic cytokines interleukin-7 (IL-7) and interleukin-15 (IL-15) from endogenous lymphocytes[58]. Treatment with single bolus of high dose T cell growth factor interleukin-2 (IL-2) shortly after TIL infusion was found to improve TIL survival and clinical efficacy[59]. Tumor derived TIL ACT has seen remarkable success with an objective tumor response rate of ~50% in patients with metastatic melanoma in phase I/II clinical trials[58,60]. Additional trials in patients with breast cancer[61], cervical cancer[62], renal cell carcinoma[63,64], and non-small cell lung carcinoma[65] have shown various rates of success.

Building on the success of TIL ACT, TCR based ACT utilizes specific anti-tumoral TCRs to genetically modify *ex vivo* expanded CD8+ effector T cells from peripheral blood to generate a pool of T cell clones that are reactive to specific tumor antigens[66,67]. TCR ACT induces potent anti-tumoral activity and initial clinical trials achieved an objective response rate of ~30% in patients with metastatic melanoma[68]. Use of select high affinity transgenic αβ TCRs redirects the engineered T cells to a highly specific and reproducible tumor immune response as seen in melanoma[69], multiple myeloma[70], viral associated malignancies[71] and acute myeloid leukemia (AML)[72]. Use of exogenous TCRs to engineer tumor antigen specific responses requires antigen presentation through the major histocompatibility complex (MHC) which allows for immune escape by tumor downregulation or loss of MHC expression[73,74]. Dependence on antigen presentation by MHC also restricts specific therapies to certain human leukocyte antigen (HLA) types with the majority of TCRs used in ACT targeting tumor antigen epitopes presented by HLA-A02:01[75]. Expansion

of TCR ACT to other patient populations with other HLA types requires extensive cancer antigen epitope discovery and identification of HLA matched antigen reactive TCRs[76,77].

CAR T cell Therapy

Chimeric antigen receptor (CAR) T cells were developed to circumvent the need for antigen presentation by MHC. CARs consist of the extracellular antigen binding domain using a single chain variable fraction (scFv) of a B cell receptor, a hinge region, a transmembrane domain, and the intracellular T cell signaling domain. This design allows for engineering MHC independent, tumor antigen specific T cells from peripheral blood[78]. Each of the components of a CAR affects its cancer antigen targeting, activation and *in vivo* function [79]. Effective cancer antigen targeting with scFv is dependent on antigen epitope binding and scFv affinity, which impact tumor antigen recognition. CAR signaling and CAR T cell activation need to be balanced to produce effective anti-tumoral CAR T activity and avoid potential toxicity from ligand-independent tonic signaling and on-target-off-tumor activation by low level antigen expression from normal tissues[79]. New scFvs are being developed to expand cancer antigens targets by CAR T cell therapy, improve receptor affinity to increase treatment efficacy and reduce toxicity, and target multiple antigens within the same CAR construct[79-81] .

The hinge region functions by providing flexibility for the extracellular region to overcome steric hindrance[79]. The length and composition of the hinge region can affect CAR expression, signaling, activation and epitope recognition[82]. The transmembrane domain functions to anchor the CAR to the T cell membrane[83]. Most transmembrane domains are derived from native T cell proteins such as CD3ζ, CD4, CD8α or CD28[79]. Effects of transmembrane domains on CAR T cell function is not fully understood however studies suggest that the transmembrane domain can influence CAR expression, CAR-mediated T cell activation, CAR stability and signaling[83,84].

The intracellular domain has been extensively investigated to optimize CAR T cell co-stimulation. First-generation CAR T cells were made with CD3ζ or FcRγ signaling domains[85]. CD3ζ alone as an intracellular domain was found to have limited persistence and IL-2 secretion, requiring exogenous IL-2 to kill target tumor cells *in vitro* [85,86]. To improve CAR T cell robustness, increase IL-2 production, and increase CAR T cell proliferation post antigen binding, second-generation CAR constructs were created with an additional co-stimulatory intracellular domain[79]. CD28 or 4-1BB (CD137) are commonly used as additional intracellular costimulatory domains in second-generation CARs[79]. Selection of either CD28 or 4-1BB affects CAR T cell differentiation, proliferation, and metabolic profile. CD28 constructs preferentially differentiate into effector memory T cells and 4-1BB domain CARs preferentially differentiate into central memory T cells[79]. Preclinical animal model studies show that 4-1BB costimulatory domain CARs have greater proliferation and persistence while CD28 costimulatory domain CARs induce more rapid expansion with shorter duration and increased toxicity post infusion[87,88]. Third-generation CARs add two co-stimulatory domains, commonly CD28 in combination with 4-1BB or OX40[54]. Third-generation CARs have produced mixed results with CD28- 4-1BB CARs inducing greater cytokine production, T cell proliferation and anti-tumoral response in a mouse model of lymphoma and pulmonary metastasis [89]. Use of third-generation CARs however did not show any additional benefit in leukemia or pancreatic cancer models over second-generation CARs[90,91].

Second-generation CARs targeting CD19 produce a robust anti-tumoral effect *in vitro* and *in vivo* against B cell malignancies. Targeting of CD19 had many advantages including high prevalence and high expression on B cell malignancies and exclusive expression to cells of the B cell lineage. Remarkable clinical responses have come from CD19 targeting CAR T cell therapy in the treatment of hematological malignancies[82]. Treatment with single infusion of second-generation CD19-CD3ζ-4-1BB CAR T cells (tisagenlecleucel) in pediatric and young adult patients with advanced refractory B cell acute leukemia (B-ALL) has led to a complete remission (CR) rate of 70~94%[87,88,92,93]. Tisagenlecleucel induced long term

disease control without need of additional therapy that was observed out to four years[94]. All patients that respond to CD19 CAR T cell therapy had persistent B cell aplasia[94]. This expected toxicity is well managed with immunoglobulin replacement[88]. Due to the unprecedented success in clinical trials, tisangenlecleucel was the first US Food and Drug Administration (FDA) approved genetically modified cellular therapy in 2017 shortly followed by second-generation CD19-CD3ζ-CD28 CAR (axicabtagene ciloleucel)[95]. Additionally in 2021 CD19 targeting CAR brexucabtagene autoleucel and lisocabtagene maraleucel were FDA approved for treatment of relapsed or refractory B cell precursor acute lymphoblastic leukemia or diffuse B cell lymphoma (DLBL), respectively [96]. B-cell mutation antigen targeting CAR (idecabtagene vicleucel) was FDA approved for treatment of relapsed or refractory multiple myeloma in 2022[96].

The success of CAR T cell therapy is not without its continued challenges and barriers. Among them are antigen escape, CAR T cell associated toxicities, on-target-off-tumor side effects, failure of adequate CAR T cell trafficking, and the immunosuppressive TME[79]. In CD19 CAR T cell therapy, resistance by antigen escape has been seen in 30-70% of patients who have recurrent disease post treatment[97]. This implicates antigen escape as a common disease resistance mechanism[97]. The major strategy to combat tumor antigen escape is targeting of multiple antigens using either dual CAR constructs in which multiple CARs are transduced into a single T cell, a mixture of CAR T cells are infused, or tandem CARs in which a single CAR contains two variable binding domains[81,98-100]. Combination therapy with low dose radiation[101,102], checkpoint inhibition[103], cancer vaccines[104,105], or other immune agonists[106,107] may increase antigen expression, induce epitope spreading or increase efficacy of CAR T cell therapy and help overcome antigen escape[97].

The most common acute CAR T cell associated toxicity is cytokine release syndrome (CRS)[108]. CRS can be life-threatening but has been well characterized in CD19 CAR T cell clinical trials and can be anticipated and managed with clinical interventions[79]. CRS is a systemic inflammatory response mediated by CAR T cell supraphysiological production of cytokines post infusion and *in vivo* T cell expansion through

cross activation[109]. CRS can range from mild with fever, fatigue, diarrhea, and myalgia to severe with hypotension, cardiac dysfunction, respiratory failure, circulatory collapse with possible progression to death[110]. Severe CRS is categorized as requiring medical and pharmacological intervention, having a fever above 38˚C for 3 or more consecutive days with elevation of two or more serum cytokines by 75-fold, or having one serum cytokine elevated above 250-fold and one clinical sign of severe toxicity[110]. Severe CRS can be further categorized by grade 1-4 depending on interventions needed[111,112].

High tumor burden, prior lymphodepletion, and higher CAR T cell doses are all correlated with increased risk and severity of CRS development[79]. Early intervention for CRS related fever, hypotension, and opportunistic infection due to pre-infusion lymphodepletion are key in mitigating CRS adverse events[110]. CRS is believed to be mediated primarily through secretion of high levels of IL-6 by CAR T cell activated myeloid cells[113]. IL-6 receptor blocking antibody (tocilizumab) is used for severe grade 4 CRS and has been shown to effectively lessen or nullify CRS related symptoms without impacting treatment efficacy of CD19 CAR T cell therapy[88,114,115]. Use of corticosteroids is reserved for severe CRS and neurological toxicities that do not respond to IL-6 blockade[112].

CAR T cell associated neurotoxicity to date have largely restricted to CD-19 CAR T clinical trials[116]. Incidence of neurotoxicity in CD19 CAR T clinical trials ranged from 20-64%[116]. The biology of CAR T cell associated neurotoxicity is still poorly understood. Common clinical manifestations include confusion, apraxia, aphasia, seizures, attention and/or calculation deficits, headache, and encephalopathy[93,109,116]. The median onset of neurologic symptoms is 4-5 days post CAR T cell infusion with most symptoms resolving by 3-8 weeks. Management of CAR T cell associated neurotoxicity include supportive care, steroids, antiseizure prophylaxis and in the concurrent case with CRS tocilizumab may be administered[116]. Clinical predictors of neurotoxicity include younger age, preexisting neurologic comorbidities, higher CAR T cell dose, higher peak CAR T cell counts, and early and/or severe CRS[116]. Animal models and clinical data suggest that high levels of cytokine release by monocytes may drive a breakdown of the blood brain barrier

however further investigation needs to be done in preclinical models for CAR T cell associated toxicities to determine the mechanism of CAR T cell associated neurotoxicity[116].

CAR T cell therapy for solid tumors

The success of CD19 targeting CAR T cell therapy has spurred the expansion of CAR T cell therapy to other tumor types such as glioblastoma (GBM) [117], non-small cell lung carcinoma (NSCLC)[118], breast cancer[119], OS[96,120] and many others[86]. CAR constructs targeting tumor associated antigens (TAAs) that have had extensive development are GD2, EGFR, mesothelin, MUC1, HER2, ROR1 and B7-H3 with more under current investigation to ensure effective tumor targeting and minimal on-target-off-tumor side effects[96]. Table 1 is a non-comprehensive list of ongoing CAR T cell clinical trials in solid malignancies. Many CAR constructs can be applied to multiple cancer types only depending on TAA surface expression to activate CAR T cell immunity. Additionally, investigation of CARs in other immune cell types such as NK cells[121] and macrophages[122] are ongoing and have shown promising pre-clinical data to date[123].

Table 1.

Antigen target	Cancer type	NCT number	phase	Brief title	status
GD2	Neuroblastoma	NCT00085930	Phase 1	Blood T-Cells and EBV Specific CTLs Expressing GD-2 Specific Chimeric T Cell Receptors to Neuroblastoma Patients (NESTLES)	Active, not recruiting
	GD2 expressing brain tumors	NCT04099797	Phase 1	C7R-GD2.CAR T Cells for Patients with GD2-expressing Brain Tumors (GAIL-B)	Recruiting
	pediatric or young adult high risk and/or relapsed/refractory Neuroblastoma and GD2-positive solid tumors	NCT03373097	Phase 1/2	Anti-GD2 CAR T Cells in Pediatric Patients Affected by High Risk and/or Relapsed/Refractory Neuroblastoma or Other GD2-positive Solid Tumors	Recruiting
	Sarcoma, Osteosarcoma, Neuroblastoma, Melanoma	NCT02107963	Phase 1	A Phase I Trial of T Cells Expressing an Anti-GD2 Chimeric Antigen Receptor in Children and Young Adults with GD2+ Solid Tumors	completed
	neuroblastoma, sarcoma, uveal melanoma, breast cancer and other GD2-positive cancer	NCT03635632	Phase 1	C7R-GD2.CART Cells for Patients with Relapsed or Refractory Neuroblastoma and Other GD2 Positive Cancers (GAIL-N)	Recruiting
	Osteosarcoma, Neuroblastoma	NCT01953900	Phase 1	iC9-GD2-CAR-VZV-CTLs/Refractory or Metastatic GD2-positive Sarcoma and Neuroblastoma (VEGAS)	Active, not recruiting
	Glioma of Spinal Cord, Glioma of Brainstem	NCT04196413	Phase 1	GD2 CAR T Cells in Diffuse Intrinsic Pontine Gliomas (DIPG) & Spinal Diffuse Midline Glioma(DMG)	Recruiting
	Neuroblastoma, Osteosarcoma	NCT03721068	Phase 1	Study of CAR T-Cells Targeting the GD2 With IL-15+iCaspase9 for Relapsed/Refractory Neuroblastoma or Relapsed/Refractory Osteosarcoma	Recruiting
	Neuroblastoma	NCT01460901	Phase 1	Study of Donor Derived, Multi-virus-specific, Cytotoxic T-Lymphocytes for Relapsed/Refractory Neuroblastoma (STALLONe)	completed
GD2/CD70	GD2 and/or CD70 positive Cancer Disease	NCT05438368	Phase 1/2	GD2/CD70 Bi-specific CAR-T Cell Therapy	Recruiting
GD2/PSMA	GD2 and PSMA positive Solid Tumor	NCT05437315	Phase 1/2	GD2/PSMA Bi-specific CAR-T Cell Therapy	Recruiting
GD2/CD56	GD2 and/or CD56 positive malignant disease	NCT05437328	Phase 1/2	GD2/CD56 Bi-specific CAR-T Cell Therapy	Recruiting
HER2	HER2 positive cancer that has spread to the brain or leptomeninges	NCT03696030	Phase 1	HER2-CAR T Cells in Treating Patients with Recurrent Brain or Leptomeningeal Metastases	Recruiting

	HER2-positive solid tumors	NCT03740256	Phase 1	Binary Oncolytic Adenovirus in Combination with HER2-Specific Autologous CAR VST, Advanced HER2 Positive Solid Tumors (VISTA)	Recruiting
	recurrent or refractory HER2-positive CNS tumors	NCT03500991	Phase 1	HER2-specific CAR T Cell Locoregional Immunotherapy for HER2-positive Recurrent/Refractory Pediatric CNS Tumors	Recruiting
	Sarcoma, HER-2 Protein Overexpression	NCT04995003	Phase 1	HER2 Chimeric Antigen Receptor (CAR) T Cells in Combination with Checkpoint Blockade in Patients with Advanced Sarcoma	Recruiting
	Ependymoma	NCT04903080	Phase 1	HER2-specific Chimeric Antigen Receptor (CAR) T Cells for Children with Ependymoma	Active, not recruiting
HER2/PD-L1	Peritoneal Carcinoma Metastatic, Pleural Effusion, Malignant	NCT04684459	Early Phase 1	Dual-targeting HER2 and PD-L1 CAR-T for Cancers with Pleural or Peritoneal Metastasis	Recruiting
IL13Ra2	leptomeningeal disease from glioblastoma, ependymoma, or medulloblastoma	NCT04661384	Phase 1	Brain Tumor-Specific Immune Cells (IL13Ralpha2-CAR T Cells) for the Treatment of Leptomeningeal Glioblastoma, Ependymoma, or Medulloblastoma	Recruiting
	Recurrent Glioblastoma, Refractory Glioblastoma	NCT04003649	Phase 1	IL13Ra2-CAR T Cells with or Without Nivolumab and Ipilimumab in Treating Patients With GBM	Recruiting
	Malignant Brain Neoplasm, Recurrent Malignant Brain Neoplasm, Refractory Malignant Brain Neoplasm	NCT04510051	Phase 1	CAR T Cells After Lymphodepletion for the Treatment of IL13Rα2 Positive Recurrent or Refractory Brain Tumors in Children	Recruiting
	stage IIIC or IV melanoma.	NCT04119024	Phase 1	Gene Modified Immune Cells (IL13Ralpha2 CAR T Cells) After Conditioning Regimen for the Treatment of Stage IIIC or IV Melanoma	Recruiting
EGFRvIII	Glioblastoma, Glioblastoma Multiforme, Glioma, Malignan	NCT05063682	Phase 1	The Efficacy and Safety of Brain-targeting Immune Cells (EGFRvIII-CAR T Cells) in Treating Patients with Leptomeningeal Disease from Glioblastoma. Administering Patients EGFRvIII -CAR T Cells May Help to Recognize and Destroy Brain Tumor Cells in Patients (CARTREMENDOUS)	Active, not recruiting
	Malignant Glioma, Glioblastoma, Brain Cancer, Gliosarcoma	NCT01454596	Phase 1/2	CAR T Cell Receptor Immunotherapy Targeting EGFRvIII for Patients With Malignant Gliomas Expressing EGFRvIII	completed
	Glioblastoma	NCT03726515	Phase 1	CART-EGFRvIII + Pembrolizumab in GBM	completed
ROR1	ROR1+ solid tumors	NCT05748938	Phase 1/2	A Study of RD14-01 in Patients With Advanced Solid Tumors	Recruiting

	ROR1+ relapsed or refractory triple negative breast cancer or non-small cell carcinoma	NCT05274451	Phase 1	A Study to Investigate LYL797 in Adults With Solid Tumors	Recruiting
	ROR1-positive hematologic chronic lymphocytic leukemia (CLL), mantle cell lymphoma (MCL), acute lymphoblastic leukemia (ALL), diffuse large B-cell lymphoma (DLBCL) and solid tumor triple negative breast cancer (TNBC)	NCT05694364	Phase 1	Dose Escalation/Dose Expansion Study of PRGN-3007 UltraCAR-T Cells in Patients With Advanced Hematologic and Solid Tumor Malignancies	Recruiting
B7-H3	Ovarian Cancer	NCT05211557	Phase 1/2	Study of Fully Human B7H3 CAR-T in Treating Recurrent Malignant Ovarian Cancer	Recruiting
	B7-H3-positive relapsed/refractory non-brainstem primary CNS tumors and brainstem high-grade neoplasms	NCT05835687	Phase 1	Loc3CAR: Locoregional Delivery of B7-H3-CAR T Cells for Pediatric Patients With Primary CNS Tumors	Recruiting
	relapsed or refractory non-CNS solid tumors	NCT04483778	Phase 1	B7H3 CAR T Cell Immunotherapy for Recurrent/Refractory Solid Tumors in Children and Young Adults	Recruiting
	relapsed/refractory B7-H3+ solid tumors	NCT04897321	Phase 1	B7-H3-Specific Chimeric Antigen Receptor Autologous T-Cell Therapy for Pediatric Patients With Solid Tumors (3CAR)	Recruiting
	recurrent advanced hepatocellular carcinoma	NCT05323201	Phase 1/2	Study Of B7H3 CAR-T Cells in Treating Advanced Liver Cancer	Recruiting
	Diffuse intrinsic pontine glioma, diffuse midline glioma, recurrent/refractory pediatric CNS tumors	NCT04185038	Phase 1	Study of B7-H3-Specific CAR T Cell Locoregional Immunotherapy for Diffuse Intrinsic Pontine Glioma/Diffuse Midline Glioma and Recurrent or Refractory Pediatric Central Nervous System Tumors	Recruiting
	Epithelial Ovarian Cancer	NCT04670068	Phase 1	Phase I Study of Autologous CAR T-Cells Targeting the B7-H3 Antigen in Recurrent Epithelial Ovarian	Recruiting
	Recurrent/refractory Glioblastoma	NCT04077866	Phase 1/2	B7-H3 CAR-T for Recurrent or Refractory Glioblastoma	Recruiting
	Recurrent glioblastoma multiforme	NCT05474378	Phase 1	B7-H3 Chimeric Antigen Receptor T Cells (B7-H3CART) in Recurrent Glioblastoma Multiforme	Recruiting
MUC-1	advanced or metastatic epithelial derived solid tumors	NCT05239143	Phase 1	P-MUC1C-ALLO1 Allogeneic CAR-T Cells in the Treatment of Subjects With Advanced or Metastatic Solid Tumors	Recruiting
	Metastatic breast cancer	NCT04020575	Phase 1	Autologous huMNC2-CAR44 T Cells for Breast Cancer Targeting Cleaved Form of MUC1 (MUC1*)	Recruiting

Unfortunately, despite many solid tumor targeting CARs producing promising pre-clinical data in a xenograft mouse model, the clinical results for solid tumor CAR T cell therapy have been less remarkable. To date there are a few successful clinical trials reported. However, these clinical trials do not achieve the same rate of clinical success compared to hematological clinical trials with CAR T cells[96]. An ongoing phase 1 clinical trial (NCT02208362) with IL13Rα2 CAR T cells reported a transient CR sustaining 7.5 months post treatment with improvements to the quality of life in one patient with recurrent multifocal GBM following multiple intracranial CAR T cell infusions[124]. A phase 1 clinical trial with GD2 CAR T cells in patients with neuroblastoma (NCT00085930) showed 3 out of 11 patients achieving CR[125]. A phase 1/2 clinical trial with HER2 CAR T cells in patients with sarcoma found 4 out of 17 patients achieving stable disease[126].

Among the major barriers to effective CAR T cell therapy ones specific to solid tumors include selection of tumor restricted antigen, tumor antigen heterogeneity, immune suppression by the TME, and failure of adequate CAR T cell trafficking and tumor infiltration[127,128]. To date, multiple approaches have been assessed to overcome these barriers but success in murine models have not been translated to human clinical trials[129,130]. We highlight some of the notable successful solid tumor target CAR T cell therapies as well as notable CAR targets that have had many hurdles and innovations to try to improve safety and efficacy in a solid tumor setting.

The major difference between B cell malignancy and solid tumor CAR T cell therapy is the lack of ubiquitously expressed tumor antigens associated with their cell lineage like in B cell malignancies[131]. TAAs in solid tumors targeted by CARs include neoantigens, tumor selective antigens, and endogenous tumor specific antigens[131]. Neoantigens such as EGFRvIII are an attractive target due to their restriction to tumor cells. EGFRvIII CAR T cells have shown promising results in murine models of GBM[132]. Clinical trials investigating the safety and efficacy of EGFRvIII CAR T cells in patients with GBM are currently underway (NCT02209376, NCT01454596). Abnormal glycosylation of extracellular glycoprotein (MUC-1) is another neoantigen targeted in CAR T cell therapy for breast and ovarian cancer. Xenograft murine models treated

with MUC-1 CAR T cells have shown significant delay in tumor progression[133] . MUC-1 CAR T cells are currently being investigated for safety and efficacy in multiple clinical trials (NCT05239143, NCT04020575).

Tumor selective antigens are overexpressed on tumor tissues but also have relatively low basal expression on normal tissues. Mesothelin (MSLN) and B7-H3 are examples of tumor selective antigens. MSLN is overexpressed in mesothelioma, ovarian, and pancreatic carcinomas and has low expression on normal peritoneal, pleural, and pericardial tissues[134]. MSLN CAR T cells have induced tumor regression and increased survival in murine models of MSLN positive patient derived xenograft tumors[135] and murine pancreatic ductal adenocarcinoma (PDAC)[136]. Unfortunately, MSLN CAR T cell therapy has had limited success in a clinical setting in solid tumors. This is due to several factors including the lack of restriction of MSLN expression to tumor tissues[137]. Early clinical trials with MSLN CAR T cells had significant on-target-off-tumor toxicity involving gastrointestinal, pulmonary and hematological tissues ranging from manageable to severe toxicity and death[138]. To reduce on-target-off-tumor toxicity dual targeting trans-signaling CAR T cells that only activate through dual receptor recognition of two antigen targets were developed and have seen promising pre-clinical results[137]. A dual targeting, trans-signaling anti-MSLN/4-1BB-anti-CAE/CD3ζ CAR construct has shown high *in vivo* anti-tumoral activity while sparing cognate healthy tissues in mice[136]. Although there are improvements to MSLN CAR safety, there has been no evidence for persistence or efficacy from intravenously infused MSLN CAR T cells in patients with MSLN positive solid tumors[137]. Barriers to CAR T cell trafficking and immune suppressive TME are among the major barriers proposed as to why MSLN CAR T cells are not clinically effective[137]. In tumor selective antigen targeting with CARs, scFv affinity and avidity are essential in preventing targeting of basal expression on normal tissue[131]. Additionally, TAAs may be heterogeneously expressed on solid tumors to which targeting with CAR T cell therapy may lead to tumor escape by antigen downmodulation[131]. Careful selection of TAAs that contribute to tumor aggressiveness or immune evasion can enhance native anti-tumoral immune therapy in the case of antigen escape by CAR T cell therapy.

CAR T cell associated toxicities are rarely seen in solid tumor CAR T cell therapy. The majority of severe systemic CAT T cell associated CRS have been reported in hematological patients targeting CD19 or BCMA[139]. CAR T cell therapies for glioma targeting antigens such as IL-13Rα2, and EGFRvIII have seen lower rates of occurrence and milder cases of CRS[140,141]. Other solid tumor targeting CAR T cell clinical trials to date have not reported any cases of CRS. This is likely due to solid tumor CAR T cell therapy being more localized, having less stimulation by tumor antigen, and having immune suppressive signals from the tumor microenvironment[115]. However, lack of adverse events also correlates with lack of efficacy with minimal to no anti-tumoral effects, comparative to the complete remissions achieved by CAR T cell therapy in hematological cancers[115].

CAR T cell therapy for osteosarcoma

The unique histological and immunological features of OS make CAR T cell therapy a particularly challenging solid tumor target as CAR T cells have to traffic through bone or cartilage matrix and also survive the immune suppressive TME of OS[41]. OS is historically known as an immunologically "cold" tumor with low CD8+ TIL to myeloid cell ratio[21]. Tumor cells and immune suppressor cells that reside within the TME suppress CAR T cell functions through a variety of mechanisms including the expression of check point molecules such as PD-L1 and secretion of soluble factors such as VEGF, IL-10 and TGFβ[142]. Additionally, careful selection of TAAs and CAR affinity dialing is needed to prevent targeting of normal tissues[131]. Tumor antigen heterogeneity also poses a high risk for tumor escape through antigen loss or down modulation due to selection pressure by CAR T cell therapy[97].

To date multiple cancer antigens targets have been identified and adapted for CAR T cell therapy in OS including human epidermal growth factor 2 (HER2), Insulin-like growth factor receptor-1 (IGFR1), receptor tyrosine orphan-like receptor 1 (ROR1), disialoganglioside (GD2), and B7 homolog 3 (B7-H3). HER2 CAR T cell therapy is currently the furthest in development having shown promising anti-tumoral effects in a murine model[126,143]. A phase 1/2 clinical trial HER2 CAR T cells showed no toxicity in HER2

positive sarcoma patients with fever post infusion being the most common adverse event[126]. 16 patients enrolled with HER2 positive relapsed or refractory sarcomas showed modest anti-tumoral activity with 4 out of 16 showing stable disease for 12 weeks to 14 months[126]. These results paved the way for further trials in patients with advanced sarcomas (NCT00902044, NCT04995003)[31]. Additionally, current phase 1 clinical trials are underway with GD2 CAR T cells in pediatric solid tumors including OS (NCT102107963). Preclinical trials with IGFR1, GD2 and ROR1 CAR T cells showed significant tumor suppression in xenograft animal models[144,145]. B7-H3 has been identified as a promising cancer antigen target in sarcomas and brain tumors and is currently being investigated as a target for CAR T cell therapy[146,147].

It is not likely that single agent CAR T cell therapy will lead to high rates of CRs in OS like in CD19 CAR T cell therapy for B cell malignancies[148]. Several strategies are being investigated to overcome the known barriers in OS for effective CAR T cell therapy and it will likely be a combination of strategies that will induce durable CRs in OS. These strategies include the following[148].

1. Affinity dialing CARs to increase specificity to tumor antigens to lower toxicity.
2. Dual targeting of CARs to increase tumor antigen coverage to prevent tumor antigen escape.
3. Combination of CAR T cell therapy with radiotherapy to increase antigen expression and induce epitope spreading.
4. Addition of chemokine receptors to increase CAR T cell trafficking and infiltration into OS.
5. TME modification of immunosuppressive cells within the TME to enhance anti-tumoral CAR T cell effects.

B7-H3 native expression and role as a tumor antigen target

B7 homolog 3 (B7-H3), also known as CD276, is an immune checkpoint molecule that has limited expression on healthy tissues such as antigen presenting cells [149]. Newly discovered as part of the B7 family, B7-H3 is thought to regulate T cell function and proliferation having found both immune activating and

inhibitory effects in different contexts[150-152]. B7-H3 is an orphan ligand currently with no definitive receptor identified[152]. B7-H3 has been found to be highly expressed in developing bones during embryogenesis and plays a role in osteoblast differentiation in mice. B7-H3 knockout mice have decreased density of osteoblasts and decreased mineralization in cortical bone[153]. Soluble B7-H3 has been found to be correlatively upregulated in the serum of patients with osteoporosis[154]. B7-H3 knockdown in MG63 a human OS cell line impaired the formation of bone[154]. B7-H3's role in bone formation and osteoblast differentiation is still being investigated although it may tie into the high prevalence of B7-H3 overexpression in OS with one study finding that 91.8% of primary OS tissues were B7-H3 positive[146].

B7-H3 has been found to be overexpressed in many tumor types including breast cancer, lung cancer, renal cell carcinoma, neuroblastoma, medulloblastoma and OS[146]. B7-H3 expression in OS is correlated with significantly shorter survival time, and increased incidence of metastasis. *In vitro* upregulation of B7-H3 expression increased invasion in OS cells in part due to the upregulation of matrix metalloproteinase-2 (MMP-2)[146]. B7-H3 also plays a role in the immune landscape of the TME with high B7-H3 expression correlating with increased infiltration of T regs and decreased infiltration of CD8+ TILs[146,152]. B7-H3 has been proposed as a pan-cancer antigen for CAR T cell therapy due to its overexpression on a variety of solid tumors[147]. Targeting of B7-H3 tumor cells may directly inhibit tumor proliferation and metastasis but may also synergistically increase anti-tumoral immune response by reprogramming the TME[147].

Use of monoclonal anti-B7-H3 antibody enoblituzumab (MGA271) in phase 1 clinical trials in patients with B7-H3 positive solid tumors was well tolerated with few dose limiting toxicities (NCT01391143, NCT02475213). Radiotherapy labeled anti-B7-H3 monoclonal antibody (clone 8H9) is currently in ongoing phase 1 clinical trial in patients with sarcomas and other cancers (NCT00089245). Novel anti-B7-H3 antibody conjugated with DNA topoisomerase I inhibitor is currently being investigated

in a multicenter phase 1/2 trial in patients with advanced malignant tumors, central nervous system cancer and neuroblastoma (NCT04145622, NCT01099644, NCT00582608).

Preclinical use of B7-H3 CAR T cell therapy showed anti-tumoral activity in xenograft mouse models of osteosarcoma inducing complete tumor control in mice treated intravenously with B7-H3 CAR T cells in both orthotopic and metastatic models of human OS[147]. Additionally, mouse orthotopic xenograft models of Ewing's sarcoma and medulloblastoma were cleared of tumors by intravenous B7-H3 CAR T cell treatment[147]. Current phase 1 clinical trials are ongoing for B7-H3 CAR T cell therapy in pediatric patients with CNS tumors (NCT04185038) and solid tumors (NCT04897321). Early reports from the B7-H3 CAR T pediatric CNS clinical trial showed no dose-limiting toxicities and one patient with sustained clinical and radiographic improvement though 12 months[155].

CXCL8 role in cancer

Chemokines and their respective receptors play a critical role in immune cell migration. Chemokines are secreted by immune and non-immune cells such as epithelial and endothelial cells[156]. Tumor cells also use chemokines as a mechanism of immune resistance[157]. CXCL8 is a chemokine normally produced by macrophages, airway smooth muscle cells, endothelial cells, and epithelial cells for the recruitment of neutrophils and other immune cells through binding receptors CXCR1 and CXCR2[158]. Overexpression of CXCL8 has been characterized in many tumor types including hepatocellular carcinoma, breast cancer, prostate cancer, lung cancer and sarcomas[159,160]. CXCL8 signaling in Ras-driven cancers has been shown to drive the recruitment of immune suppressive N2 tumor associated neutrophils (TANs) which contribute to distant metastasis and tumor neovascularization[161]. N2 TANs suppress T cell receptor expression and recruit T regs into the TME through the secretion of arginase 1 (ARG-1)[162]. High expression of CXCR1/2 on tumor derived MDSCs in a mouse model of colon carcinoma indicated that CXCL8 secretion by tumors may be a mechanism of recruitment of immune suppressor cells into the TME[163]. CXCL8 was

found to induce granulocyte MDSCs to release neutrophil extracellular nets (NETS) which were involved in metastatic progression[163].

Increasing CAR T cell trafficking is a proposed mechanism to improve CAR T cell therapy in solid tumors[96]. *In vitro* expansion and genetic modification of CAR T cells may lead to a loss of chemokine receptors further impairing CAR T cell trafficking to even high chemokine secreting tumors[164]. One proposed mechanism to improve CAR T cell trafficking is through the exogenous expression of chemokine receptors to co-opt tumor chemokine signals and increase CAR T cell homing[159]. Addition of chemokine receptor CXCR2 to GPC3 CAR T cells increased migration to tumor cells *in vitro* and *in vivo* inducing increased tumor control in an xenograft mouse model compared to GPC3 CAR T cells without exogenous CXCR2[159]. Addition of CXCR1 or CXCR2 in CD70 CAR T cells showed increased trafficking and anti-tumoral effects in xenograft mouse models of GBM, ovarian and pancreatic cancer. CXCR1/2 CD70 CAR T cells caused complete tumor regression and increased survival compared to stable or progressive disease achieved by CD70-CAR T without CXCL8 receptor[165]. This indicates that adding chemokine receptors to CAR T cells can increase their *in vivo* anti-tumoral efficacy through enhancing CAR T cell trafficking to local tumor sites[159].

Myeloid cell tumor immune suppression

The immune suppressive TME plays a major role in the failure of solid tumor CAR T cell therapy[166]. Tumor cells and residential immune cells within the TME secrete chemokines and cytokines that preferentially recruit and support immune suppressive cells such as M2 TAMs, MDSCs, N2 TANs and T regs[167]. M2 TAMs and MDSCs exert immune suppression to cytotoxic T cells through expression of checkpoint molecules such as CTLA-4 and PD-L1, secretion of cytokines such as IL-10, VEGF, IL-4, and TGFβ, and production of amino acid depleting enzymes such as ARG-1 and indoleamine 2,3-dioxygenase (IDO)[166,167].

The interaction of tumor cells and the immune cells within the TME plays a major role in cancer neo-angiogenesis, progression, and metastasis. Reprogramming of the TME through depletion of immune suppressive myeloid cells, repolarization to proinflammatory profile, blockade of migration into the TME and blockade of immune suppressive signals have been well established methods of TME modification that have shown efficacy as single agents and work synergistically with other immune therapies such as CAR T cell therapy[167]. We propose that a combination of repurposed drugs to block of monocyte migration by losartan and inhibition of MDSC mobilization by propranolol will synergistically improve CAR T cell function in a solid tumor setting.

Losartan is an angiotensin II type 1 receptor antagonist that has been shown to have immunomodulatory actions through the non-competitive inhibition of CCL2 signaling that recruits CD11b+/Ly6C+ monocytes into tumors[168]. Treatment with losartan reduces tumor burden in a mouse model of metastatic breast cancer and inhibited CD11b+/Ly6C+ monocytes into lung metastatic lesions[168]. Propranolol is a non-selective beta-blocker that has shown immune modulatory effects through the reversal of adrenergic stress[169]. Therapeutic use of propranolol has shown to partially reverse the release and differentiation of MDSC from the bone marrow by catecholamines in a mouse model[169,170]. Our group and others have shown that the combination of losartan and propranolol has TME modifying effects *in vitro* and *in vivo* in xenograft mouse models[169,171]. Most importantly we have demonstrated clinically appreciable anti-tumoral effects of losartan when combined with TKI toceranib in dogs with metastatic OS[172] and in dogs with glioma treated of combination losartan and propranolol with a cancer stem cell vaccine[173].

Conclusion

Refractory and metastatic OS is a difficult cancer to treat due the heterogeneity intratumorally and between individuals. Being a characteristically immunologically “cold” tumor OS does not elicit a strong anti-tumoral immune response. This is in part due to the immune suppressive TME composed of TAMs,

MDSCs, T regs and TANs. Canine OS is a great model for human OS due to similarities in pathogenesis, histological features, disease progression and clinical presentation. Metastatic OS in dogs has been well established as a translational model and contributed to human OS clinical trials for new therapeutics[43,46].

CAR T cell therapy has been a breakthrough in cancer immunotherapy although its successes has only been seen in patients with hematological malignancies[82]. Expansion of CAR T cell therapy to solid tumors faces unique barriers such as CAR T cell trafficking to local tumor lesions, and the immune suppressive TME[128]. Single agent CAR T cell therapy in solid tumors to date has not had clinical success[79,128]. It is likely that additional combination therapy is needed to see appreciable anti-tumoral effects[79].

Our goal is to develop canine OS as a platform to evaluate B7-H3 CAR T cell therapy in an immune competent solid tumor model. We propose to enhance B7-H3 CAR T cell therapy through the addition of chemokine receptor CXCR2 and TME modification with drugs losartan and propranolol. To achieve this, we aim to answer the following questions.

1. What is the prevalence of B7-H3 surface antigen on canine OS and normal tissues?
2. What is the activity of the human B7-H3 CAR construct in canine T cells against canine B7-H3+ OS?
3. Does the addition of chemokine receptor CXCR2 increase B7-H3 CAR T cell efficacy *in vivo*?
4. What is the effect of tumor associated immune suppressor cells on B7-H3-CXCR2 CAR T cells?

We were able to conclude that B7-H3 is a viable target for CAR T cell therapy in canine OS being widely expressed in canine OS and overexpressed in a tumor restricted manner. We determined that canine T cells engineered to express human B7-H3 CAR were activated by canine B7-H3 antigen producing IFNγ and killing B7-H3+ OS tumor cells. Activation and direct CAR T cell killing was antigen specific and gated on level of antigen expression having little activity on low B7-H3 expressing tumor cell lines. We showed that the addition of CXCR2 increased migration to canine CXCL8 and increased *in vivo* tumor control in a xenograft mouse model of canine OS. Additionally, we showed that B7-H3 positive

macrophages increased B7-H3 CAR T cell activity through antigen-CAR signaling. While there is more to be investigated on TME modification's effect on CAR T cell therapy *in vivo.* Success of this project lays the foundation for a new therapeutic for dogs with metastatic OS to which currently there are limited effective treatment modalities. Development of canine B7-H3 CAR T cell therapy can also be applied to other tumor types that express B7-H3 such as glioma and melanoma. Success of this project will also inform future avenues of investigation for pediatric trials in metastatic OS with B7-H3 CAR T cells.

Chapter 2: AIM 1- Evaluation of B7-H3 as an antigen target for CAR T cells in canine osteosarcoma

Summary

B7 homolog 3 (B7-H3) has been identified as a pan-cancer antigen target for chimeric antigen receptor (CAR) T cell therapy, being overexpressed on many solid tumor types in humans[147]. Preclinical B7-H3 CAR T cell therapy against solid tumors including osteosarcoma (OS) showed promising results[147] leading to two phase 1 clinical trials in glioma and pediatric advanced solid tumors (NCT04185038 and NCT04897321). Knowing that efforts to date for applying CAR T cell therapy to solid tumors has not yielded clinical success despite complete tumor regression in preclinical xenograft mouse models[128], we proposed to develop canine metastatic osteosarcoma as a spontaneous large animal translational model to evaluate B7-H3 CAR T cell therapy. Establishment of canine metastatic OS as a translational model for CAR T cell therapy will enable the modeling of the tumor and patient heterogeneity of OS and the complex interaction of the TME and CAR T cells in an immune competent animal.

This chapter will focus on the validation of B7-H3 as a viable tumor associated antigen target for canine B7-H3 CAR T cell therapy. To achieve this, we characterized that B7-H3 was overexpressed in canine OS both in FFPE primary tumor samples and OS cell lines. We also screened normal liver, spleen, lymph node and peripheral blood to ensure that there was differential antigen expression between tumor tissues and normal tissues. Additionally, we optimized canine CAR T cell generation for transduction efficiency, T cell expansion, and functional capacity as assessed by tumor target cell killing to ensure that we can generate clinically relevant amounts of CAR T cells from whole blood from tumor bearing dogs. We validated that the anti-human-B7-H3 CAR construct cross reacts with dog B7-H3 antigen and that canine B7-H3 CAR T cells are activated in an antigen specific manner. By developing B7-H3 CAR T cells for canine OS we can evaluate additional immune therapies that work synergistically with B7-H3 CAR T cell therapy.

Introduction

Osteosarcoma (OS) is an aggressive tumor primarily affecting children and young adults with 15-20% of patients having metastatic disease at time of diagnosis[174,175]. Patients with metastatic disease have a 5-year survival rate of less than 20% and clinical outcomes for metastatic patients have not improved in over 4 decades[174,176,177]. B7 homolog 3 (B7-H3; CD276) is a costimulatory molecule expressed normally on myeloid cells[178,179]. In addition, B7-H3 has been identified as a pan-cancer antigen due to its high surface expression in numerous solid tumor types including OS[180,181]. Other studies have shown that B7-H3 expression also drives differentiation of osteoblasts during embryogenesis and plays a role in bone mineralization[182]. In adult and pediatric OS, expression of B7-H3 has been found to be upregulated in tumors and restricted to tumor cells and myeloid cells, with limited expression on normal tissues making it a promising target for cancer immunotherapy[183]. High B7-H3 expression in OS has been correlated with decreased 5-year survival, metastatic progression, and tumor immune evasion[146,183].

Two monoclonal antibodies 8H9 and MGA271 that target B7-H3 have been used to treat B7-H3 expressing tumors. These monoclonal antibodies have been clinically demonstrated to be safe however they have had marginal anti-tumoral efficacy[184-186]. A phase 1 clinical trial using MGA271 to treat pediatric relapsed or refractory solid tumors was well tolerated with only 6% of patients experiencing grade 3/4 drug related adverse events but, did not produce profound sustained clinical activity[187].

Chimeric antigen receptor (CAR) T cells are engineered to target specific tumor antigens to induce T cell immunity through adoptive cell therapy[82]. CAR T cell therapy has shown remarkable success in B cell malignancies through the targeting of CD19[188]. Expansion of CAR T cell therapies to solid tumor malignancies aims to recreate the success of CD19 CAR T cells though the identification and targeting of solid tumor associated antigens[127].

The MGA271 B7-H3 monoclonal antibody was used to produce the single-chain variable fragment (scFv) extracellular domain in B7-H3 CAR constructs used in preclinical mouse models against pediatric

solid tumors, osteosarcoma, and glioma[147,189]. Preclinical trials of B7-H3 CAR T cells in NOD SCID gamma (NSG) mice have shown selective activity against high B7-H3 expressing tumors eliminating tumor burden and increasing survival in xenograft mouse models of human OS[147,190,191]. *In vitro* modeling of B7-H3 CAR T cell activity also shown affinity gated activation indicating a therapeutic window based on level of B7-H3 expression[147]. Phase 1 clinical trials for B7-H3 CAR T cell therapy are currently ongoing in patients with CNS tumors (NCT04185038) and pediatric patients with recurrent or refractory solid tumors (NCT04483778).

Solid tumor CAR T cell therapy faces unique challenges compared to the established CAR T cell therapies developed to treat B cell malignancies[128]. These include the immune suppressive effects of the TME, limitations to CAR T trafficking and homing to tumor sites, tumor antigen expression heterogeneity[127,128]. To date, multiple approaches have been assessed to overcome these barriers, but success in a murine model has largely not translated to success in human clinical trials[80,128]. Establishing a spontaneously occurring immune competent model for evaluating CAR T cell therapies and strategies to overcome the challenges of solid tumors would be a powerful tool in validating new CAR T cell approaches for solid tumors[192-195].

Canine OS is a well-established translational model for pediatric OS, having similar histological origin, disease progression, and a higher incidence rate than pediatric OS[22,195,196]. Canine OS recapitulates the immune suppressive tumor microenvironment (TME) characteristic of OS and individual and intra-tumoral heterogeneity not represented in a xenograft mouse model[197]. Given B7-H3's high prevalence in human OS and role in osteoblast differentiation in embryogenesis we hypothesized that B7-H3 will also have a high prevalence in canine OS and be differentially expressed from normal tissues making it a good tumor associated antigen target for CAR T cell therapy. Another group in parallel to ours showed overexpression of B7-H3 in a small sample of canine FFPE OS samples and showed activation and tumor cell killing by second-generation human B7-H3 CAR construct against canine B7-H3+ OS targets[198]. They

also found that B7-H3 CAR T cell therapy had shown no adverse side effects when administered to healthy beagles[198]. Here we demonstrate the feasibility of B7-H3 CAR T cell in canine OS by further characterizing high prevalence of B7-H3 overexpression in a wider screen of canine OS cell lines and primary FFPE OS tissues. Additionally, we optimized canine CAR T cell generation from whole blood of tumor bearing dogs for both CAR T cell yield and preservation of post-expansion anti-tumoral functionality. We also demonstrate *in vitro* activity of canine T cells expressing anti- human-B7-H3 CAR was cross reactive to canine B7-H3 antigen. Additionally, canine B7-H3 CAR T cells were activated and kill B7-H3+ canine OS cell lines in an antigen specific-affinity gated manner. These findings are notable as they more robustly show that canine OS is a viable system for the development of B7-H3 CAR T cell therapy.

Methods

Cell lines

The human erythroleukemia cell line K562 cells were stably transduced to expressed FcyRII (CD32) and canine CD86 to generate artificial antigen presenting cells (aAPCs), as previously described, and gifted by University of Pennsylvania and Dr. Nicola Mason's group[199,200]. aAPCs were conjugated with anti-canine CD3 (clone CA17.2A12, Biorad) and anti-canine CD28 (clone 5B8, Invitrogen) at a 1:1 ratio as previously described[199]. Canine osteosarcoma cell lines were provided by the FACC cell line repository and previously validated[201]. All cell lines were cultured in cell culture media containing DMEM with 10% fetal bovine serum (Corning), 2 mM L-glutamine (Gibco), 100 U/ml penicillin and 100 ug/ml streptomycin (Gibco). All cell cultures were kept at 37C and 10% CO_2.

CAR constructs

The B7-H3 CAR was shared with the University of Colorado Verneris lab by Michael Jensen, MD (Fred Hutchinson Cancer Center, Seattle, WA). This lentiviral construct contained a B7-H3 single-chain

variable fragment (scFv), an IgG4 and CD28 transmembrane domain, a 4-1BB costimulatory molecule and the CD3ζ domain. The Verneris lab cloned the CAR portion of the construct into a retroviral backbone containing a 5' LTR promoter using standard PCR-based cloning methods to create the B7-H3 CAR construct. The retroviral backbone we used was a gift from Anandani Nellan (National Cancer Institute, Bethesda, MD).

Retrovirus production

B7-H3 CAR retrovirus was produced and provided to us by Jessica Lake, MD (University of Colorado Verneris lab, Aurora, CO). 293GP cells (a gift from Dr. Terry Fry, University of Colorado, Aurora, CO) were plated in T175 flasks in Dulbecco's Modified Eagle Medium (DMEM) with 10% fetal bovine serum (FBS) and 1% anti-biotic/anti-mycotic (Gibco). Transfection occurred when cells were 90-95% confluent. Tube A contained 3.4 ml of room temperature Opti-MEM (without additives), 20.25 µg of B7-H3 vector DNA, and 10.125 µg of RD114 (envelope plasmid, gift from Anandani Nellan). Tube B contained 3.4 ml of room temperature Opti-MEM (without additives) and 100 µl of lipofectamine 2000 (Invitrogen). The tubes were left at room temperature for 10 minutes after which Tube A was added dropwise to Tube B and gently mixed. The combined mixture was left at room temperature for 30 minutes. During that time, the media was removed from the 293GP cells and 16 ml of fresh, warmed DMEM with 10% FBS (no anti-anti) was carefully added. After 30 minutes, the retroviral mixture was added to the flask, being careful not to agitate the cells. Flasks were placed at 37 degrees Celsius for 24 hours. After 24 hours, media/viral mixture was removed from flasks and 24 ml of fresh DMEM with 10% FBS and 1% anti-anti was gently added. The flasks were returned to 37 degrees Celsius. Viral collections were made at 24 and 48 hours after media replacement. The retrovirus was flash frozen in dry ice and placed in -80 degrees Celsius until use. Frozen retrovirus stocks were shared with us for the purpose of generating canine B7-H3 CAR T cells and

transported on dry ice from University of Colorado, Aurora, CO to Colorado State University, Fort Collins, CO.

Generation of anti-canine CD3/CD28 magnetic beads

Mouse anti-canine CD3 (clone CA17.2A12, Biorad) and mouse anti-canine CD28 (clone 58B, Invitrogen) antibodies were conjugated to magnetic tosyl-activated Dynabeads (Life Technologies) as previously established at a 1:1 antibody ratio[194,199].

Canine PBMC isolation and T cell activation

Canine whole blood from tumor bearing patients was provided by the Flint Animal Cancer Center (Fort Collins, CO). Peripheral blood mononuclear cells (PBMCs) were isolated using Ficoll and gravity centrifugation. Canine PBMCs were plated at a density of 2.0e6/mL in 6-well tissue culture plates to adhere monocytes for 90 minutes at 37 degrees Celsius. Peripheral blood lymphocytes (PBLs) were gently washed off with canine T cell media (cTCM), DMEM with 10% FBS and 100 U/ml penicillin and 100 ug/ml streptomycin (Gibco), 2 mM L glut, 1x essential amino acids (Gibco, cat#11130051), 1x non-essential amino acid (Gibco, cat#11140050), 0.075% Bicarbonate solution, 10 mM HEPES, and 55 uM 2-mercaptoethanol. PBLs were plated at a concentration of 1.0e6/mL in cTCM with 30 ng/mL rhIL-21(Peprotech), 100 IU rhIL-2 (Peprotech). The addition of cytokines 5 ng/mL rhIL-7 (Peprotech) and rhIL-15 (Peprotech) were also added for certain CAR T cell cultures. T cells were activated with either tosyl-activated dynabeads (Life Technologies) conjugated with canine anti-CD3/CD28 antibodies at a ratio of 3:1 beads to PBLs, 5 ug/ml PHA, or 1:1 ratio of anti-CD3/CD28 conjugated aAPCs. T cells were incubated at 37˚C for 3 days before transduction with CAR retrovirus.

CAR T cell Transduction

Non-tissue culture treated plates are coated with 24 μg/mL retronectin (Tankara) according to manufacture protocol. Frozen B7-H3 retroviral supernatant was thawed in a 37˚C water bath and aliquoted into retronectin coated 6 well plates at 2 ml/well and centrifuged at 32˚C for 2.5 hours at 2,000 G. Viral supernatant was discarded after centrifugation and activated PBLs were plated onto retroviral bound plates at a concentration of 5.0e5 cells/mL and 2 mL per well and incubated overnight at 37˚C with 10% CO_2. T cells used for CAR T cell generation optimization were transduced once before being rescued from virus and expanded in fresh cTCM media and cytokines. CAR T cells used for *in vitro* and *in vivo* assays were transduced twice before being rescued from virus and put into fresh cTCM with fresh cytokines. Half of the media was changed, and fresh cytokines are added every 2-3 days. Generated canine CAR T cells were used for analysis by day 10-14 of culture.

Flow cytometry

Canine surface expression of B7-H3 was analyzed using anti-B7-H3-APC antibody (clone 7-517, eBioscience) or isotype control mouse IgG1kappa (ThermoFisher, cat# 17-4714-82). Canine immune expression was analyzed with the following antibodies: anti-canine CD5-FITC (cloneYKIX322.3, Biorad), anti-canine CD8-alexa Fluor 647 (clone YCATE55.9, Biorad), anti-canine CD4-Pacific Blue (clone YKIX302.9, Biorad), anti-CD62L (clone FMC46, Biorad), anti-CD45RA (clone CA21,4B3, Leukocyte Antigen Biology Laboratory). Recombinant protein L-biotinylated (cat# 29997) secondary Streptavidin-PE (cat#12-4317-87, eBioscience) was used to detect B7-H3 CAR transduced cells. After staining all samples were analyzed on a Beckman Coulter Gallios flow cytometer. Flow data was analyzed by Flowjo v10.

CAR T cell activation assay

B7-H3 CAR T cells were co-cultured with canine OS cell lines. Donor matched activated non-transduced (NTD) T cells were also co-cultured with canine OS cell lines as a control for endogenous T cell

reactions. B7-H3 CAR T cell activation was measured by cytokine levels in the supernatant after 24 hours of co-culture. Canine OS cell lines were plated at 5.0e3 cells/ well in cTCM in a 96 well flat bottom plate and incubated for 24 hours at 37℃. T cells were washed 3x with 10 mL cTCM media to ensure no recombinant IL-2 contaminated the co-culture. T cells plated 1:1 effector to target (E:T) ratio with canine OS cell lines to a final volume of 250 µl/ well. Co-cultures were incubated 24 hours then 100 ul/well of supernatant was collected for IFNγ ELISA (R&D systems, cat# DY285B-05). Absorbance was read by plate reader at 450 nm.

Cell freezing

Cells were washed and pelleted before freezing. Cells were resuspended in freezing media DMEM with 10% FBS, and 10% Dimethyl Sulfoxide (DMSO) before aliquoted into 2 mL cryovials at maximum concentration 5.0e6/vial and frozen at -80C in Mr. Frosty (ThermoFisher, cat# 5100-0001). Frozen B7-H3 CAR T cells or NTD T cells were thawed in a water bath and incubated at 37˚C for 48 hours in cTCM media with cytokines matching their initial expansion culture before use in any *in vitro* assays.

Incucyte killing assay

Red fluorescence protein (RFP) labeled canine OS cell line Abrams target cells were seeded in a 96-well flat bottom plate (Corning) at 5.0e3 cells/well. Target cells were incubated for 24 hours to allow for adherence. For unlabeled cell lines caspase 3/7- GFP nuclear dye (Sartorius, cat#4440) was used per manufacturer protocol to label cell apoptosis. Effector cells were added into target cell containing wells at different E:T ratios (1:1, 1:5 or 1:20). Plates were put into an Incucyte Sx5 live-cell analysis instrument (Sartorius), images were captured every 2 hours on RFP or GFP and bright field for 48 hours. Red object count or green object count was analyzed to represent target cell count in the well for RFP tagged or Caspase 3/7-GFP labeled target cells respectively.

Immunohistochemistry

Staining was done on 4-µm thick formalin fixed paraffin embedded (FFPE) sections of primary canine osteosarcoma biopsies. The staining of FFPE canine OS slides for B7-H3 expression was done as previously described by Zhang et al [198]. Staining was done by the Human Immune Monitoring Shared Resource (HIMSR) (University of Colorado Anschutz Medical Campus, Aurora, Colorado). To semi-quantify expression levels of B7-H3, images will undergo image processing and analysis with ImageJ[202]. Images of tissues will be scored based on percentage of cells stained 0-100%. Staining intensity of cell membrane will be scored from 0-3 with a score of 0= no staining, +1= light staining, +2= intermediate staining and +3= intense staining, threshold for staining intensity will be standardized in ImageJ for all images. An expression score will be given to tissues from 0-300 calculated by (percent positive x staining intensity). This semi-quantitative data will be used to assign tissue images a score of either high>200, intermediate 200-100 or low <100 B7-H3 expression[203].

Statistical analysis

For the comparison of mean values between three or more groups normality was tested with a Shapiro-Wilk test, normally distributed data was compared with ordinary one-way ANOVA, non-normally distributed data was compared with a Kruskal-Wallis test followed by multiple comparison Dunn's test. For comparisons with two means an unpaired two tailed T test was performed. All statistical tests were performed in Graph Pad Prism 8 software.

Results

Canine CAR T cell optimization

We used a second-generation B7-H3 CAR construct and a retroviral system to generate canine B7-H3 CAR T cells **(Figure 1A)**. PBLs were isolated from whole blood from tumor bearing (n=3) and healthy

(n=3) dogs and activated to generate B7-H3 CAR T cells. Activation of PBLs was done by either anti-canine CD3/CD28 conjugated beads, PHA[204]or aAPC [199]. All conditions were in grown in cTCM media with human recombinant IL-21 on the first day. Either recombinant human IL-2 (rhIL-2) (Peprotech) or canine recombinant IL-2 (rcaIL-2) (R&D) was added into the culture media. Half the total volume of media with fresh cytokines were changed every 2-3 days. Activated canine T cells were virally transduced with one round of thawed frozen B7-H3 retroviral supernatant bound to retronectin coated plates. CAR T cells were evaluated for T cell phenotype and transduction efficiency at day 10 post activation by flow cytometry. We found that the majority of the cells was CD5+ and that CD5+ cells had a mixture of CD4+ and CD8+ cells **(Figure 1B)**. Activation method and use of either rhIL-2 or rcaIL-2 did not affect ratio of CD4+ and CD8+ T cells significantly.

We found that canine CAR T cells expanded with rhIL-2 had the best transduction efficiency with a median transduction efficiency of 16.3% across all activation conditions compared to 5.07% median transduction efficiency for rcaIL-2 cultured CAR T cells. Activation with both CD3/CD28 conjugated beads and aAPCs gave good transduction efficiency when cultured with rhIL-2 with median transduction rates of 37.2% and 16.3% respectively. T cells activated with CD3/CD28 conjugated beads had less variance between biological samples in total CAR T cells with a standard deviation of 1.48e6 compared to 4.31e6 for aAPC rhIL2 activated CAR T cells. While rcaIL-2 produced robust T cell expansion with a mean 8-fold increase in total T cells, all CAR T cell conditions grown with rcaIL-2 generated a low proportion of CAR T cells within expanded T cell cultures therefore producing a low total of CAR T cells by the end of the culture with a median of 3.08e5 CAR T cells by day 10 **(Figure 1C and D)**.

To preserve the functional capacity of canine B7-H3 CAR T cells, we also evaluated the impact of added cytokines recombinant human IL-7 and IL-15. IL-7 promotes T cell survival and inhibits apoptotic markers[205]. IL-15 induces activation, survival and proliferation of high avidity CD8+ memory T cells[206]. These additional cytokines were chosen to increase the functional phenotype of canine B7-H3 CAR T cells

during activation and expansion. Addition of IL-7 and IL-15 to CAR T cell cultures from day 1 of culture increased the killing capacity of canine B7-H3 CAR T cells compared to cultures expanded in only IL-2 and IL-21. This functional difference was assessed by *in vitro* killing of B7-H3+ canine OS target cell line. We found that B7-H3 CAR T cells cultured with additional IL-7 and IL-15 had increased rates of lysis compared to donor matched CAR T cells at the same E:T ratio that were cultured in only IL-2 and IL-21 although it was not statistically significant P-value = 0.0547 **(Figure 1E).** CAR T cells used in this assay were previously frozen and thawed demonstrating functional ability to kill B7-H3+ target cells after a freeze thaw cycle **(Supplemental** F**igure 1)**. These studies thus demonstrated that canine B7-H3 CAR T cells specifically recognized B7-H3 expressed by canine OS tumors and became activated to secrete cytokines and initiate cytolytic pathways.

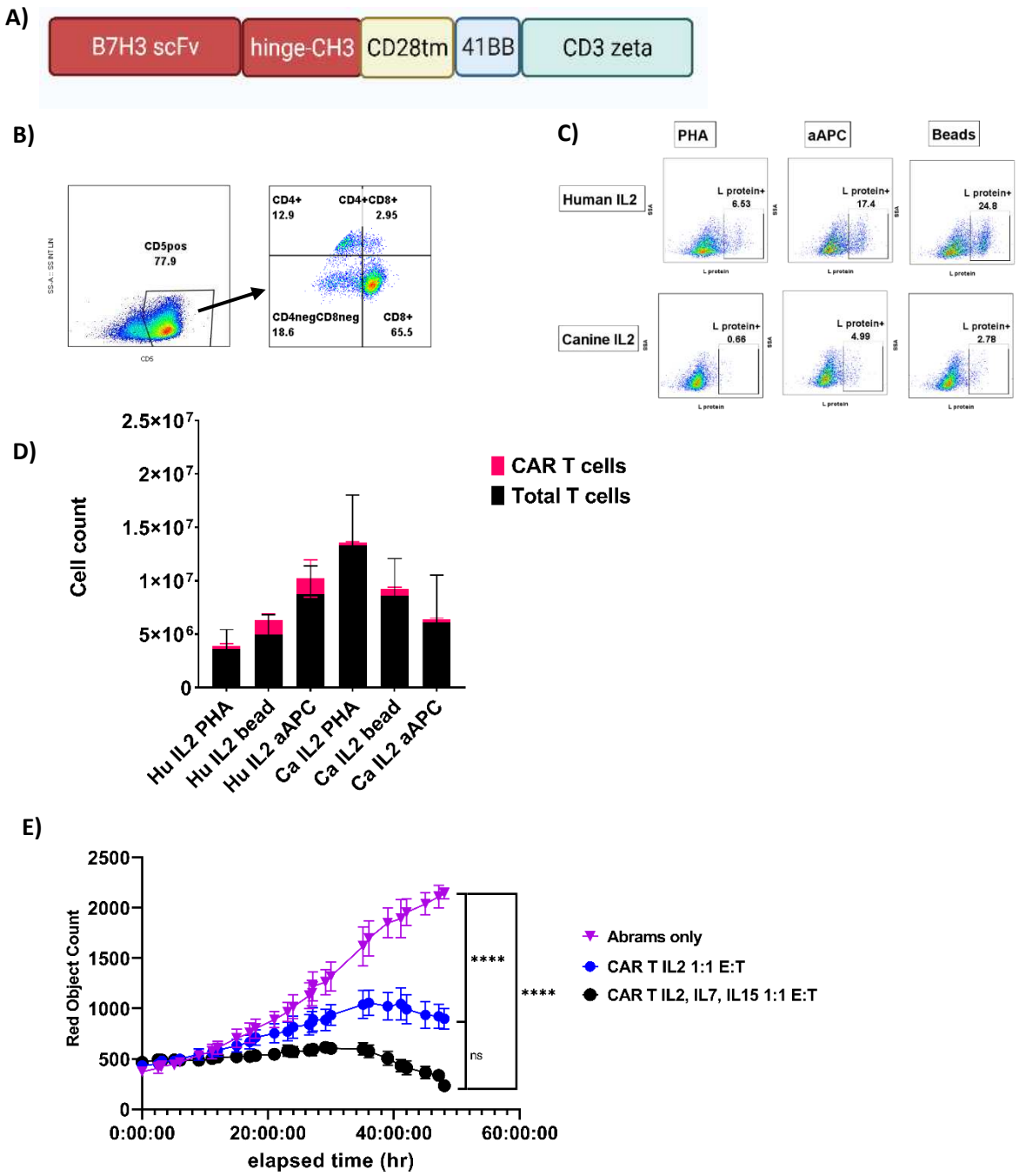

Figure 1. optimization of generation of canine B7H3 CAR T cells **A)** B7H3 CAR construct **B)** T cell phenotype of bead rhIL-2 activated canine CAR T cells at day 10 evaluated by flow cytometry for canine CD5, CD4, and CD8 expression **C)** Transduction efficiency of normal canine T cells activated by either PHA, beads or aAPCs in either rhIL-2 or rcaIL-2 **D)** canine cell expansion and B7H3 CAR T cell generation from 3 healthy dogs and 3 tumor bearing dogs. Graph shows mean ± SEM. **E)** *in vitro* killing of B7H3+ canine OS cell line Abrams by canine B7H3 CAR T cells generated with IL-21&IL-2 or IL-21, IL-2, IL-7 and IL-15. Graph shows mean ± SEM. Samples were measured in triplicate. Statistical analysis was performed using the multiple comparison Dunn's Test; *****, *P* <0.0001, ns, not significant.

B7-H3 is widely overexpressed on primary canine OS

B7-H3 surface expression on canine OS has been previously established on one canine OS cell line and 6 primary canine FFPE OS samples[191]. We expanded on those initial investigations with a screen of eight additional OS FFPE tissue biopsies and healthy dog lymph node FFPE tissues. FFPE tissues were stained using primary B7-H3 monoclonal antibody (clone RBT-B7H3) and Opal staining. In addition, we also evaluated expression by zinc fixed frozen liver, and spleen from a healthy dog (n = 1) with B7-H3 polyclonal antibody (Invitrogen cat# MA5-15693) (supplementary figure 2). Scanned images of the stained slides were analyzed using ImageJ to quantify mean florescence intensity of B7-H3 signal and percent positive expression. This analysis revealed that all eight tumor samples exhibited positive B7-H3 expression above that of normal lymph node. Two OS samples had moderate staining and three OS samples had strong staining, the remaining three OS samples had light staining **(Figure 2a)**. Semi-quantification by ImageJ to obtain H score revealed that two OS samples had intermediate expression with H score 100-200 and the remaining six OS samples had low expression with H score <100 **(Figure 2b).** In addition, we observed no to minimal B7-H3 expression by the three normal tissues evaluated (supplemental figure 2). Therefore, we concluded that B7-H3 was a safe target for CAR T cell therapy in dogs and that canine OS would likely be recognized *in vitro* by canine B7-H3 CAR T cells.

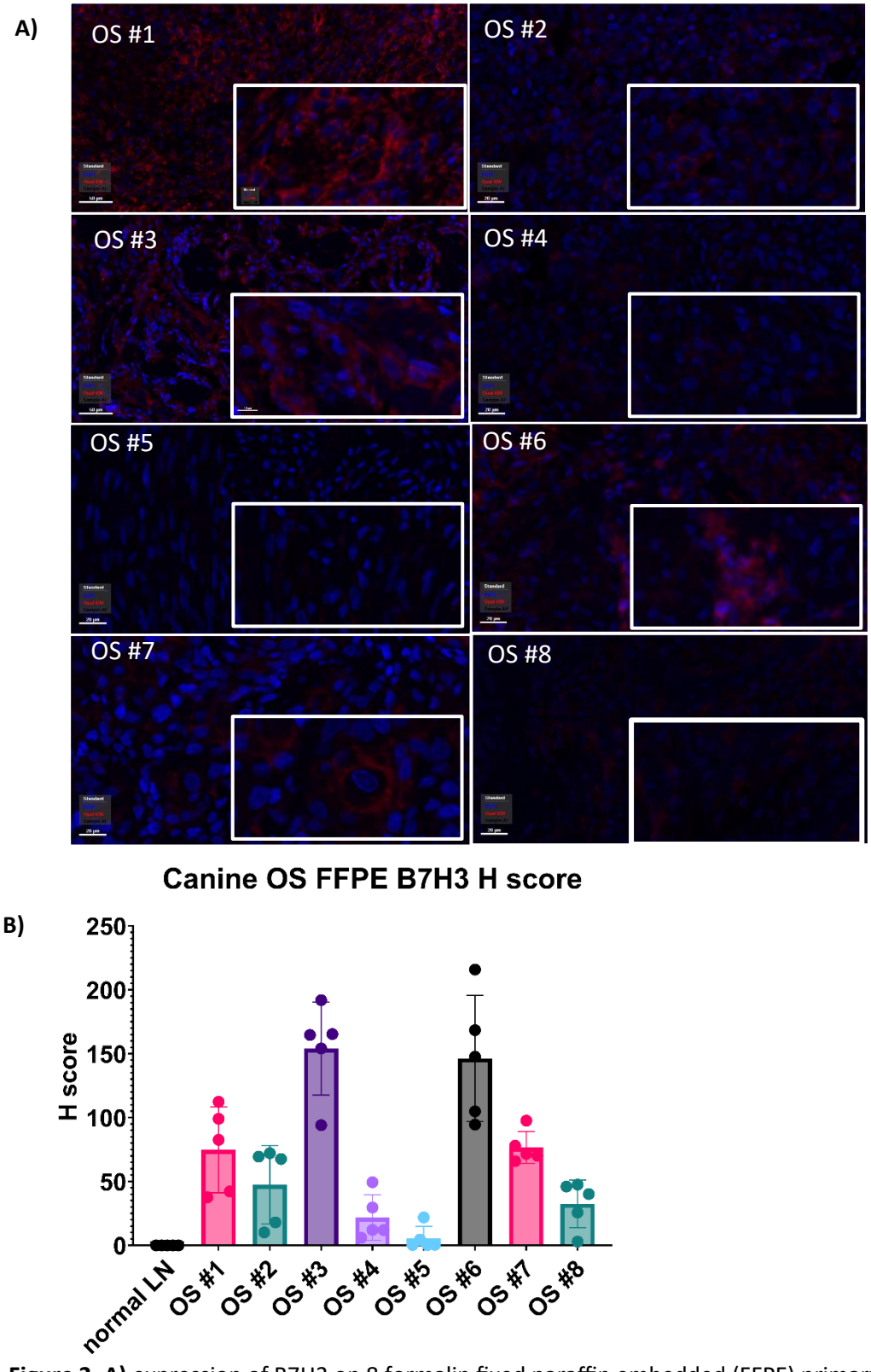

Figure 2. A) expression of B7H3 on 8 formalin fixed paraffin embedded (FFPE) primary canine osteosarcoma tissues **B)** H-score of B7-H3 expression on canine OS FFPE tissues as calculated by Imagej quantification

B7-H3 is expressed on canine OS cell lines with variable levels of expression

For use in *in vitro* assays, we screened 7 canine OS cell lines for surface expression of B7-H3 by flow cytometry. Cross reactivity of mouse anti-human B7-H3 antibody (clone 7-517) with canine B7-H3 was verified by western blot on canine Abrams OS cell line and human rhabdomyosarcoma cell line RH30 as a positive control (supplementary figure 3)**.** We found that all 7 cell lines were B7-H3 positive by antibody staining with mouse anti-human B7-H3 antibody (clone 7-517) **(Figure 3A).** Calculating the median fluorescence intensity (MFI) as a measure of level of expression we found that 5 out of 7 canine OS cell lines had high expression of B7-H3 **(Figure 3B),** with two canine OS cell lines D17 and Moresco were B7-H3 low. Evaluation of healthy dog PBMC by flow cytometry showed B7-H3 positive expression on CD11b+ monocytes and partial positive expression on CD5+ T cells (supplementary figure 4)**.**

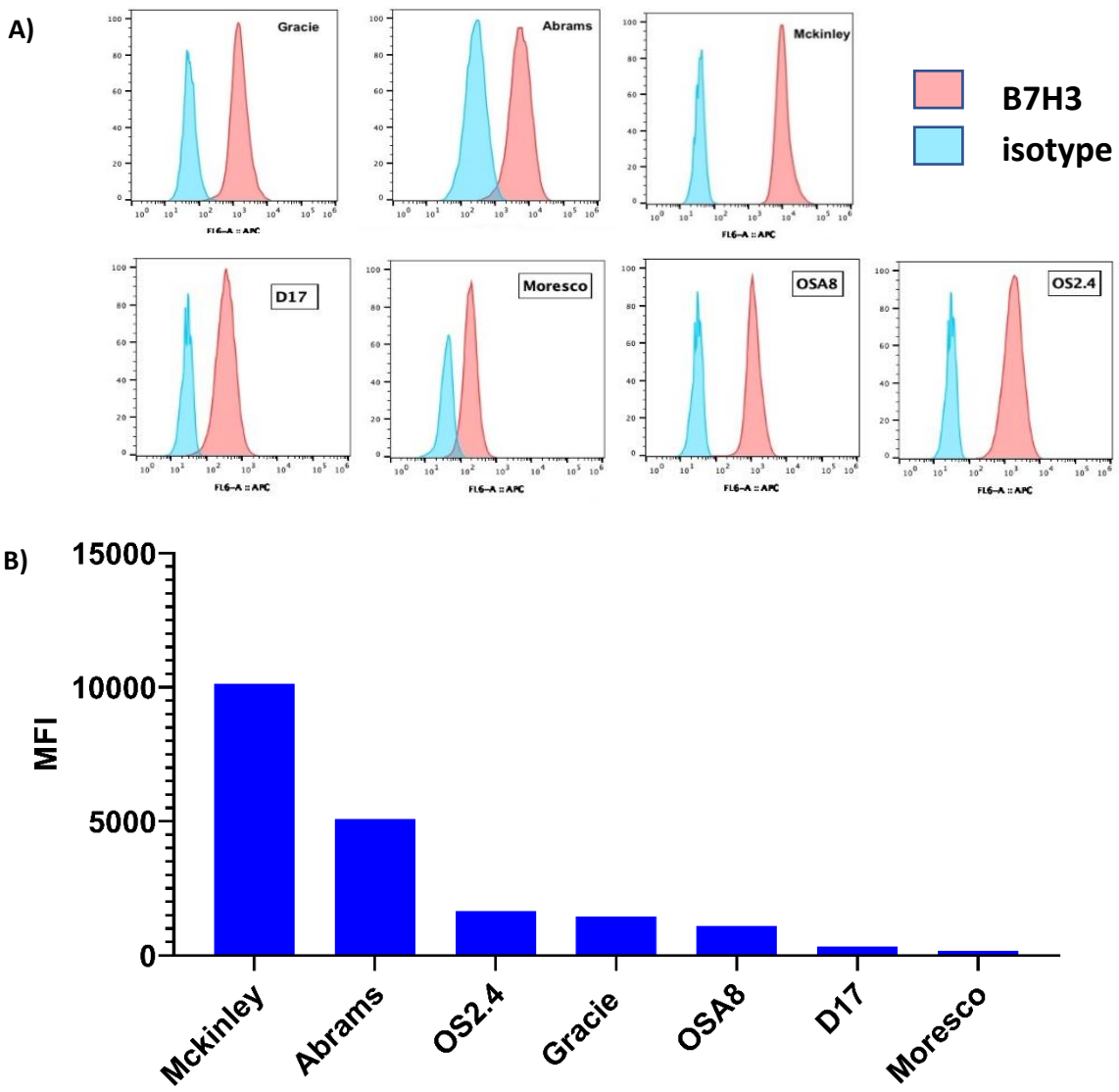

Figure 3. A) Expression of B7H3 compared to isotype control staining on canine osteosarcoma cell lines by flow cytometry **B)** mean florescence intensity of B7H3 staining on canine OS cell lines by flowcytometry

B7-H3 CAR T cells have antigen specific activity against canine OS cell lines

We evaluated the antigen specific activity of anti-human-B7-H3 CAR construct against canine B7-H3 antigen. We co-cultured canine B7-H3+ OS cell lines with canine B7-H3 CAR T cells at a 1:1 ratio and measured secreted IFNγ after 24 hours of incubation at 37˚C. We found that co-culture with B7-H3^{high} canine OS cell lines such as Abrams and McKinley produced greater secretion of IFNγ by B7-H3 CAR T cells compared to co-culture with B7-H3^{low} cell lines Moresco and D17. We also did not see activation of donor matched activated NTD T cells indicating that activation is specifically through B7-H3 CAR signaling **(Figure 4A**). To measure direct cell killing by B7-H3 CAR T cells we co-cultured canine B7-H3 CAR T cells or donor matched NTD T cells with B7-H3^{high} canine OS cell line Abrams that stably expressed RFP at a ratio of 20:1 E:T. RFP+ tumor cell growth was measured by incucyte every 2 hours for 48 hours. We found that canine B7-H3 CAR T cells lysed Abrams-RFP cells over a course of 48 hours while NTD T cells did not significantly impact Abrams-RFP growth **(Figure 4B).** To further validate B7-H3 antigen specific killing we utilized B7-H3^{low} D17 and B7-H3^{high} OSA8.0 cell lines that were tagged with apoptotic marker nuclear dye Caspase3/7-GFP and co-cultured with canine B7-H3 CAR T cells at an E:T ratio of 5:1. Caspase3/7-GFP was measured every 2 hours over a 68-hour period by incucyte. We found significant caspase3/7-GFP signal in co-cultures with B7-H3^{high} OSA8.0 target cells and not the low B7-H3 expressing D17 target cells **(Figure 4c**). B7-H3 CAR T cells demonstrated dose-dependent killing of Abrams-RFP canine OS lines with increased rate of target cell killing with increased E: T ratio **(Figure 4d)**. This indicates that generated canine B7-H3 CAR T cells had specific activity to canine B7-H3 antigen and were functionally capable of killing canine OS target cells *in vitro*.

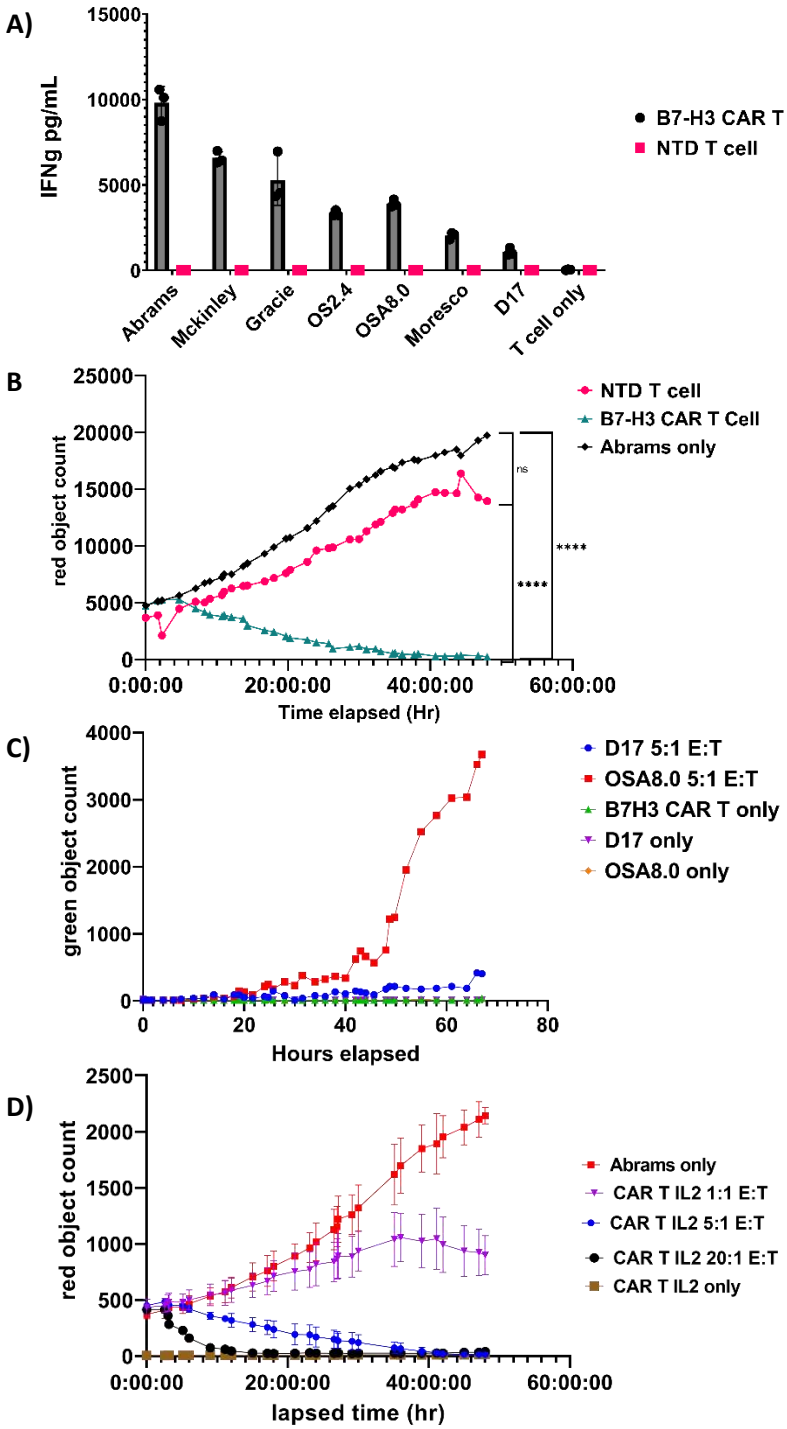

Figure 4. A) IFNγ secreted by canine B7-H3 CAR T cells or donor matched activated non-transduced (NTD) T cells co-cultured with canine OS cell lines. **B)** *in vitro* killing of Abrams-RFP OS cell line by B7-H3 CAR T cells or donor matched NTD T cells at 20:1 E:T ratio Statistical analysis was performed using the multiple group comparison Dunn's test;**** P<0.0001, ns, not significant **C)** Killing of B7-H3^{high} expressing canine OS cell line OSA8.0 and B7-H3^{low} D17 by canine B7-H3 CAR T cell as evaluated by expression of apoptotic marker caspase3/7-GFP **D)** *in vitro* killing of Abrams-RFP cell line by B7-H3 CAR T cells at various (E:T) ratios 1:1, 5:1, and 20:1. Graph shows mean ± SD. Samples were measured in triplicate.

Discussion

In this study, we optimized canine CAR generation by evaluating alternative methods of T cell activation, and additional cytokines during cell culture and expansion of canine CAR T cells. We investigated the impact of rhuIL-2 versus rcaIL-2 for CAR T cell generation. These studies revealed that that rhuIL-2 provided better CAR T cell expansion than rcaIL-2 (Figure 1C). In previous studies various stimulation methods have been published using PHA, conjugated canine antiCD3/CD28 beads, and artificial antigen presenting cells. In our study we found that conjugated canine antiCD3/CD28 beads provided the best CAR T cells generation with the least variability between biological samples (Figure 1D) supporting previously published canine CAR T cell generation protocol[194]. To optimize the functional phenotype of CAR T cells after *ex vivo* activation and expansion we investigated the addition of rhuIL-7 and rhuIL-15. We found increased functional capacity of canine CAR T cells generated with rhuIL-7 and rhuIL-15 in addition to established cytokines rhuIL-2, and rhuIL-21 (Figure 1E). We achieved consistent generation of canine B7-H3 CAR T cells with high transduction efficiency and expansion with T cells isolated from whole blood of tumor bearing dogs (n=3) that may have immune dysregulation. Therefore, use of our method of canine CAR T generation is suitable for clinical trials for client owned dogs with OS.

Zhang et al 2022 established B7-H3 as a viable cancer antigen target for canine OS showing B7-H3+ expression in six canine OS tumors and one canine OS cell line by flow cytometry and B7-H3+ expression in 6 out of 8 FFPE OS samples[198]. We expanded on the work of Zhang et al by evaluating an additional 8 primary FFPE canine OS tissue samples (Figure 2A and B) and 6 additional canine OS cell lines (Figure 3A and B) showing B7-H3 overexpression by IHC and by flow cytometry respectively. We showed that canine OS was positive for B7-H3 at various levels of expression (Figure 2b and 3b). To ensure safety in targeting B7-H3 in canines we evaluated B7-H3 expression on normal canine tissues from spleen, liver, and lymph node by IHC (Supplementary Fig.3) as well as normal canine PBMCs by flow cytometry (Supplementary Fig. 4) and found no to low expression of B7-H3 on normal tissues. Additionally, we

screened 3 canine glioma cell lines and three FFPE canine glioma samples showing positive B7-H3 overexpression (Supplemental Fig.5). This shows the potential broader utility of B7-H3 as a therapeutic target in canine tumors OS and glioma.

We showed affinity gated activation of canine B7-H3 CAR T cells through secretion of IFNγ correlating with level of B7-H3 expression by canine OS cell lines (Figure 4A). Additionally, canine B7-H3 CAR T cells induced direct cell killing in co-cultures with B7-H3^{high} cell lines OSA8.0, but not to B7-H3^{low} OS cell lines D17 as measured by apoptotic marker caspase 3/7-GFP (Figure 4C). We determined that killing activity of canine B7-H3 CAR T cells was mediated through CAR signaling with donor matched activated NTD T cells having no killing activity at a high E:T ratio of 20:1 (Figure 4B). We found that our B7-H3 CAR T cells killed high expressing B7-H3 positive canine OS cell lines in a dose dependent manner *in vitro* (Figure 4d). This shows that the already established anti-human B7-H3 CAR construct can be readily adapted to targeting canine B7-H3 positive tumors without the need of developing a canine specific B7-H3 CAR.

With this study we laid the foundation for applying B7-H3 CAR T cell therapy to canine solid tumor malignancies, specifically for canine OS. Optimization of culture conditions is an essential step in making CAR T cell studies practical for clinical evaluation in the canine cancer model. We also validated cross reactivity of the human B7-H3 CAR construct to canine B7-H3 antigen. High prevalence and differential expression of B7-H3 on canine malignancies indicates the promising wide applicability of B7-H3 CAR T cell therapy in spontaneous canine OS and glioma. Treatment of dogs with spontaneous OS can serve as a translational model for evaluating new methods to improve B7-H3 CAR T cells in a solid tumor setting for pediatric OS.

Chapter 3: AIM 2- Investigate efficacy of dual targeting B7-H3-CXCR2 CAR T cells compared to single valent B7-H3 CAR T cells against canine OS

Summary

One proposed strategy to improve CAR T cell therapy in a solid tumor setting is by increasing CAR T cell trafficking by addition of a chemokine receptor[207]. CXCL8 has been known to be co-opted by various tumor types to recruit immune suppressor cells such as N2 TANs and MDSCs which facilitate tumor immune evasion [160]. Other groups have targeted tumor secretion of CXCL8 by adding exogenous CXCL8 receptor CXCR1 or CXCR2 to CAR T cells[165]. CAR T cells expressing exogenous chemokine receptor CXCR1/2 and have shown increased trafficking and anti-tumoral effects[159,165,208]. We investigated the role of CXCL8 in canine OS and how addition of exogenous CXCR2 improved our B7-H3 CAR T cell *in vitro* and *in vivo*. We hypothesized that addition of CXCR2 to B7-H3 CAR T cells would increase migration to CXCL8 secreting tumor cell and increase *in vivo* anti-tumoral function.

We found that canine OS cell lines secrete high levels of CXCL8. We were able to generate dual valent canine B7-H3-CXCR2 CAR T cells that stably express both receptors as evaluated by flow cytometry. We showed that the human CXCR2 cross reacts with canine recombinant CXCL8 inducing migration *in vitro*. B7-H3-CXCR2 CAR T cells were activated by B7-H3 positive canine OS cell line Abrams and secreted greater levels of IL-2 and IFNγ than single B7-H3 CAR T cells. *In vitro* killing activity of canine OS tumor cells was equal between B7-H3-CXCR2 and B7-H3 CAR T cells with adherent Abrams-RFP target cells. When assessing *in vivo* function of B7-H3-CXCR2 CAR T cells against B7-H3 CAR T cells in a xenograft mouse model of canine OS we found significant increase in tumor control and persistence in peripheral blood by B7-H3-CXCR2 CAR T cells. These results indicate that the addition of chemokine CXCR2 increased antitumoral activity of B7-H3 CAR T cells. Further investigation needs to be done to determine if the increased anti-tumoral activity is mediated by increased trafficking *in vivo.*

Introduction

Development of CAR T cell therapy for solid tumors including OS have largely not been clinically success despite achieving great anti-tumoral activity in preclinical mouse models[128]. HER2 CAR T cells as an example was able to achieve complete tumor elimination in a mouse xenograft model of osteosarcoma[143]. Use of HER2 CAR T cells in phase1/2 clinical trials with patients with refractory OS however only produced SD in 4 out of 16 patients[126]. Failure of CAR T cell trafficking is a major proposed mechanism for ineffectual CAR T cell treatment in solid tumors[128]. Chemokines are secreted cytokine-like molecules that bind to chemokine receptors to mediate T cell homing[209]. Genetic modification and *ex vivo* expansion of CAR T cells has been shown to downmodulate chemokine receptors impairing native T cell homing mechanisms[64,210]. Therefore, addition of exogenous chemokine receptor CXCR2 has been used to enhance CAR T cell migration[159,165,208].

Addition of CXCR2 in GPC3 CAR T cells increased homing and produced greater *in vivo* anti-tumoral effects in a mouse xenograft model of hepatocellular carcinoma (HCC)[159]. Addition of CXCR2 in CD70 CAR T cells also increased CAR T cell migration and persistence within tumors in a xenograft mouse model of glioblastoma, ovarian and pancreatic cancer[165]. CXCR2 was selectively chosen due to its binding of CXCL8. Chemokine CXCL8 is of particular interest as it has been well characterized to have strong pro-tumor effects through the recruitment of MDSCs[163], promotion of angiogenesis[211] and positive correlation with metastatic potential[160]. Our collaborators the Verneris lab (University of Colorado, Aurora, CO) found that secretion of CXCL8 by human OS and rhabdomyosarcoma (RMS) was inducible by radiation and that addition of CXCR2 to B7-H3 CAR T cells enhanced IL-2 secretion in *in vitro* cytotoxicity assays and induced greater tumor control in a mouse orthotopic xenograft model of high CXCL8 secreting RMS[208].

Having previously shown cross-reactivity of human B7-H3 CAR construct to canine B7-H3 we hypothesize that addition of CXCR2 in canine B7-H3 CAR T cells will enhance CAR activity *in vitro* and increase homing and anti-tumoral activity in a mouse xenograft model of canine OS. Preemptively

enhancing B7-H3 CAR T cell homing through addition of CXCR2 will overcome a known barrier to efficacious CAR T cell therapy in OS[128]. Establishment of efficacy of B7-H3-CXCR2 CAR T cells in a canine OS model will pave the way for clinical trials to evaluate the safety and efficacy of B7-H3-CXCR2 CAR T cells in client owned dogs with metastatic OS.

Methods

Animals

Peripheral blood mononuclear cells (PBMCs) from EDTA anticoagulated blood samples from tumor bearing dogs from the Flint Animal Cancer Center (FACC, Fort Collins, CO) were obtained following full CSU IACUC approval. NOD-SCID-gamma (NSG) mice from Jackson laboratories were used for all mouse experiments, and these studies were covered under CSU IACUC.

Cell lines

Canine osteosarcoma cell lines were provided by the FACC cell line repository and previously validated[201]. All cell lines were cultured in cell culture media containing DMEM with 10% fetal bovine serum (Corning), 2 mM L-glutamine (Gibco), 100 U/ml penicillin and 100 ug/ml streptomycin (Gibco). All cell cultures were kept at 37C and 10% CO_2.

CAR constructs

The B7-H3 CAR was shared with the University of Colorado Verneris lab by Michael Jensen, MD (Fred Hutchinson Cancer Center, Seattle, WA). This lentiviral construct contained a B7-H3 single-chain variable fragment (scFv), an IgG4 and CD28 transmembrane domain, a 4-1BB costimulatory molecule and the CD3ζ domain. The Verneris lab cloned the CAR portion of the construct into a retroviral backbone

containing a 5' LTR promoter using standard PCR-based cloning methods to create the B7-H3 CAR construct. The retroviral backbone we used was a gift from Anandani Nellan (National Cancer Institute, Bethesda, MD). The B7-H3-CXCR2 CAR construct was created first by extracting native CXCR2 RNA from human neutrophils, conversion to cDNA by reverse transcriptase (Bio-rad iScript cDNA Synthesis kit), and amplification of the CXCR2 sequence. The CXCR2 DNA fragment was inserted into the B7-H3 CAR construct using PCR methods.

Retrovirus production

B7-H3 CAR retrovirus was produced and provided to us by Jessica Lake, MD (University of Colorado Verneris lab, Aurora, CO). 293GP cells (a gift from Dr. Terry Fry, University of Colorado, Aurora, CO) were plated in T175 flasks in Dulbecco's Modified Eagle Medium (DMEM) with 10% fetal bovine serum (FBS) and 1% anti-biotic/anti-mycotic (Gibco). Transfection occurred when cells were 90-95% confluent. Tube A contained 3.4 ml of room temperature Opti-MEM (without additives), 20.25 µg of B7-H3 or B7-H3-CXCR2 vector DNA, and 10.125 µg of RD114 (envelope plasmid, gift from Anandani Nellan). Tube B contained 3.4 ml of room temperature Opti-MEM (without additives) and 100 µl of lipofectamine 2000 (Invitrogen). The tubes were left at room temperature for 10 minutes after which Tube A was added dropwise to Tube B and gently mixed. The combined mixture was left at room temperature for 30 minutes. During that time, the media was removed from the 293GP cells and 16 ml of fresh, warmed DMEM with 10% FBS (no anti-anti) was carefully added. After 30 minutes, the retroviral mixture was added to the flask, being careful not to agitate the cells. Flasks were placed at 37 degrees Celsius for 24 hours. After 24 hours, media/viral mixture was removed from flasks and 24 ml of fresh DMEM with 10% FBS and 1% anti-anti was gently added. The flasks were returned to 37 degrees Celsius. Viral collections were made at 24 and 48 hours after media replacement. The retrovirus was flash frozen in dry ice and placed in -80 degrees Celsius until

use. Frozen retrovirus stocks were shared with us for the purpose of generating canine B7-H3 CAR T cells and transported on dry ice from University of Colorado, Aurora, CO to Colorado State University, Fort Collins, CO.

Generation of anti-canine CD3/CD28 magnetic beads

Mouse anti-canine CD3 (clone CA17.2A12, Biorad) and mouse anti-canine CD28 (clone 58B, Invitrogen) antibodies were conjugated to magnetic tosyl-activated Dynabeads (Life Technologies) as previously established at a 1:1 antibody ratio[194,199].

Canine PBMC isolation and T cell activation

Canine whole blood from tumor bearing patients was provided by the Flint Animal Cancer Center (Fort Collins, CO). Peripheral blood mononuclear cells (PBMCs) were isolated using Ficoll and gravity centrifugation. Canine PBMCs were plated at a density of 2.0e6/mL in 6 well tissue culture plates to adhere monocytes for 90 minutes at 37 degrees Celsius. Peripheral blood lymphocytes (PBLs) were gently washed off with canine T cell media (cTCM), DMEM with 10% FBS and 100 U/ml penicillin and 100 ug/ml streptomycin (Gibco), 2 mM L glutamine, 1x essential amino acids (Gibco, cat#11130051), 1x non-essential amino acid (Gibco, cat#11140050), 0.075% Bicarbonate solution, 10 mM HEPES, and 55 uM 2-mercaptoethanol. PBLs were plated at a concentration of 1.0e6/mL with 30 ng/mL rhIL-21(Peprotech), 100 IU rhIL-2 (Peprotech), 5 ng/mL rhIL-7 (Peprotech) and rhIL-15 (Peprotech). T cells were activated with tosyl-activated dynabeads (Life Technologies) conjugated with canine anti-CD3/CD28 antibodies at a ratio of 3:1 beads to PBLs. T cells were incubated at 37˚C for 3 days before transduction with CAR retrovirus.

CAR T cell Transduction

Non-tissue culture treated plates are coated with 24 µg/mL retronectin (Tankara) according to manufacture protocol. Frozen B7-H3 or B7-H3-CXCR2 retroviral supernatants were thawed in a 37˚C water bath and aliquoted into retronectin coated 6 well plates 2 ml/well and centrifuged at 32˚C for 2.5 hours at 2,000 G. PBLs are plated onto retroviral bound plates at a concentration of 5.0e5/mL and 2 mL per well and incubated overnight at 37˚C . T cells were transduced twice before being rescued from virus and expanded in fresh cTCM and cytokines. Half of the media was changed, and fresh cytokines are added every other day. Generated canine CAR T cells were used for analysis by day 10-14 of culture.

Flow cytometry

Canine surface expression of B7-H3 was analyzed using anti-B7-H3-APC antibody (clone 7-517, eBioscience) or isotype control mouse IgG2a (ThermoFisher, cat# 02-6200). Canine immune expression was analyzed with the following antibodies: anti-canine CD5-FITC (cloneYKIX322.3, Biorad), anti-canine CD8-alexa Fluor 647 (clone YCATE55.9, Biorad), anti-canine CD4-Pacific Blue (clone YKIX302.9, Biorad), anti-CD62L (clone FMC46, Biorad), anti-CD45RA (clone CA21,4B3, Leukocyte Antigen Biology Laboratory). Recombinant protein L-biotinylated (cat# 29997) secondary Streptavidin-PE (cat#12-4317-87, eBioscience) was used to detect B7-H3 CAR transduced cells. Anti-CXCR2-PEcy7 (clone 5E8, Biolegend) was used to detect human CXCR2 on transduced canine T cells. After staining all samples were analyzed on a Beckman Coulter Gallios flow cytometer. Flow data was analyzed by Flowjo v10.

Chemokine measurement

Canine OS cell lines were plated 5.0e4 cells per well in a 24 well plate in 2 mL /well. Media was changed 24 hours after the tumor cells had fully adhered to the plastic. Supernatant was collected 4 days

later, supernatant was used in technical triplicates in a canine CXCL8 ELISA (R&D, cat#DY1608). ELISA kits were used following manufacturer's protocol. Absorbance was read at 450 nm by a microplate reader. Canine B7-H3-CXCR2 CAR T cell secretion of canine CXCL8 was measured by canine CXCL8 ELISA (R&D, cat#DY1608). B7-H3-CXCR2 CAR T cells were plated at 2.5e4 cells per well in triplicate in a 96 well flat bottom plate. Supernatants were collected after 48 hours of incubation at 37˚C. cTCM was used as a negative control. ELISA kits were used following manufacturer's protocol. Absorbance was read at 450 nm by a microplate reader.

Transwell assay

To verify the cross reactivity of human CXCR2 with canine CXCL8 we performed a transwell migration assay. The lower chamber was loaded with 25 ng/ml recombinant canine CXCL8 (R&D, cat#1608-CL) in serum free DMEM, negative control serum free DMEM media or positive control DMEM media with 10% FBS. Canine B7-H3-CXCR2 CAR T cells were washed twice with serum free media to remove any serum or residual cytokines from the T cell culture media and plated at 2.5e6/ml in serum free DMEM media. 2.5e5 B7-H3-CXCR2 CAR T cells were added to the 8 um transwell insert (Corning, cat#353097). Plates were incubated at 37˚C for 4 hours. After incubation cells in the bottom well were collected and counted by trypan blue staining and hemocytometer.

CAR T cell activation assay

To measure activation of B7-H3 CAR T cells by canine B7-H3 antigen we co-cultured canine B7-H3 CAR T cells with canine osteosarcoma cell lines. Donor matched un-transduced T cells were also co-cultured with canine osteosarcoma cell lines as a control for endogenous T cell reactions. Canine

osteosarcoma cell lines were plated at 5.0e3 cells/ well in T cell media in a 96 well flat bottom plate and incubate for 24 hours at 37˚C. T cells were washed 3x with 10 mL T cell media to ensure no recombinant IL-2 contaminates the co-culture. T cells plated 5:1 effector to target (E:T) ratio with canine OS cell lines to a final volume of 250 µl/ well. Co-cultures were incubated 24 hours then 100 ul/well of supernatant was collected for IL-2 and IFNγ ELISA (R&D systems, cat# DY202-05, DY285B-05, respectively). Absorbance was read by plate reader at 450 nm.

Incucyte killing assay

Red fluorescence protein (RFP) labeled canine OS target cells were seeded in a 96-well flat bottom plate (Corning) at 5.0e3 cells/well. Target cells were incubated for 24 hours to allow for adherence. Effector cells were added into target cell containing wells at different E:T ratios (1:1, 1:5 or 1:20). Plates were put into an Incucyte Sx5 live-cell analysis instrument (Sartorius), images were captured every 2 hours on RFP and bright field for 48 hours. Red object count was analyzed to represent target cell count in the well of RFP expressing OS cell lines.

Bulk RNA-seq and analysis of canine B7-H3-CXCR2 CAR T cells

mRNA sequencing was performed on canine CAR T cells as previously described [172]. Briefly, generated canine CAR T cells or donor matched activated T cells were harvested at D10 after activation. RNA was extracted with a RNeasy mini kit (Qiagen, Hilden Germany) as to manufacturer protocol. RNA extracted was quantified by nanodrop before being frozen at -80 degrees Celsius. RNA was sent to Novogene Co. (Novogene Co., Sacramento CA) for sequencing using an Illumina platform. Samples were tested for quality control by Agilent 2100 Bioanalyzer system and by agarose gel electrophoresis. Libraries were sequenced on an Illumina PE150 (HiSeq) platform for 4.0e7 raw reads per sample. Raw reads were filtered by removing reads containing adapter and reads containing *N*>10% and for Phred scores >30. The filtered reads were analyzed using Partek Flow software version 7.0. Filtered reads were aligned with STAR

2.73a CanFam3.1 genome assembly. Aligned reads were annotated and counted using HTseq (RRID:SCR_011867). Downstream analysis of raw count data was done in R (v3.6.1) and normalized using RUVseq package RUVr function[212,213]. Normalized genes were used to find differentially expressed genes were identified using Deseq2 R package[214] requiring a P value cutoff of 0.05 and a minimum log_2 fold change of 1.5. Heatmaps were generated in R using "ComplexHeatmap" package[213]. Volcano plots were generated in R using "EnhancedVolcano" package[215].

Gene Set Enrichment Analysis (GSEA) was performed according to the user guide to determine biological pathways differentially enriched between B7-H3-CXCR2 CAR T cells and B7-H3 CAR T cells[216,217]. GSEA analysis was performed using publicly available gene sets housed in the Molecular Signatures Database (MsigDB)[218,219] using "h.all.v2023.1.Hs.symbosl.gmt", "c5.go.bp.v2023.1.Hs.symbols.gmt, "c5.go.mf.v2023.1.Hs.symbols.gmt" and "c7.all.v2023.1.Hs.symbols.gmt" as reference gene sets. Statistically significant pathways were set at P-value <0.05 and false discovery rates q <0.05.

In vivo mouse experiment

NOD-SCID-gamma (NSG) mice were injected with 1.5e5 canine OS cells (Abrams-luciferase) in 30% Matrigel subcutaneously (SC) into the right flank. Tumor implantation was confirmed through IVIS imaging before treatment. Canine CAR T cells either B7-H3 CAR (n=6) or B7-H3-CXCR2 CAR (n=7) were administered to the mice by intravenous (IV) tail vein injection on day 3 after tumor implantation at 5.0e6 CAR T cells/mouse. Engrafted tumors were monitored with serial IVIS imaging and measurement with calipers when tumors had grown large enough to palpate. Control groups were given no treatment (n=5). A selection (n=3/group) of mice were bled at day 14 post treatment to detect circulating canine T cells. Mice were humanely euthanized when tumors ulcerated through the skin or grew greater than 1.0 cm in diameter.

Statistical analysis

For the comparison of mean values between three or more groups normality was tested with a Shapiro-Wilk test, normally distributed data was compared with ordinary one-way ANOVA followed by Tukey's multiple comparisons adjustment. Non-normally distributed data was compared with a Kruskal-Wallis test followed by multiple comparison Dunn's test. For comparisons with two means an unpaired two tailed T test was performed. All statistical tests were performed in Graph Pad Prism 8 software.

Results

Addition of CXCR2 to B7-H3 CAR T cells targets canine CXCL8 chemokine in canine OS

To facilitate CAR T cell trafficking to solid tumors we evaluated the addition of chemokine receptor CXCR2 which binds to the ligand CXCL8 with our B7-H3 CAR construct **(Figure 5A)**. This dual targeting B7-H3-CXCR2 CAR was previously demonstrated by our collaborators to have superior activity in human a xenograft model of RMS when tumor cells were engineered to secrete high levels of human CXCL8[208]. The generation of dual valent B7-H3-CXCR2 CAR T cells was done as previously described with activation by anti-canine CD3/CD28 beads and two rounds of retroviral transduction with viral bound retronectin plates[194]. Canine B7-H3-CXCR2 CAR T cells were evaluated at day 10-14 for T cell markers CD5, CD4, CD8 and CAR expression by flow cytometry. We found that by day 14 the majority of the cell culture was CD5+ T cells with a mixture of CD4+ and CD8+ T cells. We confirmed dual expression of both CAR construct and CXCR2 staining of protein-L and anti-human-CXCR2 antibody with a transduction percent and 34.6% as measured by flow cytometry **(Figure 5B)**. We measured secretion of CXCL8 in 7 canine OS cell lines and found that six out of seven canine OS cell lines evaluated spontaneously produced high concentrations of canine CXCL8 **(Figure 5C).** To evaluate B7-H3-CXCR2 CAR T cell migration to canine CXCL8 we investigated the cross reactivity of human CXCR2 to canine CXCL8 using a transwell migration assay with recombinant canine CXCL8. We found that exogenous human CXCR2 induced migration of canine B7-H3-CXCR2 CAR T cells to a gradient of recombinant canine CXCL8 **(Figure 5D).** We also compared the functionality of B7-

H3-CXCR2 CAR T cells to B7-H3 CAR T cells with *in vitro* cytotoxicity assays and found that the B7-H3-CXCR2 CAR T cells had significantly greater production of IFNγ and IL-2 (P-value = 0.0414 and 0.046, respectively) when co-cultured with B7-H3+ canine OS cell line Abrams at an E:T ratio of 5:1 **(Figure 5e).** Comparison on B7-H3 CAR and B7-H3-CXCR2 CAR T cell killing of Abrams-RFP cell line *in vitro* found no difference in killing rates (supplemental figure 6).

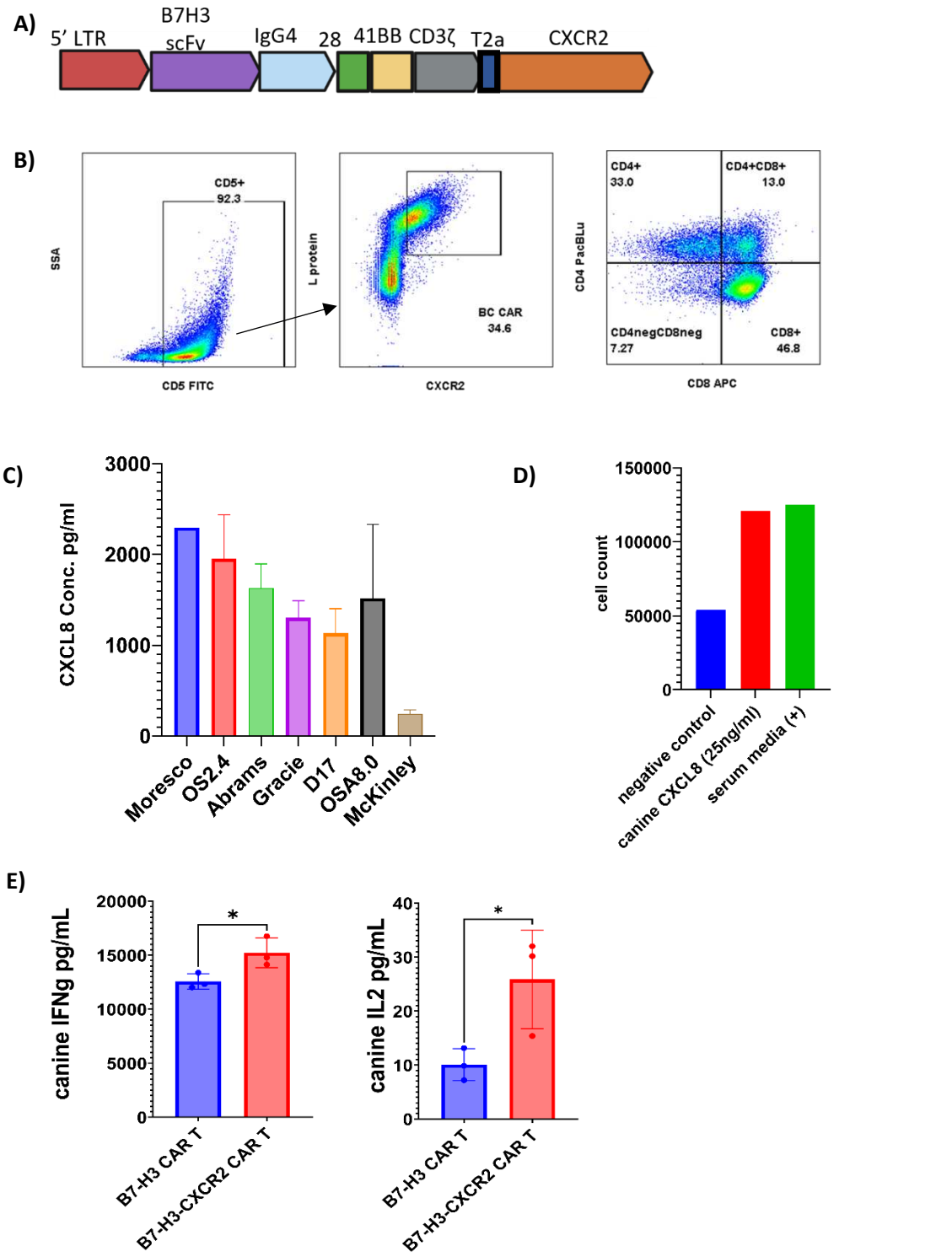

Figure 5. A) B7H3-CXCR2 CAR construct **B)** T cell phenotype by CD5, CD4 and CD8 staining of generated B7-H3-CXCR2 CAR T cells by day 14, dual expression of B7H3 and CXCR2 or transduced canine CAR T cell by flow cytometry **C)** secretion of canine CXCL8 by canine OS cell lines after 4 days at baseline. Graph is shown as means ± SD **D)** Migration of dual CAR vs to recombinant canine CXCL8 *in vitro* ***E)*** Secretion of IFNγ and IL-2 by either canine B7H3 or B7H3-CXCR2 CAR T cells co-cultured with canine OS cell line Abrams for 24 hours (P-value = 0.0414 and 0.046, respectively)

Bulk RNA sequencing of B7-H3 and B7-H3-CXCR2 CAR T cells

The difference in cytokine production between B7-H3 CAR and B7-H3-CXCR2 CAR indicates that there are intrinsic factors to CAR T cell activation contributed to the addition of CXCR2. Our collaborators the Verneris lab (University of Colorado, Aurora, CO) have also found increased oxidative respiration rates in B7-H3-CXCR2 CAR T cells (data unpublished). We found that B7-H3-CXCR2 CAR T cells secrete CXCL8 potentially auto-signaling through exogenous CXCR2 to enhance CAR T cell activation **(Figure 6A)**. To investigate the intrinsic differences between single B7-H3 CAR construct and dual targeting B7-H3-CXCR2 CAR we generated three biological replicates of B7-H3 CAR T, B7-H3-CXCR2 CAR T cells and matched activated non-transduced (NTD) T cells from whole blood from tumor bearing dogs. Cells were collected at day 10 post activation and RNA was extracted and sent to Novogene (Novogene Co., Sacramento CA) for sequencing using an Illumina platform. We found that the transcriptomic expression profile of B7-H3 CAR and B7-H3-CXCR2 CAR were different from each other and from NTD T cells **(Figure 6B)**. Comparison of B7-H3 CAR against B7-H3-CXCR CAR identified 154 differentially expressed genes (DEGs) (Log_2FC >1.5 or <1.5 and adj. P<0.05) with 65 upregulated genes and 89 downregulated genes (supplemental table 1). Additionally, there were 1149 DEGs in the comparison of B7-H3 CAR against NTD T cells and 1960 DEGs between B7-H3-CXCR2 CAR T cells and NTD T cells **(Figure 6C)**. B7-H3-CXCR2 CAR T cells have different transcriptomic expression from B7-H3 CAR T cells and cluster separately by the top 25 significant DEGs **(Figure 6D).** The most significant upregulation in our B7-H3-CXCR2 CAR T cells was in CXCR2 which is to be expected due to exogenous expression of CXCR2. An other gene that was upregulated was immune gene IL15RA. IL15RA encodes for interleukin 15 receptor subunit RA a high affinity receptor for IL-15 which is implicated in increased cell proliferation and associated with apoptosis inhibitor genes BCL2CL, BCL2-XL and BCL2[220]. CHC2-type zinc finger protein gene ZIC2 was also upregulated in B7-H3-CXCR2 CAR T cells. High mRNA expression of ZIC2 was found in CD4+ TILs correlating with a greater 5 year survival in patients with HCC[221]. ZIC2 expression in patients with HCC also positively correlated with immune infiltrating cells

including B cells, CD8+ T cells and CD4+ T cells [221]. Notably genes for other chemokine receptors such as CCR2 and CCRL2 were down regulated. It has been established that T cell activation by CD28/CD3 beads as well as activation with exogenous IL-2 downregulates CCR2 as well as CCR5 in T cells[159,210]. This may indicate that B7-H3-CXCR2 CAR T cells are more activated than B7-H3 CAR T cells[222]. Kinase insert domain (KDR) a type II tyrosine kinase receptor for vascular epithelial growth factor receptor was also downregulated in B7-H3-CXCR CAR T cells. VEGF signaling through VEGFR2 has been shown to directly suppress T cell proliferation and cytokine activity[223]**(Figure 6C)**.

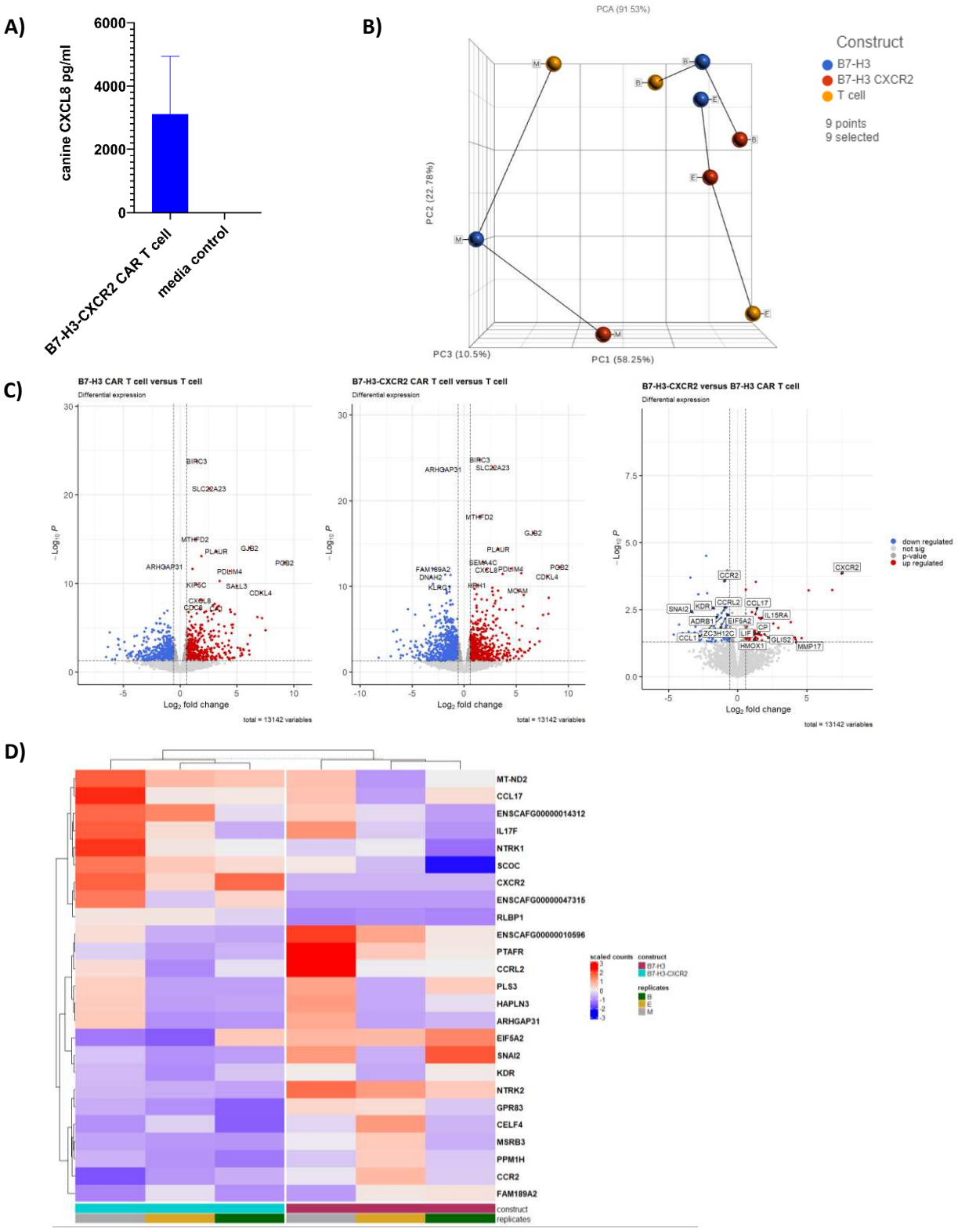

Figure 6. RNAseq B7-H3 vs B7-H3-CXCR2 CAR T A) secretion of canine CXCL8 by B7-H3-CXCR2 CAR T cells **B)** PCA plot of B7-H3-CXCR2 CAR, B7-H3 CAR, and non-transduced T cells **C)** volcano plots of B7-H3 CAR T cell compared to NTD T cells, B7-H3-CXCR2 CAR T cells to NTD T cells and B7-H3-CXCR2 CAR T cells to B7-H3 CAR T cells D**)** Heatmap of the top 25 significant DEGs between B7-H3-CXCR2 CAR T cells and B7-H3 CAR T cells

We performed GSEA[216] using the hallmarks and gene ontology biological processes and molecular functions gene sets from MsigDB[218], to better characterize biological processes of B7-H3-CXCR2 CAR T cells compared to B7-H3 CAR T cells. GSEA analysis identified 391 pathways which were significantly (FDR <0.025) upregulated in B7-H3-CXCR2 CAR T cells (Supplementary Table 2). Upregulated pathways were overrepresented by signatures associated with metabolism from the reactome pathways that involve respiration and metabolism, primarily mitochondrial translation and ATP synthase and respiratory electron transport **(Table 2).** Collectively, these transcriptional changes in B7-H3-CXCR2 CAR T cells corroborate our findings of increased cytokine production and our collaborator's findings of increased metabolic pathways compared to B7-H3 CAR T cells.

Table 2. Top 20 up regulated and down regulated pathways comparing B7-H3-CXCR2 CAR T cells with B7-H3 CAR T cells

NAME	NES	FDR q-val
HALLMARK_MYC_TARGETS_V1	2.674732	0
GOBP_RIBOSOME_BIOGENESIS	2.627747	0
GOBP_RIBOSOMAL_LARGE_SUBUNIT_BIOGENESIS	2.479399	0
HALLMARK_MYC_TARGETS_V2	2.464651	0
GOBP_RIBONUCLEOPROTEIN_COMPLEX_BIOGENESIS	2.449432	0
GOBP_RRNA_PROCESSING	2.423047	0
REACTOME_RRNA_MODIFICATION_IN_THE_NUCLEUS_AND_CYTOSOL	2.410248	0
WP_OVERVIEW_OF_PROINFLAMMATORY_AND_PROFIBROTIC_MEDIATORS	2.351442	0
REACTOME_RRNA_PROCESSING	2.33324	0
REACTOME_MITOCHONDRIAL_TRANSLATION	2.3229	0.001
GOBP_RRNA_METABOLIC_PROCESS	2.317315	0.001
GOBP_NCRNA_PROCESSING	2.288344	0.005
REACTOME_RESPIRATORY_ELECTRON_TRANSPORT_ATP_SYNTHESIS_BY_CHEMIOSMOTIC_COUPLING_AND_HEAT_PRODUCTION_BY_UNCOUPLING_PROTEINS	2.279003	0.007
REACTOME_SYNTHESIS_OF_DNA	2.252796	0.016
GOMF_RNA_POLYMERASE_ACTIVITY	2.245556	0.019
GOBP_MITOCHONDRIAL_TRANSLATION	2.242321	0.02
REACTOME_SWITCHING_OF_ORIGINS_TO_A_POST_REPLICATIVE_STATE	2.212124	0.031
WP_IMMUNE_INFILTRATION_IN_PANCREATIC_CANCER	2.203809	0.036
REACTOME_RESPIRATORY_ELECTRON_TRANSPORT	2.201844	0.037
REACTOME_MITOCHONDRIAL_PROTEIN_IMPORT	2.199672	0.038
WP_GPCRS_CLASS_A_RHODOPSINLIKE	-2.16032	0.01282772
GOMF_G_PROTEIN_COUPLED_RECEPTOR_ACTIVITY	-2.12493	0.01475028
GOMF_STEROL_BINDING	-2.11512	0.01245006
KEGG_COMPLEMENT_AND_COAGULATION_CASCADES	-2.10789	0.01179527
WP_CHOLESTEROL_METABOLISM_WITH_BLOCH_AND_KANDUTSCHRUSSELL_PATHWAYS	-2.10534	0.00983369

GOMF_PEPTIDE_RECEPTOR_ACTIVITY	-2.09423	0.00982778
REACTOME_INTEGRIN_CELL_SURFACE_INTERACTIONS	-2.05953	0.01474076
GOBP_RESPONSE_TO_AMPHETAMINE	-2.0486	0.01498626
GOBP_CD8_POSITIVE_ALPHA_BETA_T_CELL_ACTIVATION	-2.04342	0.01452137
GOBP_POSITIVE_REGULATION_OF_CYTOSOLIC_CALCIUM_ION_CONCENTRATION	-2.03822	0.01434393
REACTOME_CLASS_A_1_RHODOPSIN_LIKE_RECEPTORS	-2.02764	0.01642844
GOBP_REGULATION_OF_PROTEIN_MATURATION	-2.02666	0.01538757
GOBP_REGULATION_OF_ADENYLATE_CYCLASE_ACTIVITY	-2.02233	0.01534047
GOBP_HOMOPHILIC_CELL_ADHESION_VIA_PLASMA_MEMBRANE_ADHESION_MOLECULES	-2.01769	0.01550682
GOMF_MOLECULAR_TRANSDUCER_ACTIVITY	-2.01715	0.01453885
REACTOME_GPCR_LIGAND_BINDING	-2.01172	0.01560505
GOBP_CELL_JUNCTION_DISASSEMBLY	-2.00395	0.01780961
GOMF_STEROID_BINDING	-2.00321	0.01703951
GOBP_REGULATION_OF_T_HELPER_1_TYPE_IMMUNE_RESPONSE	-1.97705	0.02464737
GOBP_POSITIVE_REGULATION_OF_NATURAL_KILLER_CELL_MEDIATED_IMMUNITY	-1.9723	0.0258253

B7-H3-CXCR2 CAR T cells have greater in vivo anti-tumoral activity in a xenograft mouse model of OS

Finally, we conducted studies to evaluate the impact of the addition of CXCR2 to B7-H3 CAR T cells on the anti-tumoral activity in a live animal model. NSG mice with subcutaneous Abrams-luciferase tumors were treated with either B7-H3 CAR T cells generated with with a transduction efficiency of 22% (n=6), B7-H3-CXCR2 CAR T cells generated with a transduction efficiency of 24% (n=7) or no treatment control (n=5) **(Figure 7A)**. Tumor growth was monitored by IVIS imaging and measurement with calipers. To detect circulating canine T cells post infusion we bled a selection of mice from each group (n=3) at day 14 post treatment and evaluated peripheral blood by flow cytometry for circulating canine CD5+ lymphocytes. Only mice treated with B7-H3-CXCR2 CAR T cells had detectable CD5+ canine T cells in the peripheral blood **(Figure 7B).** Mice treated with B7-H3-CXCR2 CAR T cells had inhibition of tumor growth with 3 out of 7 mice experiencing complete tumor regression. Mice treated with B7-H3 CAR T cells had one mouse with complete tumor regression with the remaining 5 mice having stable disease. Control mice all had progressive growth of tumors until ulceration at which point, they were humanely euthanized on day 25 **(Figure 7C)**. Tumor growth as measured by calipers showed that mice treated with B7-H3 CAR T cells and B7-H3-CXCR2 CAR T cells had statistically smaller tumors compared to control mice (P value=0.0472 and 0.0036 respectively). Tumor growth between CAR T cell treatment groups was not statistically significant **(Figure 7D)**. Total photon flux as measured by IVIS did not show statistical significance however there was an observable trend with the control group photon flux increasing over time and the CAR T cell treated groups having stable photon flux through day 25 **(Figure 7E)**. This shows that canine B7-H3 CAR T cell treatment is effective in tumor control canine OS in a xenograft mouse model having inhibited tumor growth. B7-H3-CXCR2 CAR T cell having induced complete tumor regression in 3 out of 7 mice and stable disease in the remaining 4 mice showed greater efficacy *in vivo*.

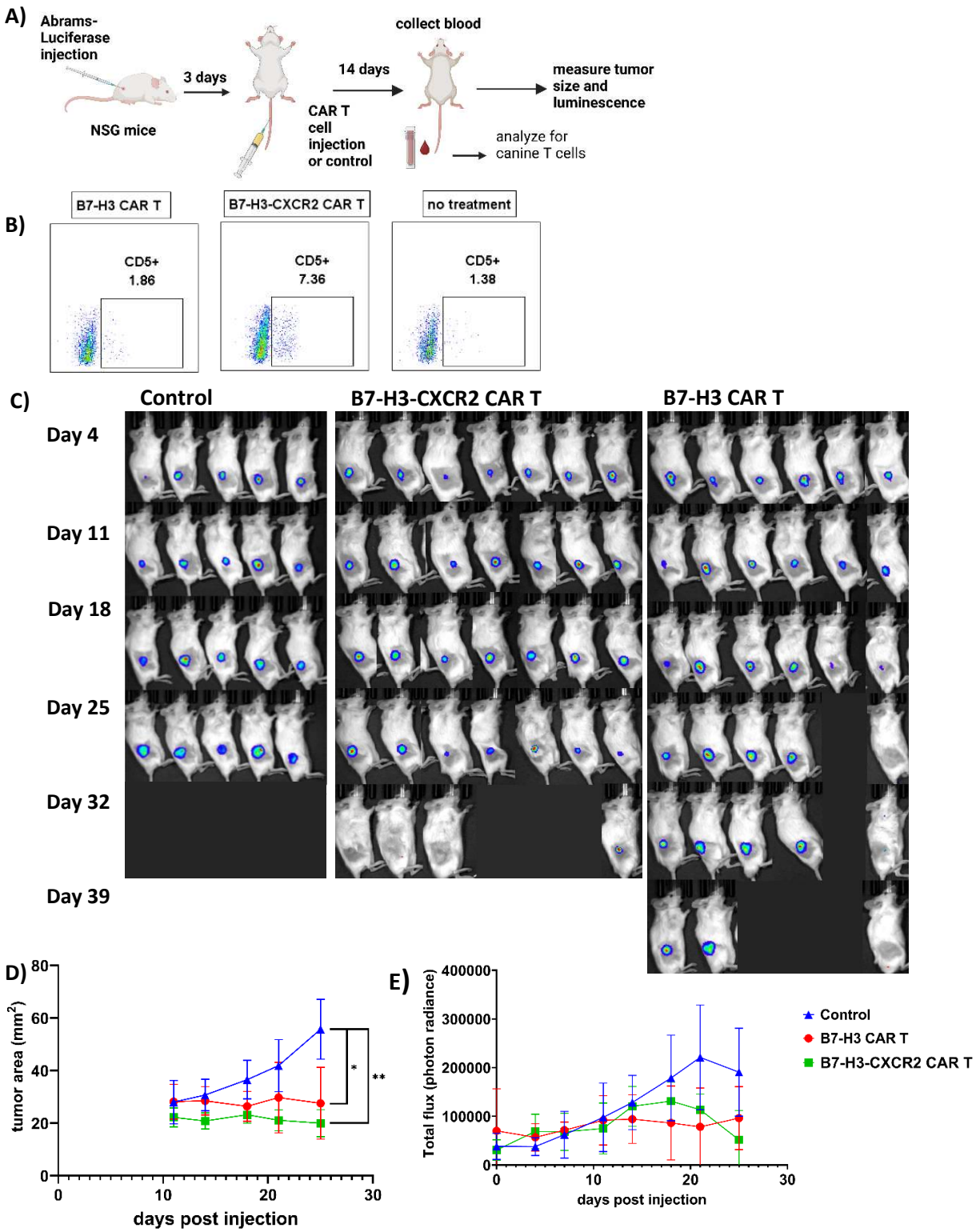

Figure 7. Abrams Luciferase tumor control by B7H3 CAR T cells **A)** experimental design **B)** canine CD5+ lymphocytes in peripheral blood of mice day 14 post treatment by flow cytometry **C)** IVIS imaging results of tumor growth over 39 weeks **D)** Tumor growth measured by calipers showing statistically different tumor growth in B7-H3 CAR T treatment vs control p-value=0.0472 and B7-H3-CXCR2 CAR T vs control p-value=0.0036 **E)** total flux of tumors as measured by IVIS

Discussion

This study is the first to our knowledge to evaluate canine B7-H3 CAR T cells in a xenograft solid tumor model. Additionally, this is the first study to demonstrate the enhanced *in vivo* anti-tumoral activity of B7-H3 CAR T cells through the addition of CXCR2 chemokine receptor in an OS xenograft model. To justify the addition of CXCR chemokine receptor we characterized secretion of its ligand CXCL8 by canine OS cell lines. We found that 6 out of 7 canine OS cell lines secreted high levels of canine CXCL8 at base line (Figure 5C) indicating that canine OS CXCL8 signaling may be co-opted to enhance CAR T cell homing to OS tumors through the addition of CXCR2. We also showed that expression of exogenous human CXCR2 drives migration in canine CAR T cells to canine recombinant CXCL8 (Figure 5D). Collectively this showed that the human B7-H3-CXCR2 CAR construct licensed by ArtisanBio (Louisville, CO) gifted to us by the Verneris lab (university of Colorado, Aurora, CO) can be readily adapted into a canine system.

In vitro activation of B7-H3 CAR was enhanced with addition of CXCR2 as measured by increased secretion of IFNγ and IL-2 when co-cultured with B7-H3^{high}-CXCL8 secreting OS cell line Abrams (Figure 5D). B7-H3-CXCR2 CAR T cells killed adherent Abrams OS cell line in a dose dependent manner but did not have improved killing from donor matched B7-H3 CAR T cells at the same E:T ratio (Supplementary Fig. 6). Taken together, these findings indicate that addition of CXCR2 does not impact *in vitro* tumor cell killing however increased cytokine production may indicate that B7-H3-CXCR2 CAR T cells are more active or more robust than B7-H3 CAR T cells. We hypothesized that this was through autocrine signaling of CXCL8 and found that canine CAR T cells secreted CXCL8 at baseline to an appreciable level (Figure 6A). Investigation of B7-H3-CXCR2 CAR T cell transcriptome by bulk RNA sequencing revealed upregulated genes involved in T cell activation such as IL15RA and ZIRC2 (Figure 6C). This suggests that addition of CXCR2 on CAR T cells increases CAR T cell activity at baseline although the exact mechanism of activation and phenotypic changes in B7-H3-CXCR2 CAR T cells compared to B7-H3 CAR T cells still need to be characterized.

To evaluate the in vivo activity of B7-H3-CXCR2 CAR T cells compared to B7-H3 CAR T cells we used an NSG mouse model. Tumor growth was controlled following IV administration of canine CAR T cells at 5.0e6 CAR T cells/mouse with both B7-H3 and B7-H3-CXCR2 CAR T cells significantly reducing tumor burden in mice compared to that of the control group (Figure7D). Additionally, B7-H3-CXCR2 CAR T cells induced greater tumor control, achieving compete tumor regression in 3 out of 7 mice as compared to B7-H3 CAR T cell treated mice that only saw 1 out of 6 mice achieve complete tumor regression (Figure 7C). Evaluation of circulating canine T cells within the peripheral blood of CAR T cell treated mice at day 14 post treatment showed that only B7-H3-CXCR2 CAR T cell mice had detectable circulating canine CD5+ lymphocytes. This may indicate that B7-H3-CXCR2 CAR T cells have better persistence post injection *in vivo* however further investigation of other tissue types including spleen and tumor need to be done to evaluate persistent CAR T cells that may be residing in tissues and not in peripheral blood. These findings therefore confirm that the addition of CXCR2 chemokine receptor to B7-H3 CAR T cells increases anti-tumoral activity *in vivo*, presumably by increasing CAR T cell trafficking to the OS tumors.

In summary, we provide critical information here necessary to advance canine CAR T cell therapy against solid cancers generally, and to treatment of OS specifically, using B7-H3 targeted CAR T cells. We also established the utility of a dual expressing vector adding a chemokine receptor CXCR2 targeting CXCL8 to improve CAR T cell tumor trafficking and tumor control by evaluating this and single B7-H3 CAR construct in a canine OS xenograft model. These studies thus pave the way for the next set of studies, which can include evaluation in clinical trials in dogs with metastatic OS as CAR T cell therapy alone, or to combine B7-H3-CXCR2 CAR T cells with strategies to remodel the immune suppressive TME by depletion of myeloid cells, as reported recently by our group for treatment of brain cancer in dogs[224].

Chapter 4: AIM 3- Investigate the effect of tumor associated macrophages and TME modifying immunotherapy on B7-H3-CXCR2 CAR T cell function

Summary

Myeloid lineage immune suppressor cells such as M2 TAMS and MDSCs within the TME contribute to the suppression of anti-tumoral T cells and tumor immune evasion. Our group has found that the combination of type 1 angiotensin II receptor blocker losartan and beta blocker propranolol have secondary immune modulating effects and work synergistically to remodel the TME to a more proinflammatory phenotype[172,173]. Our group has demonstrated synergy between losartan and propranolol with addition of a tumor lysate derived cancer vaccine to induce anti-tumoral immune response against canine glioma in a clinical setting[173]. Based on our previous experience with using losartan and propranolol to enhance immunotherapies we hypothesized that addition of repurposed drug combination losartan and propranolol would enhance B7-H3-CXCR2 CAR T cell therapy through the modification of the TME by depletion of M2 TAMs and MDSCs.

To achieve this, we used a SCID-beige mouse strain with intact myeloid lineage cells to create a xenograft canine OS model and found that mouse monocytes migrate and reside in canine OS tumors. Additionally, we found that treatment with combination losartan and propranolol significantly reduce TAMs within xenograft OS tumors. We also evaluated the effect of canine monocyte derived macrophages (MDMs) on B7-H3-CXCR2 CAR T cells *in vitro* to investigate the effect of native B7-H3 antigen signaling with either immune suppressive or proinflammatory polarized MDMs. We found that MDMs regardless of polarization enhanced B7-H3-CXCR2 CAR T cell cytotoxic activity when co-cultured for 24 hours. Co-culture with GD2 negative MDMs with GD2-CAR T cells did not enhance cytotoxic activity. This suggests that MDM enhancement of B7-H3 targeting CAR T cells is through signaling of B7-H3 antigen on MDMs through the B7-H3 CAR. In summary there is a complex relationship between myeloid cells and B7-H3-CXCR2 CAR T cells that is unique to immune modulatory antigen CAR targeting. Further investigation needs to be done

to show if TME modification through TAM depletion will be additive or inhibitory to B7-H3-CXCR2 CAR T cell antitumoral function *in vivo*.

Introduction

The immune suppressive tumor microenvironment (TME) is a major barrier for clinical success in solid tumor CAR T cell therapy[120]. OS has been known as an immunologically "cold" tumor with a lack of identified tumor neo-antigens and a low ratio of tumor infiltrating CD8+ lymphocytes to TAMs[17]. In addition, TAMs and MDSCs are known to exert immune suppressive effect to contribute to tumor immune evasion through secretion of immune suppressive cytokines such as IL-10, TGFβ, IL-4 and VEGF and through cell surface expression of checkpoint molecules such as PD-L1 [41]. Contrary to many epithelial tumors, a high proportion of TAM infiltrates in OS is correlated with reduced metastasis and greater survival in high grade OS[18,19]. This is thought to be due to the heterogenous population of pro-inflammatory M1 TAMS and anti-inflammatory M2 TAMS[41]. Treatment of patients with high grade OS with mifamurtide, an innate immune agonist that activates macrophages and monocytes, induced an increase in serum levels of proinflammatory cytokines IL-1β, IL-6 and TNF[225] and an improved 5-year survival by 13% when used with standard chemotherapy[226]. Modification of the myeloid cell component of the TME can tip the immune balance withing the TME to generate anti-tumoral immunity leading to prevention of metastatic lesions or regression of existing OS lesions[41].

Our group has found that TME modification with combination of repurposed drugs losartan and propranolol works synergistically with other immune therapies against OS and glioma in dogs[173]. Losartan a type 1 angiotensin II receptor antagonist also inhibits monocyte migration into tumors through the non-competitive inhibition of CCL2-induced ERK1/2 activity[168]. Treatment with losartan significantly slowed metastatic progression through the blockade of inflammatory monocyte recruitment and showed a significant reduction of metastasis-associated macrophages in murine models of metastatic breast and

colon cancer[168]. Additionally, treatment with losartan in combination with the tyrosine kinase inhibitor toceranib resulted in clinical benefit in 50% in dogs with lung metastatic OS[172].

Propranolol, a β-adrenergic receptor blocker, has been shown to inhibit MDSC mobilization from the bone marrow and decrease MDSC accumulation in tumors leading to a decrease in tumor growth in mice[227]. Treatment with daily losartan and propranolol in dogs with glioma depleted tumor-resident myeloid cell populations. Additionally, treatment of dogs with glioma with an allogeneic cancer stem cell vaccine generated tumor-specific immune responses and was synergistic with combination losartan and propranolol TME modification[173]. Triple therapy with losartan, propranolol and cancer stem cell vaccine generated a clinical benefit rate of 80% in dogs with glioma[173]. Therefore, we hypothesize that addition of losartan and propranolol to B7-H3-CXCR2 CAR T cell therapy will work synergistically through the depletion of tumor resident myeloid cells to modify the TME to a proinflammatory landscape increasing CAR T cell efficacy in canine OS.

Here we evaluated the effects of losartan and propranolol in a mouse xenograft model of canine OS. We found that daily administration of combination losartan and propranolol depleted CD11b+Ly6C+ macrophages from xenograft OS tumors. We also evaluated the effect of proinflammatory or anti-inflammatory polarized monocyte derived macrophages (MDMs) on B7-H3-CXCR2 CAR T cells in vitro. MDM signaling of B7-H3 to B7-H3-CXCR2 CAR T cells enhanced cytotoxic function of the CAR T cells regardless of anti-inflammatory polarization. Evaluation of losartan and propranolol with B7-H3-CXCR2 CAR T cells in a mouse xenograft model using SCID-beige mice revealed no anti-tumoral effect due to lack of persistence of canine CAR T cells in this mouse model.

Methods

Animals

Peripheral blood mononuclear cells (PBMCs) were obtained from EDTA anticoagulated blood samples from tumor bearing dogs from the Flint Animal Cancer Center (FACC) following full CSU IACUC approval. Fox Chase SCID-beige (SCID-beige) mice from Charles River were used for all mouse experiments, and these studies were covered under CSU IACUC.

In vivo mouse experiment

To evaluate the effect of losartan and propranolol on myeloid cells within OS TME, SCID-beige mice were implanted with 2.5e5 Abrams-RFP cells in HBSS with 30% Matrigel per mouse in the subcutaneous (SQ) flank. Mice were treated with daily intraperitoneal (IP) injections of either single drugs losartan (60 mg/kg) n=4, propranolol (10 mg/mouse) n=4, combination losartan and propranolol n=4, or vehicle control n=3 on day 7 when tumors were palpable. Mice were monitored for weight, and tumors were measured by calipers twice a week. Mice were humanely euthanized when tumors ulcerated through the skin or were >1.0 cm in the longest diameter. Tumor tissues were collected for analysis by flow cytometry.

To evaluate the in vivo effects of canine B7-H3-CXCR2 CAR T cells in combination with losartan and propranolol SCID-beige mice were implanted with 2.5e5 Abrams-luciferase cells in HBSS with 30% Matrigel per mouse in the right SQ flank. Tumor implantation was confirmed with IVIS imaging on day 3 post tumor inoculation prior to CAR T cell infusion. Treatment groups were control (untreated) n=6, losartan (60 mg/kg) and propranolol (10 mg/mouse) n=6, CAR T cell alone (2.5e6 B7-H3-CXCR2 CAR T cells/mouse) n=8, or CAR T combo (2.5e6 B7-H3-CXCR2 CAR T cells/mouse with losartan (60 mg/kg) and propranolol (10 mg/mouse)) n=6. Groups receiving losartan and propranolol were pre-treated with drugs 14 days prior to CAR T cell treatment. Losartan and propranolol were given daily by IP injection. Mice were monitored for weight, and tumors were measured by calipers and IVIS imaging twice a week. Mice were humanely

euthanized when tumors ulcerated through the skin or were >1.0 cm in the longest diameter. Tumor tissues were collected for analysis by flow cytometry.

Tissue single cell digestion

Excised tumors were dissociated into a single cell suspension by collagenase digestion as previously described[228]. In brief tumors were dissected into small pieces with a scalpel and incubated with collagenase for 20 minutes in 37C water bath. Digested tumor tissue was triturated through an 18-gauge needle and washed with PBS. Cell pellets were filtered through a 70-um filter and washed again with 1x PBS. If there were significant red blood cells within the cell pellet were incubated with ACK lysis buffer for 5 min on ice before being washed with 1x PBS. Single cell tumor suspensions were stained for mouse macrophage infiltrates and analyzed by flow cytometry.

Flow cytometry

Dissociated xenograft tumors were stained for mouse myeloid markers using the following antibodies, anti-mouse CD11b (clone M1/70), anti-mouse Ly6C (clone AL-21), anti-mouse Ly6G (clone 1A8), anti-mouse F4/80 (clone BM8) and anti-mouse CD11C (clone N418). A live dead stain was performed using 7AAD. Tumor cells expressed RFP and were gated on PE. Canine surface expression of B7-H3 was analyzed using anti-B7-H3-APC antibody (clone 7-517, eBioscience) or isotype control mouse IgG1kappa (ThermoFisher, cat# 17-4714-82). Canine surface expression of GD2 was analyzed using anti-human ganglioside GD2 antibody-PE (BioLegend, cat#357303) and PE-mouse IgG23a k isotpe control. Canine immune expression was analyzed with the following antibodies: anti-canine CD5-FITC (cloneYKIX322.3, Biorad), anti-canine CD8-alexa Fluor 647 (clone YCATE55.9, Biorad), anti-canine CD4-Pacific Blue (clone

YKIX302.9, Biorad). Recombinant protein L-biotinylated (ThermoFisher, cat# 29997) followed by secondary Streptavidin-PE (eBioscience, cat#12-4317-87) was used to detect B7-H3 CAR transduced cells. Anti-CXCR2-PEcy7 (clone 5E8, Biolegend) was used to detect human CXCR2 on transduced canine CAR T cells. PE anti-DYKDDDDK tag antibody (Biolegend, cat#637309) was used to detect GD2 CAR T cells. After staining all samples were analyzed on a Beckman Coulter Gallios flow cytometer. Flow data was analyzed by Flowjo v10.

Cell culture

Canine osteosarcoma cell lines were provided by the FACC cell line repository and previously validated[201]. All cell lines were cultured in cell culture media containing DMEM with 10% fetal bovine serum (Corning), 2mM L-glutamine (Gibco), 100 U/ml penicillin and 100 ug/ml streptomycin (Gibco). All cell cultures were kept at 37C and 10% CO2.

CAR constructs

The B7-H3 CAR was shared with the University of Colorado Verneris lab by Michael Jensen, MD (Fred Hutchinson Cancer Center, Seattle, WA). This lentiviral construct contained a B7-H3 single-chain variable fragment (scFv), an IgG4 and CD28 transmembrane domain, a 4-1BB costimulatory molecule and the CD3ζ domain. The Verneris lab cloned the CAR portion of the construct into a retroviral backbone containing a 5' LTR promoter using standard PCR-based cloning methods to create the B7-H3 CAR construct. The retroviral backbone we used was a gift from Anandani Nellan (National Cancer Institute, Bethesda, MD). The B7-H3-CXCR2 CAR construct was created first by extracting native CXCR2 RNA from human neutrophils, conversion to cDNA by reverse transcriptase (Bio-rad iScript cDNA Synthesis kit), and

amplification of the CXCR2 sequence. The CXCR2 DNA fragment was inserted into the B7-H3 CAR construct using PCR methods. The GD2 CAR was shared with us by Colorado State University Thamm lab (Fort Collins, CO). The murine stem cell virus (MSCV) retroviral construct contained a flag tag, GD2scFV, CD8a transmembrane domain, 4-1BB costimulatory molecule, CD3ζdomain, P2a, and truncated EGFR.

Retrovirus production

B7-H3 CAR retrovirus was produced and provided to us by Jessica Lake, MD (University of Colorado Verneris lab, Aurora, CO). GD2 CAR retrovirus was produced and provided to us by Sam Brill (Colorado State University, Thamm lab, Fort Collins, CO). 293GP cells (a gift from Dr. Terry Fry, University of Colorado, Aurora, CO) were plated in T175 flasks in Dulbecco's Modified Eagle Medium (DMEM) with 10% fetal bovine serum (FBS) and 1% anti-biotic/anti-mycotic (Gibco). Transfection occurred when cells were 90-95% confluent. Tube A contained 3.4 ml of room temperature Opti-MEM (without additives), 20.25 µg of B7-H3-CXCR2 or GD2 vector DNA, and 10.125 µg of RD114 (envelope plasmid, gift from Anandani Nellan). Tube B contained 3.4 ml of room temperature Opti-MEM (without additives) and 100 µl of lipofectamine 2000 (Invitrogen). The tubes were left at room temperature for 10 minutes after which Tube A was added dropwise to Tube B and gently mixed. The combined mixture was left at room temperature for 30 minutes. During that time, the media was removed from the 293GP cells and 16 ml of fresh, warmed DMEM with 10% FBS (no anti-anti) was carefully added. After 30 minutes, the retroviral mixture was added to the flask, being careful not to agitate the cells. Flasks were placed at 37 degrees Celsius for 24 hours. After 24 hours, media/viral mixture was removed from flasks and 24 ml of fresh DMEM with 10% FBS and 1% anti-anti was gently added. The flasks were returned to 37 degrees Celsius. Viral collections were made at 24 and 48 hours after media replacement. The retrovirus was flash frozen in dry ice and placed in -80 degrees

Celsius until use. Frozen B7-H3-CXCR2 CAR or GD2 CAR retroviral stocks were shared with us by the Verneris lab or the Thamm lab respectively for the purpose of generating canine CAR T cells.

Generation of anti-canine CD3/CD28 magnetic beads

Mouse anti-canine CD3 (clone CA17.2A12, Biorad) and mouse anti-canine CD28 (clone 58B, Invitrogen) antibodies were conjugated to magnetic tosyl-activated Dynabeads (Life Technologies) as previously established at a 1:1 antibody ratio[194,199].

Canine PBMC isolation and T cell activation

Canine whole blood from tumor bearing patients was provided by the Flint Animal Cancer Center (Fort Collins, CO). Peripheral blood mononuclear cells (PBMCs) were isolated using Ficoll and gravity centrifugation. Canine PBMCs were plated at a density of 2.0e6/mL in 6 well tissue culture plates to adhere monocytes for 90 minutes at 37 degrees Celsius. Peripheral blood lymphocytes (PBLs) were gently washed off with canine T cell media (cTCM), DMEM with 10% FBS and 100 U/ml penicillin and 100 ug/ml streptomycin (Gibco), 2 mM L glutamine, 1x essential amino acids (Gibco, cat#11130051), 1x non-essential amino acid (Gibco, cat#11140050), 0.075% Bicarbonate solution, 10 mM HEPES, and 55 uM 2-mercaptoethanol. PBLs were plated at a concentration of 1.0e6/mL with 30 ng/mL rhIL-21(Peprotech), 100IU rhIL-2 (Peprotech), 5 ng/mL rhIL-7 (Peprotech) and rhIL-15 (Peprotech). T cells were activated with tosyl-activated dynabeads (Life Technologies) conjugated with canine anti-CD3/CD28 antibodies at a ratio of 3:1 beads to PBLs. T cells were incubated at 37˚C for 3 days before transduction with CAR retrovirus.

CAR T cell Transduction

Non-tissue culture treated plates were coated with 24 µg/mL retronectin (Tankara) according to manufacturer protocol. Frozen B7-H3 or B7-H3-CXCR2 retroviral supernatant was thawed in a 37˚C water bath and aliquoted into retronectin coated 6 well plates 2 ml/well and centrifuged at 32˚C for 2.5 hours at 2,000 G. PBLs are plated onto retroviral bound plates at a concentration of 5.0e5/mL and 2 mL per well and incubated overnight at 37˚C. T cells were transduced twice before being rescued from virus and expanded in fresh cTCM media and cytokines. Half of the media was changed, and fresh cytokines are added every other day. Generated canine CAR T cells were used for analysis by day 10-14 of culture.

Macrophage conditioning

Canine monocyte derived macrophages were generated as previously described[229]. In brief, PBMCs were isolated from whole blood of tumor bearing dogs using ficoll and gravity centrifugation. Adherent cells were plated at 2.0e6 cells/ml in 24 well tissue culture plates 2 ml/well at 37˚C for 90 minutes. Non-adherent cells were removed with gentle washing and used for generation of donor matched CAR T cells. Adherent monocytes were differentiated into macrophages with 10 ng/ml recombinant human macrophage colony stimulating factor (M-CSF) (PeproTech, Rocky Hill NJ) for 7 days, refreshing media and cytokines every 3rd day. By day 7 differentiated macrophages were considered resting (M0) macrophages were then either remained M0 or polarized for 48 hours into proinflammatory macrophages (M1) with 20 ng/mL of canine IFNγ (R&D Systems Inc., Minneapolis, MN), anti-inflammatory macrophages (M2) with 20 ng/ml each of recombinant canine IL-4 and IL-13 (PeproTech, Rocky Hill NJ), or tumor media conditioned macrophages (TCM) with 1:1 mixture of fresh complete DMEM and supernatant from tumor cell line Abrams. Donor matched canine CAR T cells were then co-cultured with polarized macrophages at 2.0e6 cells/well for 24 hours at 37˚C before being used in incucyte killing assays.

Conditioned CAR T cells were washed and counted before being used in incucyte kill assays to remove any added recombinant cytokines.

Incucyte killing assay

Red fluorescence protein (RFP) or nuclight red (NLR) labeled canine OS target cells were seeded in a 96-well flat bottom plate (Corning) at 5.0e3 cells/well. Target cells were incubated for 24 hours to allow for adherence. Effector cells were added into target cell containing wells at different E:T ratios (1:1, 1:5 or 1:20). Plates were put into an Incucyte Sx5 live-cell analysis instrument (Sartorius), images were captured every 2 hours on RFP and bright field for 48 hours. Red object count was analyzed to represent target cell count in the well of RFP expressing OS cell lines.

Statistical analysis

For the comparison of mean values between three or more groups normality was tested with a Shapiro-Wilk test, normally distributed data was compared with ordinary one-way ANOVA followed by Tukey's multiple comparisons adjustment, non-normally distributed data was compared with a Kruskal-Wallis test followed by Dunn's multiple comparisons test. For comparisons with two means an unpaired two tailed T test was performed. All statistical tests were performed in Graph Pad Prism 8 software.

Results

Combination losartan and propranolol blocks monocyte migration into xenograft canine OS tumors

To evaluate the effect of losartan and propranolol on the TME we utilized a SCID-beige mouse strain as they have intact myeloid lineage cells unlike that of NSG mice. SCID-beige mice are still immune

compromised lacking T cells, B cells and having impaired NK cells making them able to accept xenograft canine OS tumors[230]. Canine OS Abrams-RFP tumor cells were implanted subcutaneously in SCID-beige mice. Mice were treated on day 5 post tumor inoculation with repurposed TME modifying drugs (n=4) losartan (60 mg/kg), propranolol (10 mg/mouse) or combination (combo) losartan (60 mg/kg) and propranolol (10 mg/mouse) or a vehicle control (n=3). Mice were monitored by weight and tumors were measured blinded to treatment groups with calipers. Mice were humanely euthanized when the tumors ulcerated through the skin or grew >1.0cm in the largest diameter. Tumors were excised and processed into a single cell suspension and evaluated by flow cytometry for infiltrating mouse myeloid cells **(Figure 8a)**.

We found that treatment with either losartan, propranolol, or combo had no effect on tumor growth or survival in the mice compared to vehicle control **(Figure 8b)**. Mouse myeloid cells migrated to and infiltrated into dog xenograft OS tumors as evaluated by antibody staining by flow cytometry **(Figure 8c).** Immune suppressive TAMs were identified as CD11b+Ly6c^{high} cells withing the tumor. There was a significant decrease in CD11b+Ly6c^{high} TAMs in mice treated with combination losartan and propranolol but not in either of the single drug treated groups (one-way ANOVA P=0.0428. Dunnett's multiple comparisons test control vs combo p=0.025) **(Figure 8e)**.

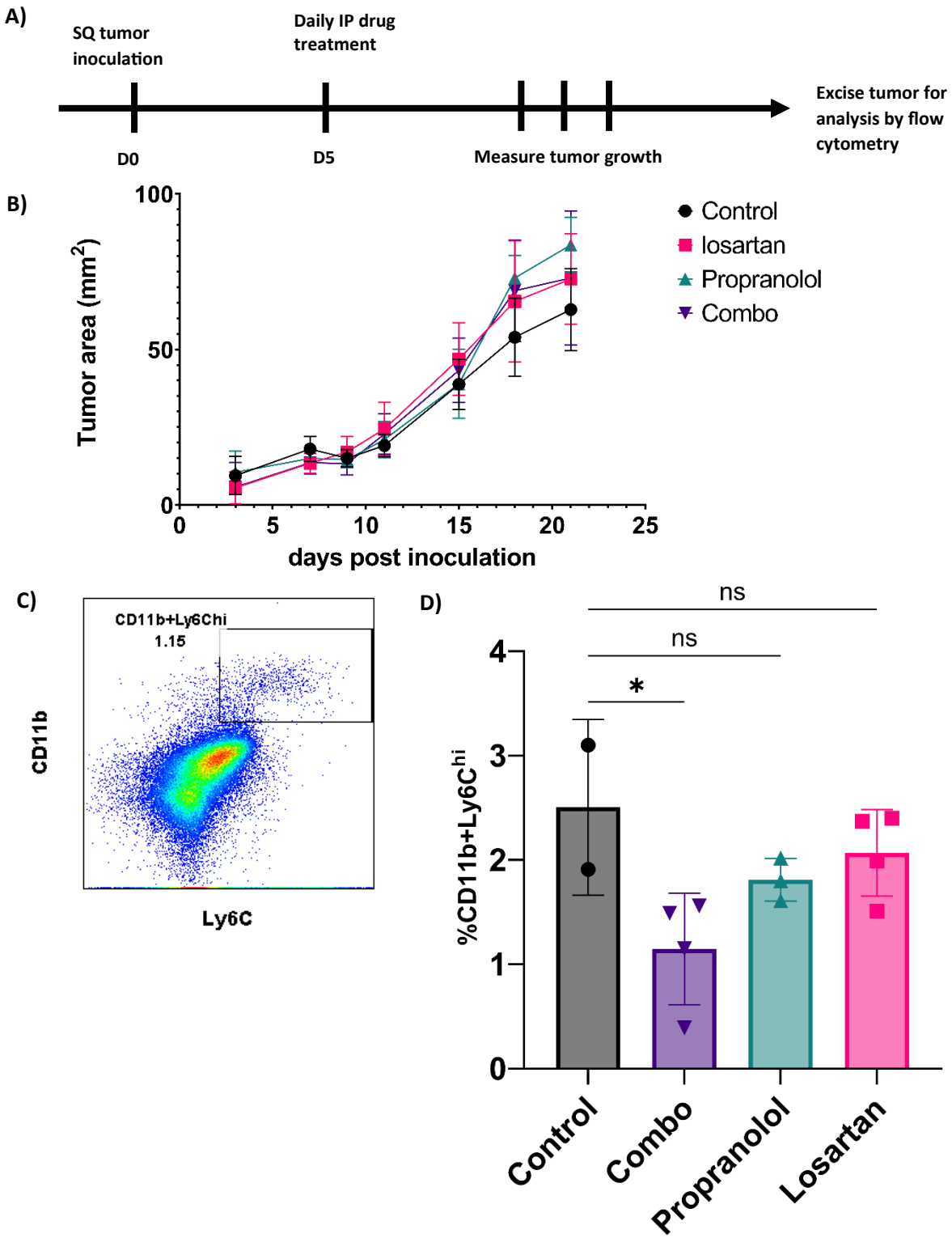

Figure 8. Migration of mouse myeloid cells into canine OS xenograft tumors and the effects of losartan and propranolol A) experimental design **B)** tumor growth of SQ implanted Abrams-RFP tumors in SCID-beige mice **C)** representative plot of mouse myeloid cell infiltrates in xenograft canine OS tumors **D)** percentages of CD11b+Ly6C^{high} tumor associated macrophages as evaluated by flow cytometry. One-way ANOVA P=0.0428. Dunnett's multiple comparisons test control vs combo p=0.025

Monocyte derived macrophages enhance B7-H3-CXCR2 CAR T cell activity in vitro

To evaluate the effects of macrophages on CAR T cells we developed an *in vitro* cell culture system using donor matched monocyte derive macrophages (MDMs) co-cultured with B7-H3-CXCR CAR T cells isolated from whole blood from tumor bearing dogs (n=3). Canine monocyte derived macrophages were generated and polarized following our previously established protocol[229]. In brief, the adherent fraction of canine PBMCs was isolated from whole blood, non-adherent cells were separated for CAR T cell generation. Adherent monocytes were differentiated with 10 ng/ml M-CSF and remained resting (M0) or polarized at day 7 to M1, M2 or, tumor media conditioned macrophages (TCM). Duplicate wells of macrophages were made and detached at day 9 to evaluate B7-H3 expression by flow cytometry. We found that canine monocyte derived macrophages were B7-H3 positive with various levels of expression depending on polarization as calculated by median florescence intensity (MFI) with TCMs having highest MFI and M0s having lowest MFI **(Figure 9A and B).**

2.0e6 donor matched B7-H3-CXCR2 CAR T cells were co-cultured with polarized MDMs at day 10 for 24 hours at 37 ˚C for macrophage conditioning. Naïve and macrophage conditioned B7-H3-CXCR CAR T cells were plated with target canine Abrams-RFP OS cells in triplicate at an E:T ratio of 5:1. Tumor growth was measured by red object count by Incucyte every 2 hours for 48 hours. We found that M1, M2, TCM and M0 polarized macrophage conditioned CAR T cells had significantly increased rates of killing compared to naïve CAR T cells as evaluated by non-parametric ANOVA Kruskal-Wallis test p value <0.0001 and Dunn's multiple comparisons test P value <0.0001, <0.0001, and 0.001, for M1, M2 and M0 respectively **(Figure 9C)**.

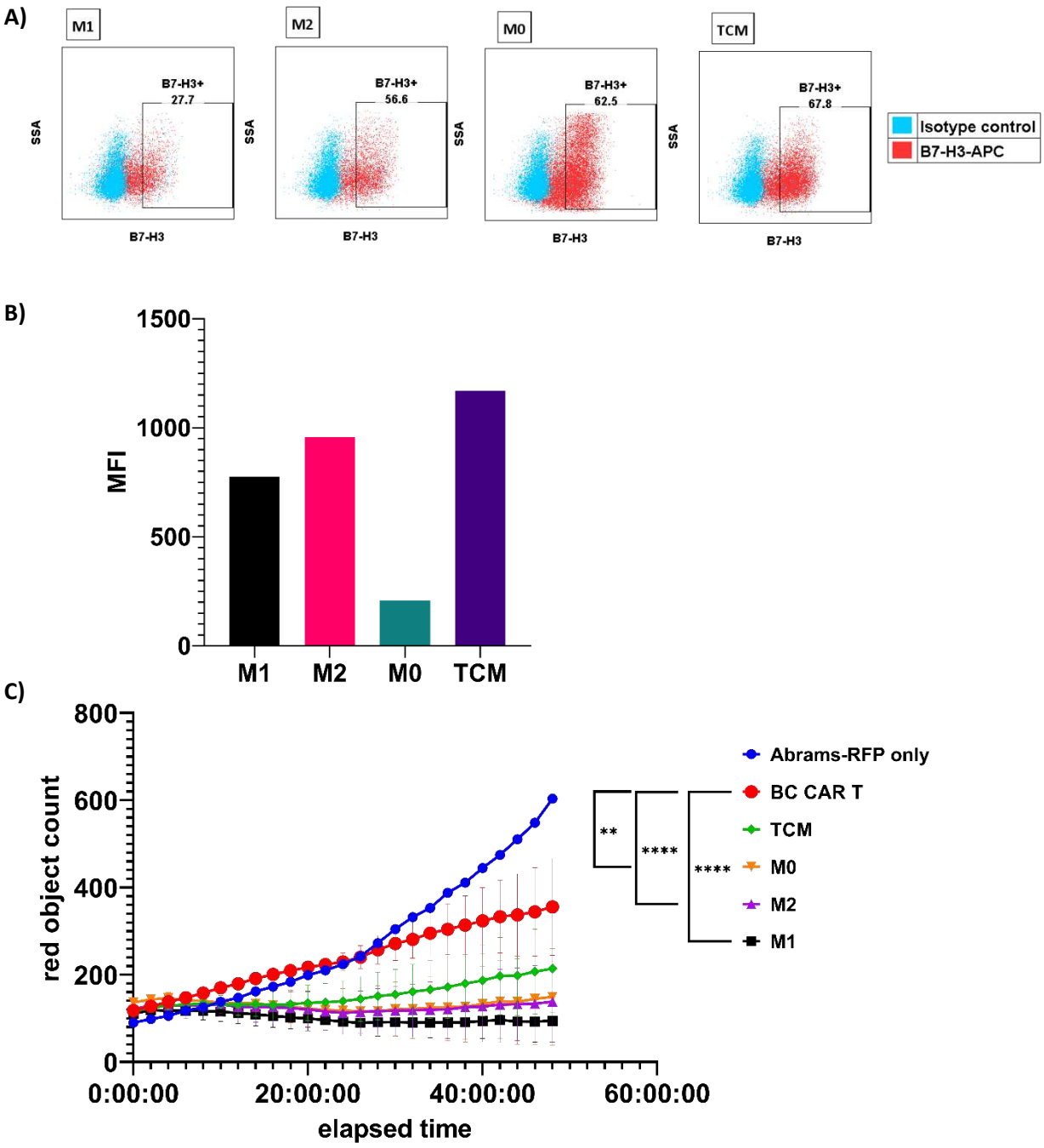

Figure 9. Effect of monocyte derive macrophages on B7-H3-CXCR2 CAR T cells in *vitro* **A)** B7-H3 expression on canine monocyte derived macrophages by flow cytometry **B)** median fluorescence intensity of B7-H3 on polarized canine monocyte derived macrophages resting M0, proinflammatory M1, or immune suppressive M2 or tumor media conditioned TCM **C)** Killing of canine OS target cells by B7-H3-CXCR2 CAR T cells at 5:1 effector to target ratio. CAR T cells are either naïve (BC CAR T) or conditioned for 24 hours with M1, M2, M0, or TCM polarized macrophages. Data is depicted graphically as mean ± SEM. Statistical differences were determined using nonparametric Kruskal-Wallis test, followed by Dunn's multiple comparisons test (*$p \leq 0.05$, **$p \leq 0.01$, ***$p \leq 0.001$, **** $p \leq 0.0001$), ns for non-significant

Macrophage enhancement of B7-H3 CAR is due to B7-H3 antigen priming

To investigate if enhancement of B7-H3-CXCR2 CAR T cells was through binding of B7-H3 from MDMs, we repeated the above experiment using GD2-CAR T cells. Disialoganglioside (GD2) is a ganglioside overexpressed in neuroectodermal tumors[142]. We found that canine MDMs did not show any surface expression of GD2 **(Figure 10A).** Canine OS cell line OSA8.0 overexpressed GD2 as evaluated by flow cytometry **(Figure 10B)**. Expression of GD2 CAR using an anti-flag antibody was evaluated by flow cytometry at day 10 and showed a 14% transduction efficiency **(Figure 10C)**. GD2 CAR T cells were co-cultured with polarized donor matched MDMs for 24 hours on day 10 at 37°C. Naïve or macrophage conditioned GD2 CAR T cells were co-cultured with NucLight red expressing OSA8.0 (OSA8.0-NLR) cells at and E:T ratio of 5:1. Tumor cell growth was measured by red object count by Incucyte every 2 hours over 24 hours. We found that macrophage conditioning with GD2 CAR T cells did not enhance or inhibit GD2 CAR T cell killing of GD2 positive canine OS target cells *in vitro.* Ordinary one-way ANOVA p value <0.0001 with Tukey's multiple comparisons between naïve GD2 CAR T or MDM conditioned CAR T cells and OSA8.0 alone adjusted P<0.0001 and no significance between naïve GD2 CAR T cells and any MDM conditioned CAR T cell conditions **(Figure 10D)**.

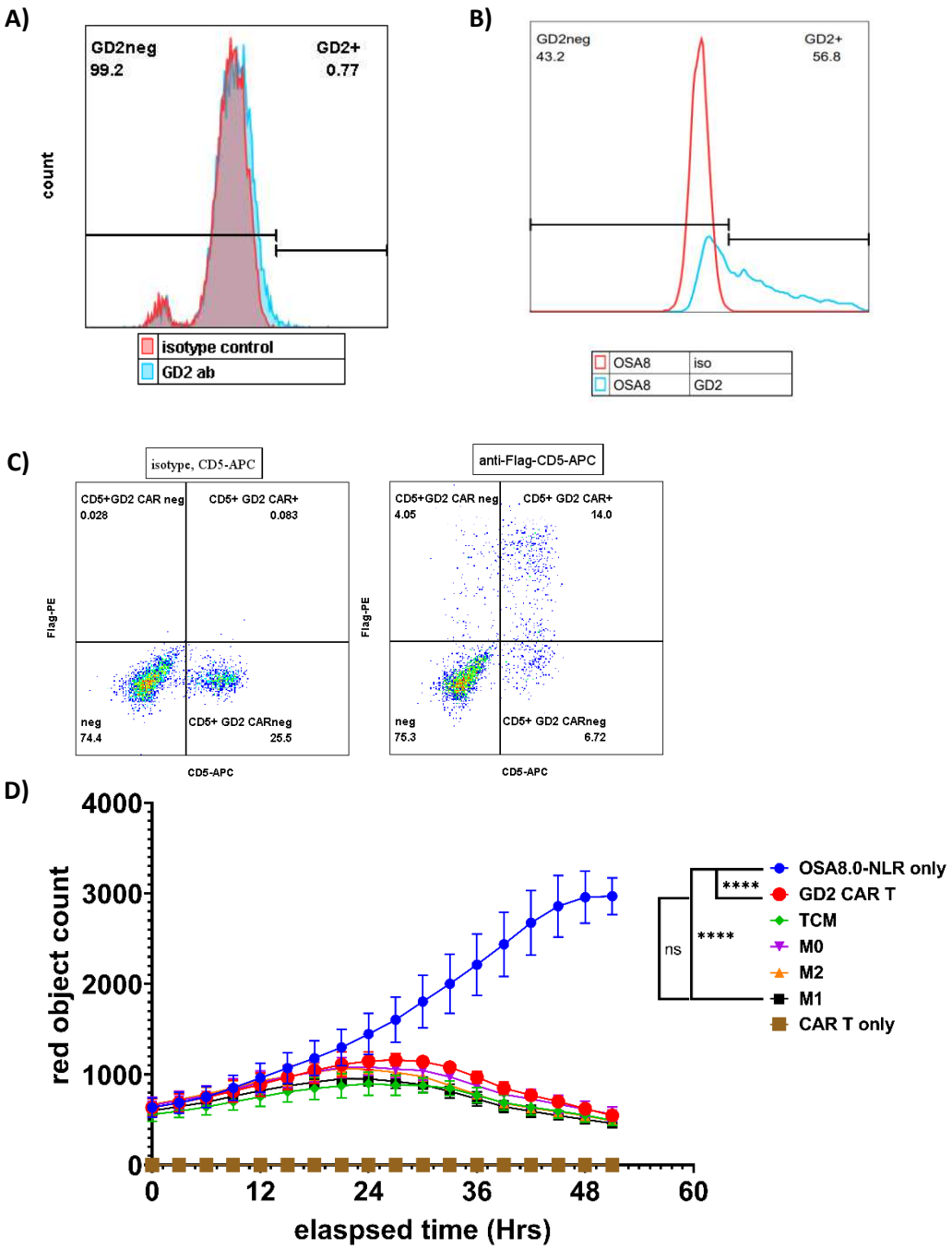

Figure 10. Effect of monocyte derive macrophages on GD2 CAR T cells *in vitro* A) expression GD2 on canine monocyte derive macrophages by flow cytometry **B)** expression of GD2 on canine OSA8.0 OS cell line by flow cytometry **C)** GD2 CAR and CD5 expression on transduced canine T cells by flow cytometry **D)** *In vitro* killing of canine OS target cells by naïve or macrophage conditioned GD2 CAR T cells over 48 at a E:T ratio of 5:1. CAR T cells are either naïve (GD2 CAR T) or conditioned for 24 hours with M1, M2, M0, or TCM polarized macrophages. Data is depicted graphically as mean ± SEM. Statistical differences were determined using ordinary one-way ANOVA, followed by Tukey's multiple comparisons adjustment (*$p \leq 0.05$, **$p \leq 0.01$, ***$p \leq 0.001$, **** $p \leq 0.0001$), ns for non-significant.

In vivo effects of TME modification by losartan and propranolol with B7-H3-CXCR2 CAR T cells

To investigate the *in vivo* effects of losartan and propranolol TME modification on B7-H3-CXCR2 CAR T cell therapy we use our SCID-beige canine OS xenograft model. SCID-beige mice were split into four treatment groups 1) B7-H3-CXCR2 CAR T: 2.5e6 B7-H3-CXCR2 CAR T cell (n=8), 2) CAR T combo: 2.5e6 B7-H3-CXCR2 CAR T cells with combination losartan (60 mg/kg) and propranolol (10 mg/mouse) (n=6), 3) losartan/propranolol: losartan and propranolol (n=6), 4) control: untreated (n=6). Mice in CAR T combo and losartan/propranolol groups were pretreated with drugs for 14 days prior to CAR T cell infusion. Mice were inoculated SQ with Abrams-luciferase cells 3 days prior to CAR T cell infusion. To prevent the effects of losartan from interfering with CAR T cell trafficking, the CAR T combo group was taken of losartan for 24 hours pre and post CAR T cell injection. Tumor implantation was confirmed by IVIS imaging on day 3 post tumor implantation prior to CAR T cell injections **(Figure 11A)**. B7-H3-CXCR2 CAR T cells were generated as previously described using 50 mL of whole blood from a tumor bearing dog[194]. Briefly, PBLs were isolated from whole blood and activated with anti-canine CD3/CD28 beads for 3 days. Activated T cells were transduced twice with B7-H3-CXCR2 retroviral bound on retronectin coated plates. CAR T cell dosing in mice is calculated based on total T cell count and transduction efficiency measured by protein-L staining analyzed by flow cytometry. B7-H3-CXCR2 CAR T cell transduction efficiency was 34.2% and a total of 7.3e6 T cells were injected I.V. by tail vein per mouse to achieve 2.5e6 CAR T cells per mouse.

Tumor growth was monitored by blinded serial caliper measurements and IVIS imaging. Mice were humanely euthanized when tumors ulcerated through the skin or grew greater than 1.0 cm at the longest diameter. We found that there was no significant tumor reduction in any of the groups **(Figure 11B)**. There was no benefit to survival in any of the treatment groups compared to control. However, there was a trend of decreased survival by CAR T combo group (median survival = 25 days) compared to control (median survival = 34 days) **(Figure 11C)**.

We hypothesized that the cessation of losartan 24 hours pre and post CAR T cell infusion may cause a rebound of TAMs promoting tumor growth more than the control mice. This has been previously demonstrated in a mouse model of mammary tumors with CCR2 blockade[231]. Tumors were excised at endpoint and processed into a single cell suspension and stained for anti-mouse CD11b and F4/80 to detect mouse TAMs. We found that there was no significant difference in percentage of TAMs between treatment groups **(Figure 11D)**.

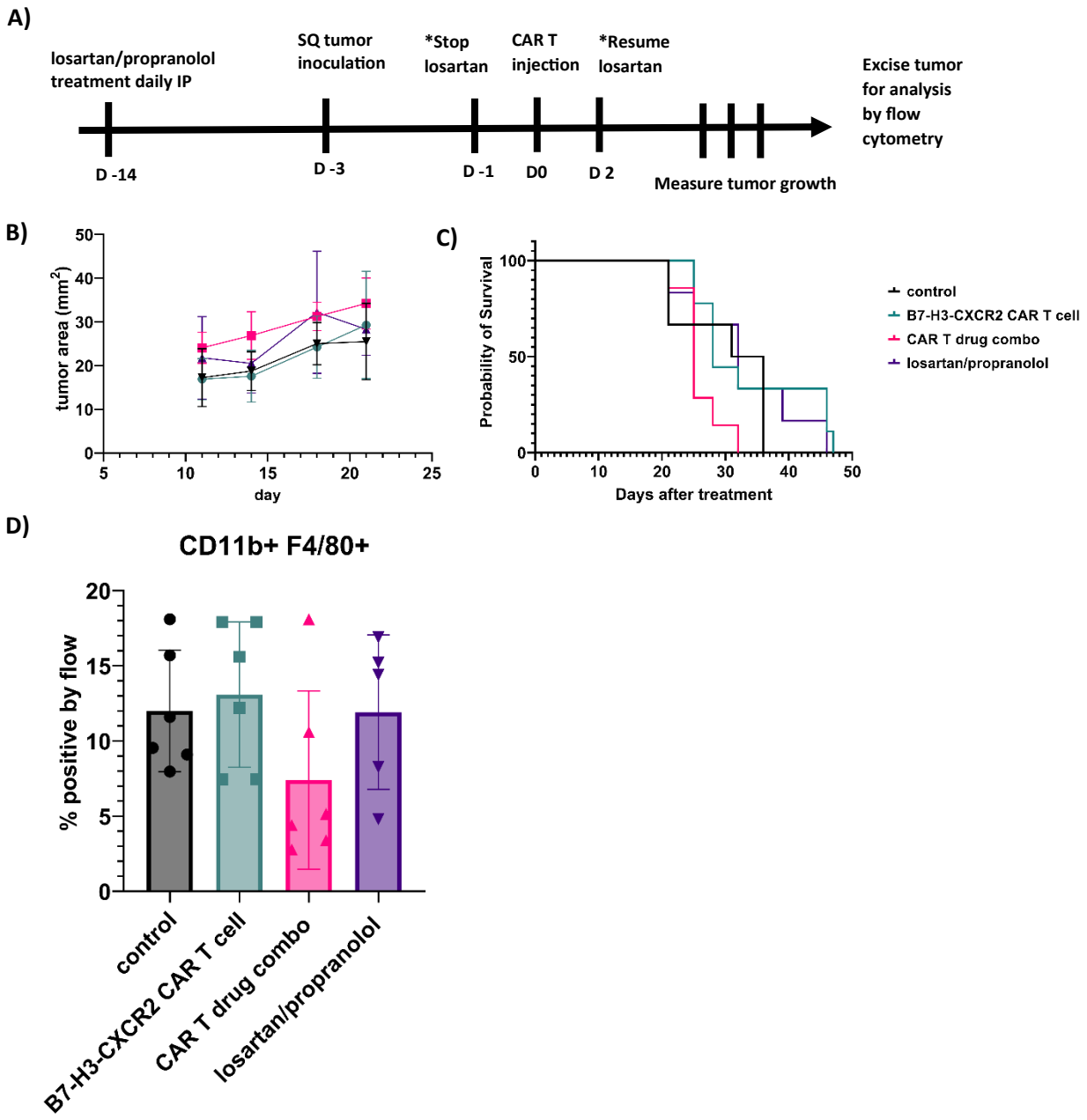

Figure 11. Effect of losartan and propranolol on B7-H3-CXCR2 CAR T cells in a SCID-beige xenograft OS model **A)** experimental design **B)** tumor growth of canine xenograft Abrams-Luc tumors treated with vehicle control, B7-H3-CXCR2 CAR T cells, CAR T cells with losartan and propranolol combo or losartan and propranolol **C)** Kaplan-Meyer survival curves of SCID beige mice with Abrams-Luc SQ tumors treated with vehicle control, B7-H3-CXCR2 CAR T cells, CAR T cells with losartan and propranolol combo or losartan and propranolol. **D)** CD11b+F4/80+ TAMs from excised Abrams-Luc tumors as measured by flow cytometry

To investigate the effects of losartan cessation in our mouse model, we repeated our mouse experiment adjusting the administration of losartan and propranolol. CAR T combo and losartan/propranolol treated mice were not pre-treated with losartan and propranolol but instead given losartan and propranolol on day 1 post tumor inoculation and given drug continuously without cessation. All other variables remained the same as the previous experiment **(Figure 12A)**. We found that there was no significant difference in tumor growth in all groups **(Figure 12B).** We observed that there was no significant difference in survival amongst all the treatment groups. The trend that we previously saw in decreased survival amongst the CAR T combo group was reversed with a median survival time of 34 days for all groups **(Figure 12C)**. Since we did not see an anti-tumoral effect from either CAR T cell treated groups we evaluated the tumors for infiltrating canine T cells by flow cytometry. We found that there were no significant canine lymphocyte infiltrates as seen by anti-canine CD45 and CD5 staining **(figure 12D)**.

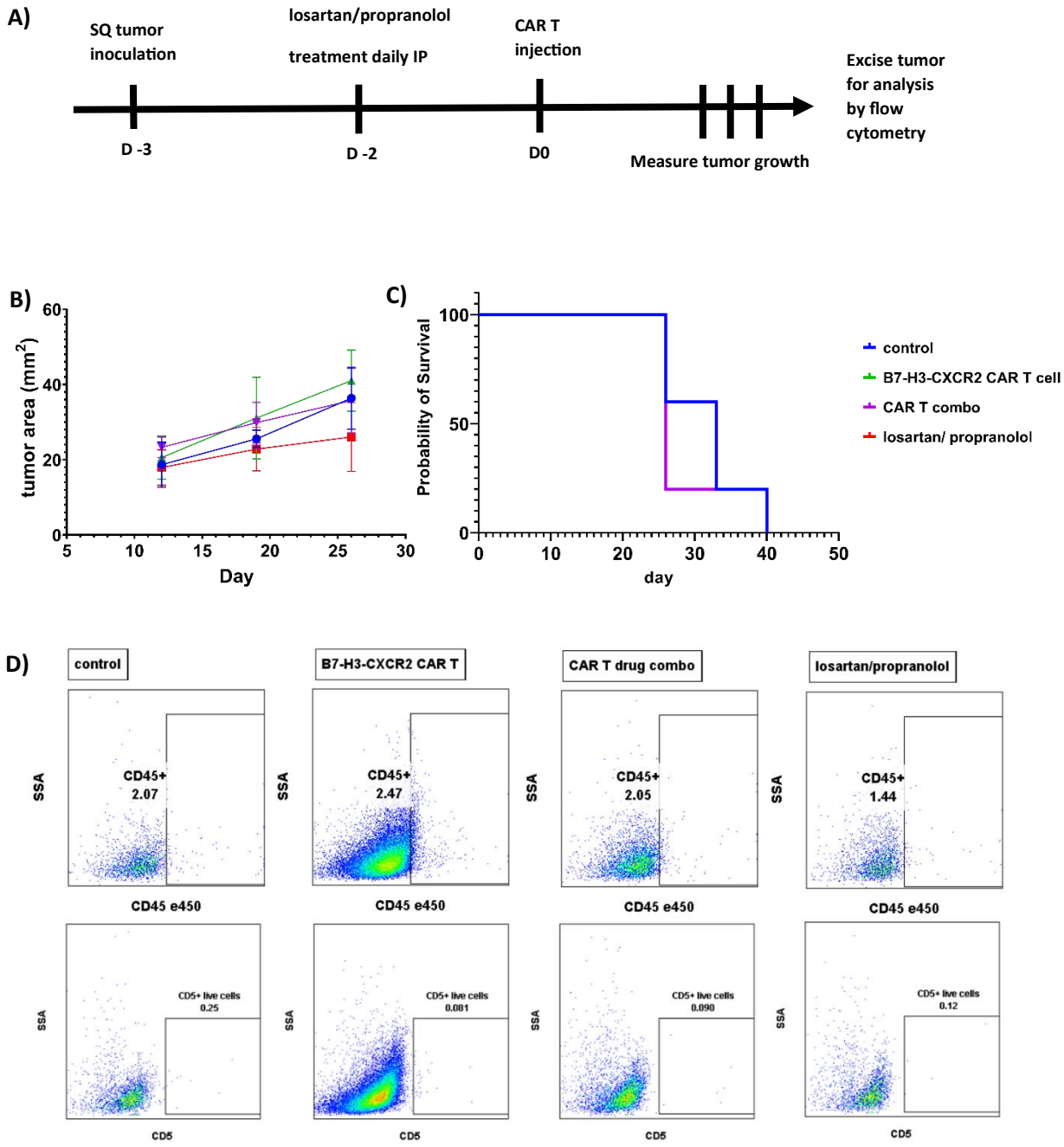

Figure 12. A) experimental design **B)** tumor growth of for mice implanted with SQ Abrams-luc tumors treated with either control, BC CAR , BC CAR T combo or losartan/ propranolol **C)** Kaplan-Meyer survival curves for mice implanted with SQ Abrams-luc tumors treated with either control, BC CAR , BC CAR T combo or losartan/ propranolol **D)** representative flow plots of canine CD45+ and CD5+ cells within the tumor of mice implanted with SQ Abrams-luc tumors treated with either control, BC CAR , BC CAR T combo or losartan/ propranolol

We hypothesized that since SCID-beige mice still have functional myeloid lineage cells and dysfunctional NK cells that the intact immune cells within SCID-beige mice may be deleting the xenograft canine CAR T cells. We used a small sample of SCID-beige mice with SQ implanted Abrams-Luc tumors and treated them either with B7-H3 CAR T cells (n=3), B7-H3-CXCR2 CAR T cells (n=3) or no treatment control (n=1). Generated CAR T cells were labeled with CellTrace violet cell proliferation kit (Invitrogen cat#C34557) prior to injection **(Figure 13A)**. CAR T treated mice were injected with high dose 1.0e7 CAR T cells/mouse by tail vein (n=3) on day 7 post tumor implantation. Mice were euthanized on day 4 post CAR T injection and tumor, spleen, bone marrow and peripheral blood was collected for analysis by flow cytometry **(Figure 13B)**. Tissues were processed into a single cell suspension and stained with anti-canine CD45-APC and anti-canine CD5-PE. We did not find significant amounts of canine lymphocytes by cell trace violet or anti-canine CD45 staining in either the tumor **(figure 13C)** or peripheral blood **(figure 13d).** There were also no detectable canine lymphocytes within the spleen, or bone marrow (supplemental figure 6).

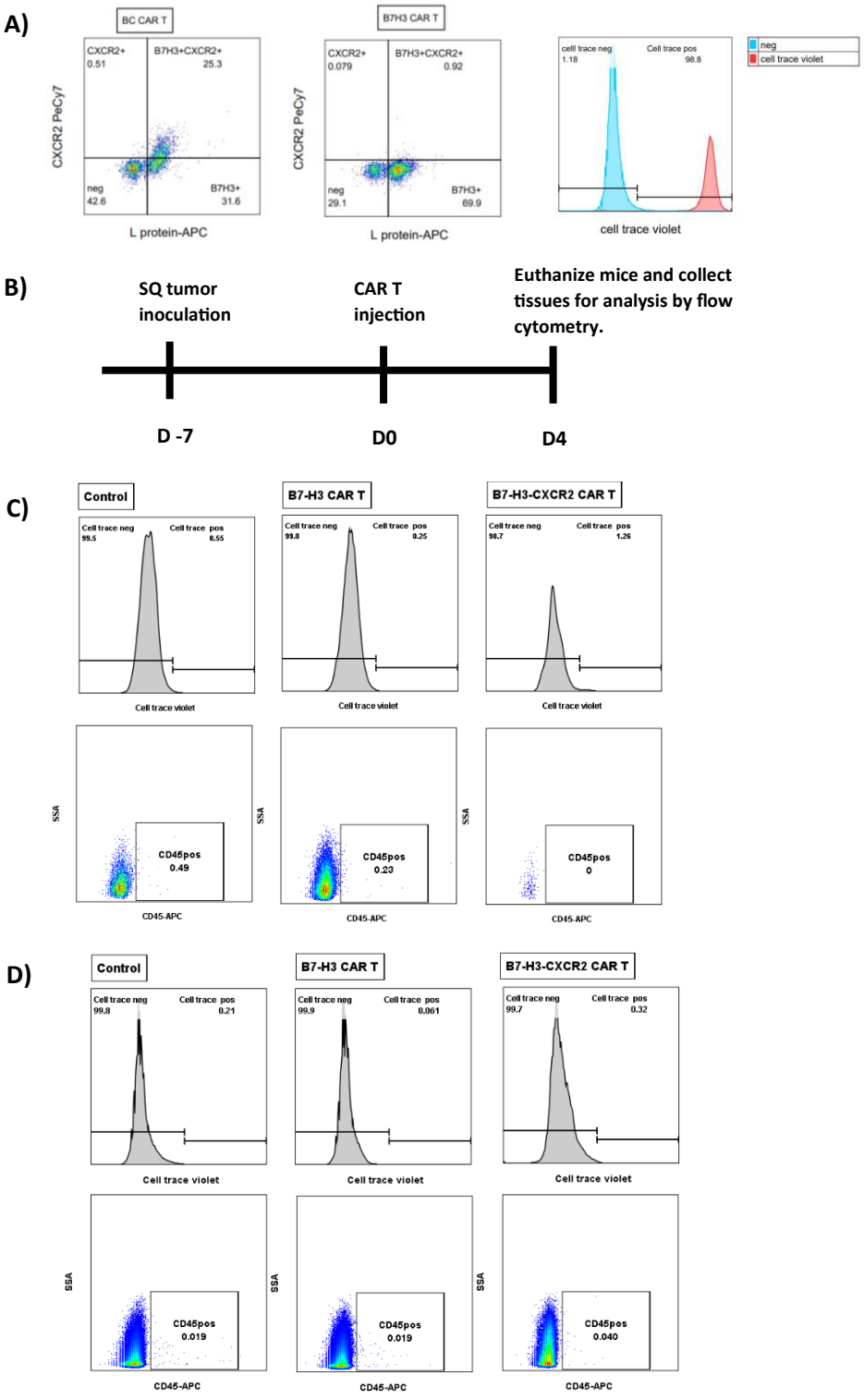

Figure 13. A) CAR T cell transduction efficiency measured at day 14 of generation and stained with CellTrace violet **B)** experimental design **C)** tumors analyzed by flow cytometry for cell trace violet positive cells and anti-canine CD45 **D)** PBMC analyzed by flow cytometry for cell trace violet positive cells and anti-canine CD45.

Discussion

In this study we used a SCID-beige mouse strain to model the interaction of myeloid suppressor cells withing the TME and B7-H3-CXCR2 CAR T cells. SCID-beige mice were selected to model the myeloid cell component as the NOD-SCID-gamma (NSG) mouse model that is standard in CAR T cell preclinical models has defective myeloid lineage cells. While the severe immune deficiency in NSG mice make it amenable to hematopoietic xenografts, the reduced mature macrophage population and reduced DC function due to defects in IL-1 secretion do not make it a good model for myeloid cell interactions within the TME[232]. SCID-beige mice maintain intact macrophages and dendritic cells but do not have mature B cell and T cell populations, and have defective NK cells populations with reduced capacity for degranulation[230]. This impairment of adaptive immunity makes SCID-beige mice amenable to xenografts and have been successfully used to model human CAR T cell therapy for human ovarian carcinoma and mesothelioma[233-235].

Our group has previously shown that treatment of combination losartan and propranolol paired with an allogenic cancer stem cell vaccine induced an overall clinical benefit of 80% in dogs with glioma [173]. TME modification by losartan is mediated though its function as a competitive CCL2 inhibitor which blocks monocyte migration in tumor sites, significantly decreasing TAM populations in a mouse model of metastatic breast cancer[168]. Additionally, the β-adrenergic receptor blocker propranolol has been shown to reduce the bone marrow mobilization of MDSCs reducing their population within the TME and increasing CD8+ and NK cell populations within the TME[170,236]. Therefore, we hypothesized that treatment with combination losartan and propranolol would modify the TME in OS to reduce TAMs and MDSCs. We showed that SCID-beige mouse myeloid cells migrate to canine OS xenograft subcutaneous tumors and infiltrate into the tumors. Additionally, treatment with combination losartan and propranolol 5 days after tumor implantation significantly reduces the percentage of immune suppressive CD11b+Ly6c^{high} TAMs within a canine OS xenograft mouse model (Figure 8D).

The immune suppression by the TME is classically thought to be largely exerted through TAMs that make up for over 50% of the immune cells within the TME in OS[237]. TAMs within OS are characterized as a mix of proinflammatory M1 and anti-inflammatory M2 although it is worth noting that biologically TAMs exist on a spectrum of functional states[238]. Immune suppression by TAMS is exerted through cell surface signaling through checkpoint molecules such as PD-L1, secreted factors such as TGFβ, IL-4 and IL-10 and through promotion of angiogenesis through secretion of proangiogenic factors such as vascular endothelial growth factor (VEGF), TNF and CXCL8[238]. We investigated the impact of monocyte derived macrophages (MDMs) on B7-H3-CXCR2 CAR T cells *in vitro*. We polarized canine MDMs to be either classically proinflammatory M1, immune suppressive M2, resting M0 or immune suppressive with tumor media conditioning (TCM) from canine OS cell line Abrams-RFP supernatant as previously described and validated[229]. We hypothesized that MDMs polarized to immune suppressive phenotypes M2 and TCM would inhibit the killing activity of B7-H3-CXCR2 CAR T cells against B7-H3+ canine OS tumor cells. We found that all macrophage conditioned B7-H3-CXCR2 CAR T cells had greater killing activity than that of naïve B7-H3 CAR T cells that had not been co-cultured with MDMs (Figure 9C). We found that MDMs were B7-H3+ with M1 MDMs having the greatest level of expression and M0s having the lowest according to median florescence intensity (Figure 9A and B). MDMs had much lower level of B7-H3 expression than that of high expressing canine OS cell lines but comparable to that of low expressing tumor cell lines such as Moresco or D17. We propose that the increase in killing activity by MDM conditioned B7-H3-CXCR2 CAR T cells was due to the signaling of B7-H3 from the macrophages through the B7-H3 CAR prior to co-culture with the target tumor cells. B7-H3+ macrophages act as a source of target antigen to prime B7-H3 CAR T cells prior to tumor cell co-culture.

To further investigate the mechanism of CAR T cell enhancement by macrophage conditioning we used a different CAR construct targeting GD2 which is not expressed on macrophages (Figure 11A). We found that conditioning of GD2 CAR T cells with MDMs did not enhance or dampen GD2 CAR T cell killing

against GD2 high expressing canine OS cell OSA8.0-NLR *in vitro* regardless of polarization. This indicates that the CAR T cell enhancement we see with macrophage conditioning may be unique to B7-H3 targeting CAR T cells as B7-H3 is a co-stimulatory molecule with known native expression on myeloid lineage cells such as macrophages[149].

Macrophages and other myeloid cells may act as a source of antigen for B7-H3 targeting CAR T cells which may confound our method of TME modification through TAM and MDSC depletion through administration of losartan and propranolol. Although we know that myeloid lineage immune suppressor cells within the TME exert a strong immune suppressive force especially to anti-tumoral lymphocytes, activation of B7-H3 CAR by TAMs may potentially be immune stimulatory based on our *in vitro* data. Myeloid immune suppressor cells such as TAMs and MDSCs also recruit and induce immune suppression of other cell types such as tumor associated neutrophils (TANs), and regulatory T cells[167]. Additionally, secreted factors from immune suppressor cells remodel the tumor vasculature inducing hypoxic areas and impairing anti-tumoral lymphocyte infiltration into the tumor[238]. To investigate the effect of combination losartan and propranolol on B7-H3-CXCR2 CAR T cells and to evaluate if TAM depletion by blocking of monocyte migration would have a net positive or negative effect on CAR T cell treatment, we evaluated B7-H3-CXCR2 CAR T cell therapy with and without losartan and propranolol in our a canine OS xenograft SCID-beige mouse model.

We found no benefit to either B7-H3-CXCR2 CAR T cell treatment or with CAR T cell treatment in combination with losartan and propranolol (Figure 11B). There was no significant survival benefit to any of the groups however that was a trend for the CAR T cell drug combo group doing worse than the control untreated group (Figure 11C). We hypothesize this is due to the 24-hour cessation of losartan treatment both pre and post CAR T cell injection causing a rebound of TAMs contributing to greater tumor growth than that of even untreated mice[231]. We repeated the experiment giving continuous losartan treatment and starting losartan and propranolol treatment one day post tumor implantation instead of pretreating

11 days before (Figure 12A). We found the decrease in survival in the CAR T drug combo group was reversed back to that of the control group (Figure 12C). We however did not see any tumor suppression or survival benefit in any CAR T treatment group (Figure 12B). We looked for persistent tumor infiltrating canine lymphocytes within the tumor by anti-canine CD45 and anti-canine CD5 staining and analysis by flow cytometry and did not find any canine CD45+ or CD5+ cells within the tumor (Figure 12D).

We hypothesized that the remaining intact immune system of the SCID-beige mice was detecting and deleting canine T cells before the CAR T cells had a chance to enact an antitumor effect. We used a small sample of SCID-beige mice and treated with CellTrace violet labeled high dose B7-H3 CAR T (n=3), B7-H3-CXCR2 CAR T (n=3) or no treatment control (n=1) at day 7 post SQ tumor implantation with Abrams-Luc OS cell line (Figure 13A and B). We euthanized all the mice on day 4 post CAR T injection and collected tumor, spleen, bone marrow and peripheral blood to try and detect CAR T cells by flow cytometry. We could not find significant CellTrace violet+, CD45+ or CD5+ cells in any of the tissues indicating that the CAR T cells were not persisting long enough to have an anti-tumoral effect (Figure 13 C and D, Supplementary figure 6). Although other groups have used SCID-beige mice with human xenograft CAR T cells in ovarian and mesothelioma models and seen antitumoral effects and persistence of their xenograft human CAR T cells[234,235] canine CAR T cells do not persist in SCID-beige mice. SCID-beige mice are clearly not a viable mouse strain to model canine xenograft CAR T cells due to the lack of persistence of canine CAR T cells. Although more investigation needs to be done to determine if it is the mouse immune cells that are detecting and deleting the canine CAR T cells, we know that canine CAR T cells persist and can be detected at day 14 post injection with NSG mice.

NSG mice are severely immune compromised with dendritic cells and macrophages that are both impaired in function and reduced in numbers compared to immune competent mice[239]. NSG mice, while the standard for CAR T cell xenograft models, are not ideal for modeling the interaction of the myeloid cell component of the TME with CAR T cell therapy in combination with TME modifying drugs. NSG mice could

be used to get a preliminary view as the myeloid cell types are still present and may be affected by CCL2 blockade and repolarization with propranolol. Use of propranolol in an NSG mouse model of human xenograft melanoma did find reduction in tumor and inhibition of angiogenesis, they however did not report any immune modulating effects of propranolol and contributed the effects of propranolol to direct tumor cell beta adrenergic receptor blockade[240]. To get a fuller picture of tumor associated myeloid suppressor cell interaction with CAR T cells a fully immune competent model is needed. Either a fully mouse system or canine OS can be used as an immune competent model for TME modification in conjunction with B7-H3-CXCR2 CAR T cell therapy based on the work we've established. Losartan and propranolol have been shown effective in a canine clinical trial with metastatic OS and in canine glioma in combination with other immunotherapies either TKI inhibitor or cancer stem cell vaccine[172,173].

In summary we showed that mouse myeloid cells do infiltrate canine xenograft OS tumors and that TAM depletion by combination TME modulating drugs losartan and propranolol can be modeled in a SCID-beige mouse strain. TAMs may be a source of antigen for anti-B7-H3 CAR T cell enhancing their function *in vitro*. It remains to be seen if collectively the immune suppressive TME with B7-H3 expression is stimulatory or inhibitory to B7-H3 targeting CAR T cells. Canine CAR T cells in SCID-beige mice do not persist long enough to have an antitumoral effect. Further investigation needs to be done to model the interaction of the TME within OS on B7-H3-CXCR2 CAR T cells with and without TME modification by losartan and propranolol.

Chapter 5: Conclusions and future directions

Summary

Chimeric antigen receptor (CAR) T cell therapy is a revolutionary innovation in adoptive cell therapy. Despite incredible success in treating B cell malignancies through the targeting of B cell lineage antigen CD19, application of CAR T cell therapies to other malignancies has not seen the same clinical success especially in solid tumors. B7 homolog 3 (B7-H3) is a checkpoint molecule that has been found to be overexpressed on many different solid tumor types including sarcomas and gliomas. Refractory or metastatic osteosarcoma (OS) has few effective treatment options to which CAR T cell immunotherapy would be a welcomed addition. Establishment of canine OS as a large animal, immune competent spontaneous cancer model for B7-H3 CAR T cell therapy would serve as a translational platform for improving CAR T cell therapy in a solid tumor setting as well as offer a new treatment option for dogs with metastatic OS.

This thesis investigates B7-H3 as a tumor antigen target in canine OS for CAR T cell therapy. The body of work we have performed for this dissertation addressed the existing knowledge gaps regarding B7-H3 expression on canine OS, and anti-human B7-H3 CAR antigen specific targeting of canine B7-H3. This thesis also expands on the established works to optimize canine CAR T cell generation for both improved CAR T cell yield and post expansion activity. We further investigated the effects of the addition of chemokine receptor CXCR2 on B7-H3 CAR T cell anti-tumoral efficacy through increased CAR T cell trafficking to chemokine signal CXCL8 both *in vitro* and *in vivo*. Finally, we investigated the effect of tumor microenvironment (TME) modification with repurposed drugs propranolol and losartan on canine OS in a murine model and how macrophage signaling effects B7-H3-CXCR2 CAR T cell function. Taken together our findings align with the current literature and show that canine OS is a feasible model for B7-H3 CAR T cell therapy and that addition of chemokine receptor CXCR2 increases CAR T cell persistence and antitumoral effect *in vivo*.

Conclusions

B7-H3 is proposed as a "pan-cancer" antigen being overexpressed on many sarcomas and CNS tumors[147]. Zhang et al 2022 found that B7-H3 was also overexpressed in canine OS[198], we also further validated this in parallel with the addition of 6 canine OS cell lines and 8 FFPE primary OS tumor biopsies showing positive B7-H3 overexpression above that of screened normal canine spleen, liver, peripheral blood, and lymph node. We optimized canine B7-H3 CAR T cell generation from isolation of peripheral blood lymphocytes from whole blood of tumor bearing dogs. Our findings for optimal activation and transduction methods align with published protocol for generating canine CD20 CAR T cells[194]. Additionally, we found that supplementation of recombinant human IL-7 and IL-15 increase canine B7-H3 CAR T cell killing efficiency of B7-H3 positive canine OS target cells *in vitro*.

We evaluated B7-H3 CAR T cell activity *in vitro* and showed that canine B7-H3 CAR T cells were activated and produced IFNγ when co-cultured with canine B7-H3 positive OS cell lines. B7-H3 CAR T cell activation correlated with the level of expression of B7-H3 antigen with B7-H3^{high} OS cell lines such as Abrams and McKinley induced the greatest amount of IFNγ production while B7-H3^{low} OS cell lines D17 and Moresco induced the least IFNγ production. We also confirmed that activation of canine CAR T cells was through the B7-H3 CAR as donor matched activated T cells did not produce IFNγ when co-cultured with canine OS cell lines. We validated cross reactivity and affinity gating of the human B7-H3 CAR construct with canine B7-H3 antigen through target cell killing of B7-H3^{high} OS cell lines Abrams and OSA8.0 over 48 hours *in vitro* but did not kill B7-H3^{low} D17. Further, we showed cross reactivity of anti-human B7-H3 antibody (clone 7-517) with isolated canine B7-H3 protein by western blot (supplemental). Collectively these findings show that B7-H3 is a viable target for canine OS having high frequency of overexpression on canine OS tissues as well as low to no expression on normal tissues. Application of the existing human B7-H3 CAR construct to dogs is also feasible in both generation of canine B7-H3 CAR T cells and with cross

reactivity of human B7-H3 CAR with canine B7-H3 antigen. Developing anti-B7-H3 CAR T cells for dogs can serve as an important translational model to improve treatment options in metastatic OS in both pet dogs and human patients. Use of the dog model can also be used to gather more clinically relevant insights for improvements of B7-H3 CAR T cell therapy in a spontaneously occurring, immune competent OS model bridging the gap between murine models and human clinical trials.

Limitations of study

While we did show no or low expression of B7-H3 in a select number of normal tissues we did not do an extensive screen of normal tissues to ensure safety of B7-H3 CAR T cell targeting in dogs. Further screening can be done on other major tissue organs such as normal heart, lung, kidney, and brain to further validate the safety of B7-H3 CAR T cell targeting in dogs. We know that our B7-H3 CAR is affinity gated, not being activated by low expressing B7-H3+ cell lines such as D17. Further work to quantify antigen expression and B7-H3 CAR activation through quantification of B7-H3 surface molecules and generation of low, moderate, and high expressing cell lines can be done to ensure safety of B7-H3 CAR T cells in dogs[147]. Zhang et al. 2022 demonstrated that high dose administration of second generation B7-H3 CAR T cells in healthy beagles did not show any CAR T cell associated severe adverse side effects. While we can infer based on this data that our B7-H3 CAR T cells will not be activated by low levels of B7-H3 on normal tissues, any application of B7-H3 CAR T cells into a canine patient will require careful monitoring for CAR T cell associated adverse events. It is also known that increased tumor burden positively correlates with risk of CAR T cell associated adverse events specifically the incidence of cytokine release syndrome. So, while B7-H3 CAR T cells may not target normal tissues specifically we cannot conclude at this time that it will be safe in antigen positive tumor bearing dogs.

Future directions

Our work established the feasibility of targeting B7-H3 for CAR T cell therapy in canine OS. With the generation of canine B7-H3 CAR T cells optimized the application of B7-H3 CAR T cells is readily applicable to other tumor types that overexpress B7-H3. We have found three canine glioma cell lines and two FFPE glioma samples are also positive for B7-H3 expression (supplemental fig 5). Further screening can be done to expand B7-H3 CAR T cell targeting to other B7-H3 positive tumor types. Screening of B7-H3 expression can be done on available canine tumor cell lines including melanoma, mammary carcinoma, hemangiosarcoma, transitional cell carcinoma, mast cell tumor, thyroid carcinoma, soft tissue sarcoma and histiocytic sarcoma. B7-H3 positive cell lines would need to be validated with B7-H3 staining of primary tumor biopsies. Additionally, validation needs to be done to show B7-H3 CAR T cell activity and direct cell killing of other B7-H3 positive tumor types.

Based on canine CD20 CAR T cell therapy in dogs with lymphoma we know that canine CAR T cells expressing human CAR constructs are detected by the canine immune system with canine CAR reactive antibodies being detected at day 18 post infusion, limiting canine CAR T persistence if using a CAR derived from mouse or human. To fully establish B7-H3 CAR T cell therapy as an effective treatment for metastatic OS in dogs and to be able to evaluate long term outcomes and anti-tumoral effectiveness, generation of a fully canine CAR construct will need to be done to avoid detection and deletion of CAR T cells by the dog's native immunity.

Efficacy of dual targeting B7-H3-CXCR2 CAR construct against single agent B7-H3 CAR T cells in canine osteosarcoma

Conclusions

CAR T cell therapy as a single agent in solid tumors has largely not been shown to be clinically effective [128]. One major barrier to clinical success in solid tumors such as OS is the failure of CAR T cell

trafficking to local tumor sites from the circulatory system[128,207]. Modification with exogenous chemokine receptors in addition to CAR targeting to improve CAR T cell has been shown to increase CAR T cell efficacy without additional toxicity[159,165,207]. Hence, we investigated the addition of human CXCR2 as a chemokine receptor with our B7-H3 CAR. Investigation of CXCR2-CXCL8 signaling revealed that canine OS cell lines secreted high levels of chemokine CXCL8 and that human CXCR2 cross reacts with canine CXCL8 by *in vitro* trans-well migration assay. While B7-H3-CXCR2 CAR T cells did not enhance target cell killing *in vitro* we did find enhanced secretion of proinflammatory cytokines IFNγ and IL-2. We investigated the transcriptomic differences between B7-H3-CXCR2 CAR and B7-H3 CAR T cells showing upregulating in metabolic pathways and immune genes such as IL15Rα by B7-H3-CXCR2 CAR T cells. In mice with xenograft B7-H3+ CXCL8 secreting tumors we found anti-tumoral activity by B7-H3-CXCR2 CAR T cells than that of B7-H3 CAR T cells at the same dose of 5.0e6 CAR T cells/mouse with a greater proportion of the mice achieving complete tumor elimination. Altogether our findings show increased anti-tumoral efficacy of B7-H3 CAR T cells that is enhanced with the addition of chemokine receptor CXCR2.

Limitations of study

A limitation of this study is the lack of increased survival data within the mice treated with either B7-H3 CAR T cells or B7-H3-CXCR2 CAR T cells. While mice treated with dual targeting B7-H3-CXCR2 CAR T cells had greater tumor responses we were not able to show an increase in survival by B7-H3-CXCR2 treated mice since many of the mice also experienced unexplained adverse events such as jaundice and hind limb paresis which is suspected due to graft versus host disease (GVHD) due to the canine CAR T cell. Further investigation needs to be done on the adverse effects of canine CAR T cell treatment in our mice as the classical signs of GVHD such as hair loss, diarrhea or fever were not seen in any of the mice. H&E staining of affected mouse livers showed large immune infiltrates. Future studies should be done at a lower dose of canine CAR T cells especially the B7-H3-CXCR2 CAR T cells as they have been shown to be more immunologically active *in vitro*. Treatment in future studies with client owned dogs with metastatic OS will

be done with autologous CAR T cells therefore possible GVHD due to CAR T cell dose would not be a concern.

Additionally, we showed *in vitro* migration of canine B7-H3-CXCR2 CAR T cells to recombinant canine CXCL8 by transwell migration assay with a single replicate. Additional technical and biological replicates of this experiment would more robustly show the cross reactivity of the human CXCR2 to canine CXCL8. Use of anti-human CXCR2 blocking antibody to block migration would also more definitively show that it is signaling through exogenous canine CXCL8 that induces migration in our canine B7-H3-CXCR2 CAR T cells. Addition of canine B7-H3 CAR T cells to the migration assay would show the effect of exogenous CXCR2 on migration to show that increase in migration is due to CXCR2 signaling.

We used a NSG mouse strain to show *in vivo* efficacy of our B7-H3 CAR T cell with increased tumor control by our dual targeting B7-H3-CXCR2 CAR T cell. This mouse stain is severely immune compromised which allows for the engraftment of xenograft OS tumors as well as persistence of intravenously injected canine CAR T cells and is the standard strain used in mouse modeling for CAR T cell therapy. However, use of the NSG mouse strain does not accurately recreate the TME of OS that is a large component to tumor immune evasion. Although we saw complete tumor elimination in our mice that we do not expect complete remission in the clinical setting based on previous track record of solid tumor CAR T cell clinical research pipeline[96,128]. An immune competent animal model would more accurately indicate expected results in a clinical setting.

We used a subcutaneous tumor model when our goal is to use B7-H3 CAR T cells in a metastatic OS setting. Injecting Abrams-luciferase tumor cells IV creates a metastatic model with tumors forming in the lungs[241]. A lung metastatic OS mouse model and would have given more accurate insights into CAR T cell efficacy in metastatic OS.

Future directions

Our study found that B7-H3-CXCR2 CAR T cells had increased cytokine production and upregulation of metabolic pathways compared to B7-H3 CAR T cells. We hypothesized that this was due to autocrine signaling of endogenous CXCL8 from the CAR T cells to exogenous CXCR2. Further investigation can be done by blocking of CXCL8 signaling through anti-canine CXCL8 antibody and/or use of an anti-human CXCR2 blocking antibody would show if CXCL8 signaling increased activation status and metabolic pathways in B7-H3-CXCR2 CAR T cells.

Future studies need to be done to evaluate the *in vivo* trafficking of our B7-H3-CXCR2 CAR T cells compared to B7-H3 CAR T cells. Additional mouse experiments comparing B7-H3-CXCR2 CAR T cells with B7-H3 CAR T cells should be conducted to evaluate the spleen, bone marrow, peripheral blood, and tumor at set endpoints to measure kinetics and quantify enrichment of CAR T cells in certain tissues. This would verify if increased tumor control was due to increased trafficking of B7-H3-CXCR2 CAR T cells to the tumor. Antigen recognition by CAR T cells also can induce post infusion *in vivo* expansion of CARs which could have only been detected by sampling of tumor and major lymphoid organs.

Effect of tumor associated macrophages and TME modifying immunotherapy on B7-H3-CXCR2 CAR T cell function

Conclusions

Our group has previously established that losartan inhibits monocyte migration and decreases establishment of TAMs through the blockade of CCL2 signaling. Additionally, our group has shown that propranolol works synergistically with losartan by inhibition of MDSC mobilization[168,170,172]. Therefore, we hypothesized that TME modification by losartan and propranolol would reduce TAM and MDSC populations within OS tumors and enhance B7-H3-CXCR2 CAR T cell function.

We found that treatment of combination losartan and propranolol significantly decreased the percentage of mouse immune suppressive CD11b+Ly6C^{high} TAMs within canine OS tumors. Conditioning of B7-H3-CXCR2 CAR T cells with donor matched monocyte derived macrophages (MDMs) enhanced tumor cell killing by B7-H3-CXCR2 CAR T cells regardless of macrophage polarization to immune suppressive or proinflammatory phenotypes. CAR T cell enhancement by MDMs was not seen when we used anti-GD2 CAR T cells that did not have CAR antigen expression on macrophages.

Evaluation of B7-H3-CXCR2 CAR T cells with combination losartan and propranolol revealed that cessation of losartan worsened survival compared to untreated control in SCID-beige mice, although this finding was not significant. Repetition with continuous losartan administration reversed this finding and survival of CAR T drug combo was not different to that of untreated controls. Treatment of B7-H3-CXCR2 CAR T cells did not induce any treatment benefit above untreated control mice. We found that this was due to a lack of CAR T cell persistence in the SCID-beige mouse model as shown by analysis of bone marrow, peripheral blood, spleen, and tumor by flow cytometry. To our knowledge this is the first study looking at the interaction of combination TME modifying drugs losartan and propranolol on CAR T cell therapy. We also took a preliminary look at the unique interaction of immune suppressive macrophages and B7-H3 targeting CAR T cells showing that even M2 polarized macrophages improved anti-B7-H3 CAR T cell function likely through macrophage B7-H3 antigen recognition by B7-H3 CAR.

Limitations of study

A limitation of this study was the small number of SCID-beige mice that we used in our losartan and propranolol experiment with n=3 for control, n=4 for each treatment group. While we did find significant differences in TAMs between control and combination losartan and propranolol treated groups it would be valuable to evaluate our findings with additional mice. Furthermore, treatment with B7-H3-CXCR2 CAR T cells in SCID-beige mice did not have any anti-tumoral benefit unlike in our NSG mouse model due to lack of persistence of our canine CAR T cells in SCID-beige mice. Further consideration of mouse

strain needs to be taken for modeling the interaction of CAR T cells and myeloid cell TME modification *in vivo*.

Enhancement of B7-H3-CXCR2 by macrophage conditioning *in vitro* through B7-H3 signaling could have been further validated with an anti-B7-H3 blocking antibody to see if blocking B7-H3-CAR signaling reversed the effect of macrophage conditioning. Additional biological replicates with macrophage conditioning with GD2-CAR T cells could have been done to more robustly show that CAR T cells without antigen recognition are not enhanced by macrophage co-culture as we only did one biological replicate.

Future directions

Further studies need to be done to model the complex interaction of the myeloid cell component within the TME on B7-H3-CXCR2 CAR T cells. This will likely have to be achieved using an immune competent model to recapitulate the myeloid cell population within the TME. This can be achieved through a fully mouse model using mouse OS tumor and mouse B7-H3-CXCR2 CAR T cells or with a spontaneously occurring dog metastatic OS model using the work we've done so far with canine B7-H3-CXCR2 CAR T cells. Use of NSG canine xenograft OS model can be used to give a preliminary look at the interaction between B7-H3-CXCR2 CAR T cells and losartan and propranolol as NSG mice do have dendritic cells and macrophages. The results of this may not be fully clinically relevant however as NSG mature macrophages are reduced in number and function at base line due to defects in IL-1 secretion[239].

Additional studies to validate the safety in the administration of B7-H3-CXCR2 CAR T cells in dogs need to be done before evaluating efficacy in client owned dogs with metastatic OS. We are currently purposing a 3+3 safety trial in client owned dogs with metastatic OS to evaluate the safety of treatment of B7-H3-CXCR2 CAR T cells (supplemental fig 8). Starting treatment group with low dose CAR T cells 5.0e5 CAR T cells/kg and escalating to 1.0e6/kg and then 2.5e6 CAR T cells/kg. Establishment of B7-H3-CXCR2 CAR T cells as a clinical therapy for dogs with metastatic OS can bring a new form of immune therapy to

this veterinary species. Additionally, application of CAR T cells to canine OS will also act a platform to improve solid tumor B7-H3-CXCR2 CAR T cell therapy through the investigation of additional combination therapies such as TME modification, immune checkpoint blockade or use of radiation to stimulate chemokine production and tumor antigen presentation.

Future directions

This study establishes B7-H3 CAR T cell therapy for canine OS. In the future we hope to expand our CAR T cell program to apply B7-H3 CAR T cell therapy to multiple tumor types such as glioma, melanoma, and soft tissue sarcoma in dogs. We also hope to expand our CAR T cell work to a clinical trial in dogs with metastatic osteosarcoma to evaluate safety and efficacy with combination losartan and propranolol. Pending the results of the first ever solid tumor CAR T cell trail in dogs we hope to use canine OS as a platform for investigate further combination therapies such as checkpoint inhibitors or new CAR T cell constructs in metastatic canine OS as a translational model for pediatric OS. Additionally further investigation of the possible stimulatory priming effect of macrophages on B7-H3 CAR T cells can be done. Investigating administration of B7-H3 CAR T cells to lymph nodes to prime with antigen presenting cells before circulating to tumors can be done. Additionally, simulation of antigen presenting cells to upregulate B7-H3 with systemic administration of immune stimulants such as IFNγ or TNF could possibly make a more favorable environment for B7-H3 CAR T cells pre-infusion.

References

1. Ritter J, Bielack S. Osteosarcoma. *Annals of oncology* 2010;21:vii320-vii325.
2. Luetke A, Meyers PA, Lewis I, et al. Osteosarcoma treatment–where do we stand? A state of the art review. *Cancer treatment reviews* 2014;40:523-532.
3. Mirabello L, Troisi RJ, Savage SA. International osteosarcoma incidence patterns in children and adolescents, middle ages and elderly persons. *International journal of cancer* 2009;125:229-234.
4. Stiller C, Bielack S, Jundt G, et al. Bone tumours in European children and adolescents, 1978–1997. Report from the Automated Childhood Cancer Information System project. *European journal of cancer* 2006;42:2124-2135.
5. Mirabello L, Pfeiffer R, Murphy G, et al. Height at diagnosis and birth-weight as risk factors for osteosarcoma. *Cancer Causes & Control* 2011;22:899-908.
6. Misaghi A, Goldin A, Awad M, et al. Osteosarcoma: a comprehensive review. *SICOT J* 2018;4:12.
7. Kundu ZS. Classification, imaging, biopsy and staging of osteosarcoma. *Indian journal of orthopaedics* 2014;48:238-246.
8. Doyle LA. Sarcoma classification: an update based on the 2013 World Health Organization Classification of Tumors of Soft Tissue and Bone. *Cancer* 2014;120:1763-1774.
9. Shao YW, Wood GA, Lu J, et al. Cross-species genomics identifies DLG2 as a tumor suppressor in osteosarcoma. *Oncogene* 2019;38:291-298.
10. Chen X, Bahrami A, Pappo A, et al. Recurrent somatic structural variations contribute to tumorigenesis in pediatric osteosarcoma. *Cell reports* 2014;7:104-112.
11. Wunder JS, Gokgoz N, Parkes R, et al. TP53 mutations and outcome in osteosarcoma: a prospective, multicenter study. *Journal of Clinical Oncology* 2005;23:1483-1490.
12. Berman SD, Calo E, Landman AS, et al. Metastatic osteosarcoma induced by inactivation of Rb and p53 in the osteoblast lineage. *Proceedings of the National Academy of Sciences* 2008;105:11851-11856.
13. Ladanyi M, Cha C, Lewis R, et al. MDM2 gene amplification in metastatic osteosarcoma. *Cancer research* 1993;53:16-18.
14. Yoshida A, Ushiku T, Motoi T, et al. MDM2 and CDK4 immunohistochemical coexpression in high-grade osteosarcoma: correlation with a dedifferentiated subtype. *The American journal of surgical pathology* 2012;36:423-431.
15. Ji J, Quindipan C, Parham D, et al. Inherited germline ATRX mutation in two brothers with ATR-X syndrome and osteosarcoma. *American journal of medical genetics Part A* 2017;173:1390-1395.
16. Inagaki Y, Hookway E, Williams K, et al. Dendritic and mast cell involvement in the inflammatory response to primary malignant bone tumours. *Clinical sarcoma research* 2016;6:1-8.
17. Heymann M-F, Lézot F, Heymann D. The contribution of immune infiltrates and the local microenvironment in the pathogenesis of osteosarcoma. *Cellular immunology* 2019;343:103711.
18. Dumars C, Ngyuen J-M, Gaultier A, et al. Dysregulation of macrophage polarization is associated with the metastatic process in osteosarcoma. *Oncotarget* 2016;7:78343.
19. Buddingh EP, Kuijjer ML, Duim RA, et al. Tumor-Infiltrating Macrophages Are Associated with Metastasis Suppression in High-Grade Osteosarcoma: A Rationale for Treatment with Macrophage Activating AgentsImpact of Macrophages on Osteosarcoma Metastases. *Clinical Cancer Research* 2011;17:2110-2119.
20. Meyers PA. Muramyl tripeptide (mifamurtide) for the treatment of osteosarcoma. *Expert review of anticancer therapy* 2009;9:1035-1049.

21. Casey DL, Cheung N-KV. Immunotherapy of pediatric solid tumors: treatments at a crossroads, with an emphasis on antibodies. *Cancer immunology research* 2020;8:161-166.

22. Cascio MJ, Whitley EM, Sahay B, et al. Canine osteosarcoma checkpoint expression correlates with metastasis and T-cell infiltrate. *Veterinary Immunology and Immunopathology* 2021;232:110169.

23. Fritzsching B, Fellenberg J, Moskovszky L, et al. CD8+/FOXP3+-ratio in osteosarcoma microenvironment separates survivors from non-survivors: a multicenter validated retrospective study. *Oncoimmunology* 2015;4:e990800.

24. Koirala P, Roth ME, Gill J, et al. Immune infiltration and PD-L1 expression in the tumor microenvironment are prognostic in osteosarcoma. *Scientific reports* 2016;6:30093.

25. Hartley GP, Chow L, Ammons DT, et al. Programmed Cell Death Ligand 1 (PD-L1) Signaling Regulates Macrophage Proliferation and ActivationPD-L1 Regulates Macrophage Proliferation and Activation. *Cancer immunology research* 2018;6:1260-1273.

26. Keung EZ, Burgess M, Salazar R, et al. Correlative analyses of the SARC028 trial reveal an association between sarcoma-associated immune infiltrate and response to pembrolizumabsarcoma-associated immune infiltrate and Anti-PD1 therapy. *Clinical Cancer Research* 2020;26:1258-1266.

27. Le Cesne A, Marec-Berard P, Blay J-Y, et al. Programmed cell death 1 (PD-1) targeting in patients with advanced osteosarcomas: results from the PEMBROSARC study. *European journal of cancer* 2019;119:151-157.

28. Paoluzzi L, Cacavio A, Ghesani M, et al. Response to anti-PD1 therapy with nivolumab in metastatic sarcomas. *Clinical sarcoma research* 2016;6:1-7.

29. Eilber F, Giuliano A, Eckardt J, et al. Adjuvant chemotherapy for osteosarcoma: a randomized prospective trial. *Journal of Clinical Oncology* 1987;5:21-26.

30. Simon MA, Aschliman M, Thomas N, et al. Limb-salvage treatment versus amputation for osteosarcoma of the distal end of the femur. *JBJS* 1986;68:1331-1337.

31. Raymond AK, Jaffe N. Osteosarcoma multidisciplinary approach to the management from the pathologist's perspective. *Pediatric and adolescent osteosarcoma* 2010:63-84.

32. Meltzer PS, Helman LJ. New horizons in the treatment of osteosarcoma. *New England Journal of Medicine* 2021;385:2066-2076.

33. Mirabello L, Troisi RJ, Savage SA. Osteosarcoma incidence and survival rates from 1973 to 2004. *Cancer* 2009;115:1531-1543.

34. Rosen G, Marcove RC, Caparros B, et al. Primary osteogenic sarcoma. The rationale for preoperative chemotherapy and delayed surgery. *Cancer* 1979;43:2163-2177.

35. O'Kane G, Cadoo K, Walsh E, et al. Perioperative chemotherapy in the treatment of osteosarcoma: a 26-year single institution review. *Clinical sarcoma research* 2015;5:1-8.

36. Crenn V, Biteau K, Amiaud J, et al. Bone microenvironment has an influence on the histological response of osteosarcoma to chemotherapy: retrospective analysis and preclinical modeling. *American journal of cancer research* 2017;7:2333.

37. Marko TA, Diessner BJ, Spector LG. Prevalence of metastasis at diagnosis of osteosarcoma: an international comparison. *Pediatric blood & cancer* 2016;63:1006-1011.

38. Meazza C, Scanagatta P. Metastatic osteosarcoma: a challenging multidisciplinary treatment. *Expert review of anticancer therapy* 2016;16:543-556.

39. Moukengue B, Lallier M, Marchandet L, et al. Origin and Therapies of Osteosarcoma. *Cancers* 2022;14:3503.

40. Beck J, Ren L, Huang S, et al. Canine and murine models of osteosarcoma. *Veterinary Pathology* 2022;59:399-414.

41. Corre I, Verrecchia F, Crenn V, et al. The osteosarcoma microenvironment: a complex but targetable ecosystem. *Cells* 2020;9:976.

42. Gustafson DL, Duval DL, Regan DP, et al. Canine sarcomas as a surrogate for the human disease. *Pharmacology & therapeutics* 2018;188:80-96.

43. Schiffman JD, Breen M. Comparative oncology: what dogs and other species can teach us about humans with cancer. *Philosophical Transactions of the Royal Society B: Biological Sciences* 2015;370:20140231.

44. Edmunds GL, Smalley MJ, Beck S, et al. Dog breeds and body conformations with predisposition to osteosarcoma in the UK: a case-control study. *Canine medicine and genetics* 2021;8:1-22.

45. Selmic L, Burton J, Thamm D, et al. Comparison of carboplatin and doxorubicin-based chemotherapy protocols in 470 dogs after amputation for treatment of appendicular osteosarcoma. *Journal of veterinary internal medicine* 2014;28:554-563.

46. Fan TM, Khanna C. Comparative aspects of osteosarcoma pathogenesis in humans and dogs. *Veterinary sciences* 2015;2:210-230.

47. McNeill C, Overley B, Shofer F, et al. Characterization of the biological behaviour of appendicular osteosarcoma in Rottweilers and a comparison with other breeds: a review of 258 dogs. *Veterinary and comparative oncology* 2007;5:90-98.

48. Craig LE, Dittmer KE, Thompson KG. Bones and joints. *Jubb, Kennedy & Palmer's pathology of domestic animals* 2015;1:16-163.

49. Meuten DJ. *Tumors in domestic animals*: John Wiley & Sons, 2020.

50. Klein MJ, Siegal GP. Osteosarcoma: anatomic and histologic variants. *American journal of clinical pathology* 2006;125:555-581.

51. Nagamine E, Hirayama K, Matsuda K, et al. Diversity of histologic patterns and expression of cytoskeletal proteins in canine skeletal osteosarcoma. *Veterinary pathology* 2015;52:977-984.

52. LeBlanc AK, Mazcko CN, Cherukuri A, et al. Adjuvant Sirolimus Does Not Improve Outcome in Pet Dogs Receiving Standard-of-Care Therapy for Appendicular Osteosarcoma: A Prospective, Randomized Trial of 324 DogsAdjuvant Sirolimus in Canine Appendicular Osteosarcoma. *Clinical Cancer Research* 2021;27:3005-3016.

53. Skorupski KA, Uhl J, Szivek A, et al. Carboplatin versus alternating carboplatin and doxorubicin for the adjuvant treatment of canine appendicular osteosarcoma: a randomized, phase III trial. *Veterinary and comparative oncology* 2016;14:81-87.

54. Rohaan MW, Wilgenhof S, Haanen JBAG. Adoptive cellular therapies: the current landscape. *Virchows Archiv* 2019;474:449-461.

55. Esfahani K, Roudaia L, Buhlaiga N, et al. A Review of Cancer Immunotherapy: From the Past, to the Present, to the Future. *Current Oncology*, 2020;87-97.

56. June CH, Riddell SR, Schumacher TN. Adoptive cellular therapy: a race to the finish line. *Science translational medicine* 2015;7:280ps287-280ps287.

57. Spiess PJ, Yang JC, Rosenberg SA. In vivo antitumor activity of tumor-infiltrating lymphocytes expanded in recombinant interleukin-2. *Journal of the National Cancer Institute* 1987;79:1067-1075.

58. Rosenberg SA, Yang JC, Sherry RM, et al. Durable complete responses in heavily pretreated patients with metastatic melanoma using T-cell transfer immunotherapycomplete regressions in melanoma. *Clinical cancer research* 2011;17:4550-4557.

59. Atkins MB, Lotze MT, Dutcher JP, et al. High-dose recombinant interleukin 2 therapy for patients with metastatic melanoma: analysis of 270 patients treated between 1985 and 1993. *Journal of clinical oncology* 1999;17:2105-2105.

60. Andersen R, Donia M, Ellebaek E, et al. Long-lasting complete responses in patients with metastatic melanoma after adoptive cell therapy with tumor-infiltrating lymphocytes and an attenuated IL2 regimen. *Clinical cancer research* 2016;22:3734-3745.

61. Lee HJ, Kim Y-A, Sim CK, et al. Expansion of tumor-infiltrating lymphocytes and their potential for application as adoptive cell transfer therapy in human breast cancer. *Oncotarget* 2017;8:113345.

62. Stevanović S, Draper LM, Langhan MM, et al. Complete regression of metastatic cervical cancer after treatment with human papillomavirus–targeted tumor-infiltrating T cells. *Journal of Clinical Oncology* 2015;33:1543.

63. Leisegang M, Turqueti-Neves A, Engels B, et al. T-Cell Receptor Gene–Modified T Cells with Shared Renal Cell Carcinoma Specificity for Adoptive T-Cell Therapy. *Clinical cancer research* 2010;16:2333-2343.

64. Andersen R, Westergaard MCW, Kjeldsen JW, et al. T-cell Responses in the Microenvironment of Primary Renal Cell Carcinoma—Implications for Adoptive Cell TherapyT-cell Responses in Primary RCC—Implications for ACT. *Cancer immunology research* 2018;6:222-235.

65. Ben-Avi R, Farhi R, Ben-Nun A, et al. Establishment of adoptive cell therapy with tumor infiltrating lymphocytes for non-small cell lung cancer patients. *Cancer Immunology, Immunotherapy* 2018;67:1221-1230.

66. Yee C, Thompson J, Byrd D, et al. Adoptive T cell therapy using antigen-specific CD8+ T cell clones for the treatment of patients with metastatic melanoma: in vivo persistence, migration, and antitumor effect of transferred T cells. *Proceedings of the National Academy of Sciences* 2002;99:16168-16173.

67. Schumacher TN. T-cell-receptor gene therapy. *Nature Reviews Immunology* 2002;2:512-519.

68. Johnson LA, Morgan RA, Dudley ME, et al. Gene therapy with human and mouse T-cell receptors mediates cancer regression and targets normal tissues expressing cognate antigen. *Blood, The Journal of the American Society of Hematology* 2009;114:535-546.

69. Robbins PF, Morgan RA, Feldman SA, et al. Tumor regression in patients with metastatic synovial cell sarcoma and melanoma using genetically engineered lymphocytes reactive with NY-ESO-1. *Journal of Clinical Oncology* 2011;29:917.

70. Stadtmauer EA, Faitg TH, Lowther DE, et al. Long-term safety and activity of NY-ESO-1 spear T cells after autologous stem cell transplant for myeloma. *Blood advances* 2019;3:2022-2034.

71. Doran SL, Stevanović S, Adhikary S, et al. T-cell receptor gene therapy for human papillomavirus–associated epithelial cancers: a first-in-human, phase I/II study. *Journal of Clinical Oncology* 2019;37:2759.

72. Chapuis AG, Egan DN, Bar M, et al. T cell receptor gene therapy targeting WT1 prevents acute myeloid leukemia relapse post-transplant. *Nature medicine* 2019;25:1064-1072.

73. Rath JA, Arber C. Engineering Strategies to Enhance TCR-Based Adoptive T Cell Therapy. *Cells* 2020;9:1485.

74. Garrido F, Ruiz-Cabello F, Aptsiauri N. Rejection versus escape: the tumor MHC dilemma. *Cancer immunology, immunotherapy* 2017;66:259-271.

75. Zhang J, Wang L. The emerging world of TCR-T cell trials against cancer: a systematic review. *Technology in cancer research & treatment* 2019;18:1533033819831068.

76. Joglekar AV, Li G. T cell antigen discovery. *Nature methods* 2021;18:873-880.

77. Perez C, Gruber I, Arber C. Off-the-shelf allogeneic T cell therapies for cancer: opportunities and challenges using naturally occurring “universal” donor T cells. *Frontiers in immunology* 2020;11:583716.

78. Gross G, Waks T, Eshhar Z. Expression of immunoglobulin-T-cell receptor chimeric molecules as functional receptors with antibody-type specificity. *Proceedings of the National Academy of Sciences* 1989;86:10024-10028.

79. Sterner RC, Sterner RM. CAR-T cell therapy: current limitations and potential strategies. *Blood Cancer Journal* 2021;11:69.

80. Townsend MH, Shrestha G, Robison RA, et al. The expansion of targetable biomarkers for CAR T cell therapy. *Journal of Experimental & Clinical Cancer Research* 2018;37:1-23.

81. Hegde M, Mukherjee M, Grada Z, et al. Tandem CAR T cells targeting HER2 and IL13Rα2 mitigate tumor antigen escape. *The Journal of clinical investigation* 2016;126:3036-3052.

82. June CH, O'Connor RS, Kawalekar OU, et al. CAR T cell immunotherapy for human cancer. *Science* 2018;359:1361-1365.

83. Bridgeman JS, Hawkins RE, Bagley S, et al. The optimal antigen response of chimeric antigen receptors harboring the CD3ζ transmembrane domain is dependent upon incorporation of the receptor into the endogenous TCR/CD3 complex. *The Journal of Immunology* 2010;184:6938-6949.

84. Guedan S, Posey Jr AD, Shaw C, et al. Enhancing CAR T cell persistence through ICOS and 4-1BB costimulation. *JCI insight* 2018;3.

85. Brocker T, Karjalainen K. Signals through T cell receptor-zeta chain alone are insufficient to prime resting T lymphocytes. *The Journal of experimental medicine* 1995;181:1653-1659.

86. Eshhar Z, Waks T, Gross G, et al. Specific activation and targeting of cytotoxic lymphocytes through chimeric single chains consisting of antibody-binding domains and the gamma or zeta subunits of the immunoglobulin and T-cell receptors. *Proceedings of the National Academy of Sciences* 1993;90:720-724.

87. Lee DW, Kochenderfer JN, Stetler-Stevenson M, et al. T cells expressing CD19 chimeric antigen receptors for acute lymphoblastic leukaemia in children and young adults: a phase 1 dose-escalation trial. *The Lancet* 2015;385:517-528.

88. Maude SL, Frey N, Shaw PA, et al. Chimeric antigen receptor T cells for sustained remissions in leukemia. *New England Journal of Medicine* 2014;371:1507-1517.

89. Zhong X-S, Matsushita M, Plotkin J, et al. Chimeric antigen receptors combining 4-1BB and CD28 signaling domains augment PI3kinase/AKT/Bcl-XL activation and CD8+ T cell–mediated tumor eradication. *Molecular therapy* 2010;18:413-420.

90. Abate-Daga D, Lagisetty KH, Tran E, et al. A novel chimeric antigen receptor against prostate stem cell antigen mediates tumor destruction in a humanized mouse model of pancreatic cancer. *Human gene therapy* 2014;25:1003-1012.

91. Milone MC, Fish JD, Carpenito C, et al. Chimeric receptors containing CD137 signal transduction domains mediate enhanced survival of T cells and increased antileukemic efficacy in vivo. *Molecular therapy* 2009;17:1453-1464.

92. Turtle CJ, Hanafi L-A, Berger C, et al. CD19 CAR–T cells of defined CD4+: CD8+ composition in adult B cell ALL patients. *The Journal of clinical investigation* 2016;126:2123-2138.

93. Grupp SA, Maude SL, Shaw PA, et al. Durable remissions in children with relapsed/refractory all treated with t cells engineered with a CD19-targeted chimeric antigen receptor (CTL019). *Blood* 2015;126:681.

94. Maude SL, Laetsch TW, Buechner J, et al. Tisagenlecleucel in children and young adults with B-cell lymphoblastic leukemia. *New England Journal of Medicine* 2018;378:439-448.

95. Leick MB, Maus MV, Frigault MJ. Clinical perspective: treatment of aggressive B cell lymphomas with FDA-approved CAR-T cell therapies. *Molecular Therapy* 2021;29:433-441.

96. Patel U, Abernathy J, Savani BN, et al. CAR T cell therapy in solid tumors: A review of current clinical trials. *EJHaem* 2022;3:24-31.

97. Majzner RG, Mackall CL. Tumor antigen escape from CAR T-cell therapy. *Cancer discovery* 2018;8:1219-1226.

98. Zhang H, Gao L, Liu L, et al. A Bcma and CD19 bispecific CAR-T for relapsed and refractory multiple myeloma. *Blood* 2019;134:3147.

99. Dai H, Wu Z, Jia H, et al. Bispecific CAR-T cells targeting both CD19 and CD22 for therapy of adults with relapsed or refractory B cell acute lymphoblastic leukemia. *Journal of hematology & oncology* 2020;13:1-10.

100. Wilkie S, van Schalkwyk MC, Hobbs S, et al. Dual targeting of ErbB2 and MUC1 in breast cancer using chimeric antigen receptors engineered to provide complementary signaling. *Journal of clinical immunology* 2012;32:1059-1070.

101. Weiss T, Weller M, Guckenberger M, et al. NKG2D-Based CAR T Cells and Radiotherapy Exert Synergistic Efficacy in GlioblastomaRadiotherapy Augments NKG2D CAR T Cells against Glioblastoma. *Cancer research* 2018;78:1031-1043.

102. DeSelm C, Palomba ML, Yahalom J, et al. Low-dose radiation conditioning enables CAR T cells to mitigate antigen escape. *Molecular Therapy* 2018;26:2542-2552.

103. Gargett T, Yu W, Dotti G, et al. GD2-specific CAR T cells undergo potent activation and deletion following antigen encounter but can be protected from activation-induced cell death by PD-1 blockade. *Molecular Therapy* 2016;24:1135-1149.

104. Tanaka M, Tashiro H, Omer B, et al. Vaccination Targeting Native Receptors to Enhance the Function and Proliferation of Chimeric Antigen Receptor (CAR)-Modified T CellsVaccination to Enhance CAR-T-Cell Function. *Clinical Cancer Research* 2017;23:3499-3509.

105. Slaney CY, Von Scheidt B, Davenport AJ, et al. Dual-specific Chimeric Antigen Receptor T Cells and an Indirect Vaccine Eradicate a Variety of Large Solid Tumors in an Immunocompetent, Self-antigen SettingCAR T Cells Eradicate Large Syngeneic Tumors. *Clinical cancer research* 2017;23:2478-2490.

106. Majzner RG, Heitzeneder S, Mackall CL. Harnessing the immunotherapy revolution for the treatment of childhood cancers. *Cancer Cell* 2017;31:476-485.

107. Khalil DN, Smith EL, Brentjens RJ, et al. The future of cancer treatment: immunomodulation, CARs and combination immunotherapy. *Nature reviews Clinical oncology* 2016;13:273-290.

108. Frey NV, Porter DL. Cytokine release syndrome with novel therapeutics for acute lymphoblastic leukemia. *Hematology 2014, the American Society of Hematology Education Program Book* 2016;2016:567-572.

109. Brudno JN, Kochenderfer JN. Toxicities of chimeric antigen receptor T cells: recognition and management. *Blood, The Journal of the American Society of Hematology* 2016;127:3321-3330.

110. Davila ML, Riviere I, Wang X, et al. Efficacy and toxicity management of 19-28z CAR T cell therapy in B cell acute lymphoblastic leukemia. *Science translational medicine* 2014;6:224ra225-224ra225.

111. Porter DL, Hwang W-T, Frey NV, et al. Chimeric antigen receptor T cells persist and induce sustained remissions in relapsed refractory chronic lymphocytic leukemia. *Science translational medicine* 2015;7:303ra139-303ra139.

112. Lee DW, Gardner R, Porter DL, et al. Current concepts in the diagnosis and management of cytokine release syndrome. *Blood, The Journal of the American Society of Hematology* 2014;124:188-195.

113. Singh N, Hofmann TJ, Gershenson Z, et al. Monocyte lineage–derived IL-6 does not affect chimeric antigen receptor T-cell function. *Cytotherapy* 2017;19:867-880.

114. Neelapu SS, Locke FL, Bartlett NL, et al. Axicabtagene ciloleucel CAR T-cell therapy in refractory large B-cell lymphoma. *New England Journal of Medicine* 2017;377:2531-2544.

115. Siegler EL, Kenderian SS. Neurotoxicity and cytokine release syndrome after chimeric antigen receptor T cell therapy: insights into mechanisms and novel therapies. *Frontiers in immunology* 2020;11:1973.

116. Hunter BD, Jacobson CA. CAR T-Cell Associated Neurotoxicity: Mechanisms, Clinicopathologic Correlates, and Future Directions. *JNCI: Journal of the National Cancer Institute* 2019;111:646-654.

117. Petersen CT, Krenciute G. Next generation CAR T cells for the immunotherapy of high-grade glioma. *Frontiers in Oncology* 2019;9:69.

118. Qu J, Mei Q, Chen L, et al. Chimeric antigen receptor (CAR)-T-cell therapy in non-small-cell lung cancer (NSCLC): current status and future perspectives. *Cancer immunology, immunotherapy* 2021;70:619-631.

119. Corti C, Venetis K, Sajjadi E, et al. CAR-T cell therapy for triple-negative breast cancer and other solid tumors: preclinical and clinical progress. *Expert Opinion on Investigational Drugs* 2022;31:593-605.

120. Zhu J, Wan R, Huang W. CAR T targets and microenvironmental barriers of osteosarcoma. *Cytotherapy* 2022.

121. Marofi F, Abdul-Rasheed OF, Rahman HS, et al. CAR-NK cell in cancer immunotherapy; A promising frontier. *Cancer Science* 2021;112:3427-3436.

122. Chen Y, Yu Z, Tan X, et al. CAR-macrophage: A new immunotherapy candidate against solid tumors. *Biomedicine & Pharmacotherapy* 2021;139:111605.

123. Pan K, Farrukh H, Chittepu VCSR, et al. CAR race to cancer immunotherapy: from CAR T, CAR NK to CAR macrophage therapy. *Journal of Experimental & Clinical Cancer Research* 2022;41:1-21.

124. Brown CE, Alizadeh D, Starr R, et al. Regression of Glioblastoma after Chimeric Antigen Receptor T-Cell Therapy. *New England Journal of Medicine* 2016;375:2561-2569.

125. Louis CU, Savoldo B, Dotti G, et al. Antitumor activity and long-term fate of chimeric antigen receptor–positive T cells in patients with neuroblastoma. *Blood* 2011;118:6050-6056.

126. Ahmed N, Brawley VS, Hegde M, et al. Human epidermal growth factor receptor 2 (HER2)–specific chimeric antigen receptor–modified T cells for the immunotherapy of HER2-positive sarcoma. *Journal of clinical oncology* 2015;33:1688.

127. Newick K, O'Brien S, Moon E, et al. CAR T cell therapy for solid tumors. *Annual review of medicine* 2017;68:139-152.

128. Marofi F, Motavalli R, Safonov VA, et al. CAR T cells in solid tumors: challenges and opportunities. *Stem cell research & therapy* 2021;12:1-16.

129. Ma S, Li X, Wang X, et al. Current progress in CAR-T cell therapy for solid tumors. *International journal of biological sciences* 2019;15:2548.

130. Schmidts A, Maus MV. Making CAR T cells a solid option for solid tumors. *Frontiers in immunology* 2018;9:2593.

131. Newick K, Moon E, Albelda SM. Chimeric antigen receptor T-cell therapy for solid tumors. *Molecular Therapy - Oncolytics* 2016;3:16006.

132. Johnson LA, Scholler J, Ohkuri T, et al. Rational development and characterization of humanized anti–EGFR variant III chimeric antigen receptor T cells for glioblastoma. *Science translational medicine* 2015;7:275ra222-275ra222.

133. Wilkie S, Picco G, Foster J, et al. Retargeting of human T cells to tumor-associated MUC1: the evolution of a chimeric antigen receptor. *The Journal of Immunology* 2008;180:4901-4909.

134. Morello A, Sadelain M, Adusumilli PS. Mesothelin-Targeted CARs: Driving T Cells to Solid TumorsMesothelin: A Rising Star in Cancer Immunotherapy. *Cancer discovery* 2016;6:133-146.

135. Zhao Y, Moon E, Carpenito C, et al. Multiple Injections of Electroporated Autologous T Cells Expressing a Chimeric Antigen Receptor Mediate Regression of Human Disseminated TumorAutologous RNA CAR T Cells Mediate Tumor Regression. *Cancer research* 2010;70:9053-9061.

136. Adachi K, Kano Y, Nagai T, et al. IL-7 and CCL19 expression in CAR-T cells improves immune cell infiltration and CAR-T cell survival in the tumor. *Nature biotechnology* 2018;36:346-351.

137. Klampatsa A, Dimou V, Albelda SM. Mesothelin-targeted CAR-T cell therapy for solid tumors. *Expert opinion on biological therapy* 2021;21:473-486.

138. Bonifant CL, Jackson HJ, Brentjens RJ, et al. Toxicity and management in CAR T-cell therapy. *Molecular Therapy-Oncolytics* 2016;3:16011.

139. Brudno JN, Maric I, Hartman SD, et al. T cells genetically modified to express an anti–B-cell maturation antigen chimeric antigen receptor cause remissions of poor-prognosis relapsed multiple myeloma. *Journal of Clinical Oncology* 2018;36:2267-2280.

140. Brown CE, Alizadeh D, Starr R, et al. Regression of glioblastoma after chimeric antigen receptor T-cell therapy. *New England Journal of Medicine* 2016;375:2561-2569.

141. O'Rourke DM, Nasrallah MP, Desai A, et al. A single dose of peripherally infused EGFRvIII-directed CAR T cells mediates antigen loss and induces adaptive resistance in patients with recurrent glioblastoma. *Science translational medicine* 2017;9:eaaa0984.

142. Chulanetra M, Morchang A, Sayour E, et al. GD2 chimeric antigen receptor modified T cells in synergy with sub-toxic level of doxorubicin targeting osteosarcomas. *American Journal of Cancer Research* 2020;10:674.

143. Rainusso N, Brawley V, Ghazi A, et al. Immunotherapy targeting HER2 with genetically modified T cells eliminates tumor-initiating cells in osteosarcoma. *Cancer gene therapy* 2012;19:212-217.

144. Huang X, Park H, Greene J, et al. IGF1R-and ROR1-specific CAR T cells as a potential therapy for high risk sarcomas. *PLoS One* 2015;10:e0133152.

145. Park JA, Cheung N-KV. GD2 or HER2 targeting T cell engaging bispecific antibodies to treat osteosarcoma. *Journal of hematology & oncology* 2020;13:1-16.

146. Wang L, Zhang Q, Chen W, et al. B7-H3 is overexpressed in patients suffering osteosarcoma and associated with tumor aggressiveness and metastasis. *PloS one* 2013;8:e70689.

147. Majzner RG, Theruvath JL, Nellan A, et al. CAR T Cells Targeting B7-H3, a Pan-Cancer Antigen, Demonstrate Potent Preclinical Activity Against Pediatric Solid Tumors and Brain TumorsB7-H3 CAR T Cells Demonstrate Potent Preclinical Activity. *Clinical Cancer Research* 2019;25:2560-2574.

148. Lin Z, Wu Z, Luo W. Chimeric Antigen Receptor T-Cell Therapy: The Light of Day for Osteosarcoma. *Cancers* 2021;13:4469.

149. Yang S, Wei W, Zhao Q. B7-H3, a checkpoint molecule, as a target for cancer immunotherapy. *International Journal of Biological Sciences* 2020;16:1767.

150. Picarda E, Ohaegbulam KC, Zang X. Molecular Pathways: Targeting B7-H3 (CD276) for Human Cancer ImmunotherapyCancer Immunotherapies against B7-H3. *Clinical Cancer Research* 2016;22:3425-3431.

151. Li D, Xiang S, Shen J, et al. Comprehensive understanding of B7 family in gastric cancer: expression profile, association with clinicopathological parameters and downstream targets. *International journal of biological sciences* 2020;16:568.

152. Zou W, Chen L. Inhibitory B7-family molecules in the tumour microenvironment. *Nature Reviews Immunology* 2008;8:467-477.

153. Suh W-K, Wang S, Jheon A, et al. The immune regulatory protein B7-H3 promotes osteoblast differentiation and bone mineralization. *Proceedings of the National Academy of Sciences* 2004;101:12969-12973.

154. Feng P, Zhang H, Zhang Z, et al. The interaction of MMP-2/B7-H3 in human osteoporosis. *Clinical Immunology* 2016;162:118-124.

155. Vitanza NA, Wilson AL, Huang W, et al. Intraventricular B7-H3 CAR T cells for diffuse intrinsic pontine glioma: preliminary first-in-human bioactivity and safety. *Cancer discovery* 2023;13:114-131.

156. Kulkarni N, Pathak M, Lal G. Role of chemokine receptors and intestinal epithelial cells in the mucosal inflammation and tolerance. *Journal of Leucocyte Biology* 2017;101:377-394.

157. Stone MJ, Hayward JA, Huang C, et al. Mechanisms of regulation of the chemokine-receptor network. *International journal of molecular sciences* 2017;18:342.

158. Matsushima K, Baldwin ET, Mukaida N. Interleukin-8 and MCAF: novel leukocyte recruitment and activating cytokines. *Interleukins: molecular biology and immunology* 1992;51:236-265.

159. Liu G, Rui W, Zheng H, et al. CXCR2-modified CAR-T cells have enhanced trafficking ability that improves treatment of hepatocellular carcinoma. *European Journal of Immunology* 2020;50:712-724.

160. Liu Q, Li A, Tian Y, et al. The CXCL8-CXCR1/2 pathways in cancer. *Cytokine & Growth Factor Reviews* 2016;31:61-71.

161. Sparmann A, Bar-Sagi D. Ras-induced interleukin-8 expression plays a critical role in tumor growth and angiogenesis. *Cancer cell* 2004;6:447-458.

162. Rotondo R, Barisione G, Mastracci L, et al. IL-8 induces exocytosis of arginase 1 by neutrophil polymorphonuclears in nonsmall cell lung cancer. *International journal of cancer* 2009;125:887-893.

163. Alfaro C, Teijeira A, Oñate C, et al. Tumor-Produced Interleukin-8 Attracts Human Myeloid-Derived Suppressor Cells and Elicits Extrusion of Neutrophil Extracellular Traps (NETs) Effects of IL8 on MDSC. *Clinical Cancer Research* 2016;22:3924-3936.

164. Jena B, Dotti G, Cooper LJ. Redirecting T-cell specificity by introducing a tumor-specific chimeric antigen receptor. *Blood, The Journal of the American Society of Hematology* 2010;116:1035-1044.

165. Jin L, Tao H, Karachi A, et al. CXCR1-or CXCR2-modified CAR T cells co-opt IL-8 for maximal antitumor efficacy in solid tumors. *Nature communications* 2019;10:4016.

166. Fonkoua LAK, Sirpilla O, Sakemura R, et al. CART Cell Therapy and the Tumor Microenvironment: Current Challenges and Opportunities. *Molecular Therapy-Oncolytics* 2022.

167. Cao JW, Chow L, Dow S. Strategies to overcome myeloid cell induced immune suppression in the tumor microenvironment. *Frontiers in Oncology* 2023;13:1324.

168. Regan DA-O, Coy JW, Chahal KA-O, et al. The Angiotensin Receptor Blocker Losartan Suppresses Growth of Pulmonary Metastases via AT1R-Independent Inhibition of CCR2 Signaling and Monocyte Recruitment.

169. Ammons DT, MacDonald CR, Chow L, et al. Chronic adrenergic stress and generation of myeloid-derived suppressor cells: Implications for cancer immunotherapy in dogs. *Veterinary and Comparative Oncology* 2023;21:159-165.

170. Ammons DT, MacDonald CR, Chow L, et al. Chronic adrenergic stress and generation of myeloid-derived suppressor cells: Implications for cancer immunotherapy in dogs. *Veterinary and Comparative Oncology* 2023;21:159-165.

171. Regan DP, Coy JW, Chahal KK, et al. The angiotensin receptor blocker losartan suppresses growth of pulmonary metastases via AT1R-independent inhibition of CCR2 signaling and monocyte recruitment. *The Journal of Immunology* 2019;202:3087-3102.

172. Regan DP, Chow L, Das S, et al. Losartan blocks osteosarcoma-elicited monocyte recruitment, and combined with the kinase inhibitor toceranib, exerts significant clinical benefit in canine metastatic osteosarcoma. *Clinical Cancer Research* 2022;28:662-676.

173. Ammons DT, Guth A, Rozental AJ, et al. Reprogramming the canine glioma microenvironment with tumor vaccination plus oral losartan and propranolol induces objective responses. *Cancer Research Communications* 2022;2:1657-1667.

174. Kager L, Zoubek A, Pötschger U, et al. Primary metastatic osteosarcoma: presentation and outcome of patients treated on neoadjuvant Cooperative Osteosarcoma Study Group protocols. *Journal of clinical oncology* 2003;21:2011-2018.

175. Harris MA, Hawkins CJ. Recent and ongoing research into metastatic osteosarcoma treatments. *International Journal of Molecular Sciences* 2022;23:3817.

176. Bacci G, Ferrari S, Bertoni F, et al. Long-term outcome for patients with nonmetastatic osteosarcoma of the extremity treated at the istituto ortopedico rizzoli according to the istituto ortopedico rizzoli/osteosarcoma-2 protocol: an updated report. *Journal of clinical oncology* 2000;18:4016-4027.

177. Allison DC, Carney SC, Ahlmann ER, et al. A meta-analysis of osteosarcoma outcomes in the modern medical era. *Sarcoma* 2012;2012.

178. Vigdorovich V, Ramagopal UA, Lazar-Molnar E, et al. Structure and T cell inhibition properties of B7 family member, B7-H3. *Structure* 2013;21:707-717.

179. Castellanos JR, Purvis IJ, Labak CM, et al. B7-H3 role in the immune landscape of cancer. *American journal of clinical and experimental immunology* 2017;6:66.

180. Wang L, Kang FB, Shan BE. B7-H3-mediated tumor immunology: friend or foe? *International journal of cancer* 2014;134:2764-2771.

181. Kontos F, Michelakos T, Kurokawa T, et al. B7-H3: An Attractive Target for Antibody-based Immunotherapy. *Clinical Cancer Research* 2021;27:1227-1235.

182. Suh W-K, Wang SX, Jheon AH, et al. The immune regulatory protein B7-H3 promotes osteoblast differentiation and bone mineralization. *Proceedings of the National Academy of Sciences* 2004;101:12969-12973.

183. He L, Li Z. B7-H3 and its role in bone cancers. *Pathology-Research and Practice* 2019;215:152420.

184. Loo D, Alderson RF, Chen FZ, et al. Development of an Fc-Enhanced Anti–B7-H3 Monoclonal Antibody with Potent Antitumor ActivityDevelopment of Fc-Enhanced Anti–B7-H3 Monoclonal Antibody. *Clinical cancer research* 2012;18:3834-3845.

185. Fauci JM, Sabbatino F, Wang Y, et al. Monoclonal antibody-based immunotherapy of ovarian cancer: targeting ovarian cancer cells with the B7-H3-specific mAb 376.96. *Gynecologic oncology* 2014;132:203-210.

186. Kramer K, Kushner BH, Modak S, et al. Compartmental intrathecal radioimmunotherapy: results for treatment for metastatic CNS neuroblastoma. *Journal of neuro-oncology* 2010;97:409-418.

187. Powderly J, Cote G, Flaherty K, et al. Interim results of an ongoing Phase I, dose escalation study of MGA271 (Fc-optimized humanized anti-B7-H3 monoclonal antibody) in patients with refractory B7-H3-expressing neoplasms or neoplasms whose vasculature expresses B7-H3. *Journal for immunotherapy of cancer* 2015;3:1-2.

188. Shah NN, Lee DW, Yates B, et al. Long-term follow-up of CD19-CAR T-cell therapy in children and young adults with B-ALL. *Journal of Clinical Oncology* 2021;39:1650.

189. Talbot LJ, Chabot A, Funk A, et al. A novel orthotopic implantation technique for osteosarcoma produces spontaneous metastases and illustrates dose-dependent efficacy of B7-H3-CAR T cells. *Frontiers in Immunology* 2021:2209.

190. Lichtman EI, Du H, Shou P, et al. Preclinical Evaluation of B7-H3–specific Chimeric Antigen Receptor T Cells for the Treatment of Acute Myeloid LeukemiaB7-H3–specific CAR T Cells for AML. *Clinical Cancer Research* 2021;27:3141-3153.

191. Zhang Y, He L, Sadagopan A, et al. Targeting radiation-resistant prostate cancer stem cells by B7-H3 CAR T cells. *Molecular cancer therapeutics* 2021;20:577-588.

192. Panjwani MK, Atherton MJ, MaloneyHuss MA, et al. Establishing a model system for evaluating CAR T cell therapy using dogs with spontaneous diffuse large B cell lymphoma. *Oncoimmunology* 2020;9:1676615.

193. Guijarro MV, Ghivizzani SC, Gibbs CP. Animal models in osteosarcoma. *Frontiers in oncology* 2014;4:189.

194. Rotolo A, Atherton MJ, Kasper BT, et al. Genetic re-direction of canine primary T cells for clinical trial use in pet dogs with spontaneous cancer. *STAR Protoc* 2021;2:100905.

195. Rodriguez CO. Using canine osteosarcoma as a model to assess efficacy of novel therapies: can old dogs teach us new tricks? *Current Advances in Osteosarcoma* 2014:237-256.

196. LeBlanc AK, Mazcko CN. Improving human cancer therapy through the evaluation of pet dogs. *Nature Reviews Cancer* 2020;20:727-742.

197. Overgaard NH, Fan TM, Schachtschneider KM, et al. Of mice, dogs, pigs, and men: choosing the appropriate model for immuno-oncology research. *ILAR journal* 2018;59:247-262.

198. Zhang S, Black RG, Kohli K, et al. B7-H3 Specific CAR T Cells for the Naturally Occurring, Spontaneous Canine Sarcoma Model. *Molecular Cancer Therapeutics* 2022;21:999-1009.

199. Panjwani MK, Smith JB, Schutsky K, et al. Feasibility and safety of RNA-transfected CD20-specific chimeric antigen receptor T cells in dogs with spontaneous B cell lymphoma. *Molecular Therapy* 2016;24:1602-1614.

200. Suhoski MM, Golovina TN, Aqui NA, et al. Engineering artificial antigen-presenting cells to express a diverse array of co-stimulatory molecules. *Molecular therapy* 2007;15:981-988.

201. Fowles J, Dailey D, Gustafson D, et al. The Flint Animal Cancer Center (FACC) Canine Tumour Cell Line Panel: a resource for veterinary drug discovery, comparative oncology and translational medicine. *Veterinary and comparative oncology* 2017;15:481-492.

202. Crowe AR, Yue W. Semi-quantitative determination of protein expression using immunohistochemistry staining and analysis: an integrated protocol. *Bio-protocol* 2019;9:e3465-e3465.

203. Walker R. Quantification of immunohistochemistry—issues concerning methods, utility and semiquantitative assessment I. *Histopathology* 2006;49:406-410.

204. Sakai O, Igase M, Mizuno T. Optimization of canine CD20 chimeric antigen receptor T cell manufacturing and in vitro cytotoxic activity against B-cell lymphoma. *Veterinary and comparative oncology* 2020;18:739-752.

205. ElKassar N, Gress RE. An overview of IL-7 biology and its use in immunotherapy. *Journal of immunotoxicology* 2010;7:1-7.

206. Pilipow K, Roberto A, Roederer M, et al. IL15 and T-cell Stemness in T-cell–Based Cancer ImmunotherapyIL15 in T-cell Therapy of Cancer. *Cancer research* 2015;75:5187-5193.

207. White LG, Goy HE, Rose AJ, et al. Controlling Cell Trafficking: Addressing Failures in CAR T and NK Cell Therapy of Solid Tumours. *Cancers* 2022;14:978.

208. Jessica L, Kevin W, Alexander H, et al. 125 Co-opting IL-8 to enhance efficacy of B7H3 CAR T cells against pediatric sarcoma. *Journal for ImmunoTherapy of Cancer* 2021;9:A134.

209. Hughes CE, Nibbs RA-O. A guide to chemokines and their receptors.

210. Jena B, Dotti G, Cooper LJN. Redirecting T-cell specificity by introducing a tumor-specific chimeric antigen receptor. *Blood* 2010;116:1035-1044.

211. Ning Y, Manegold PC, Hong YK, et al. Interleukin-8 is associated with proliferation, migration, angiogenesis and chemosensitivity in vitro and in vivo in colon cancer cell line models. *International journal of cancer* 2011;128:2038-2049.

212. Risso D, Ngai J, Speed TP, et al. Normalization of RNA-seq data using factor analysis of control genes or samples. *Nature biotechnology* 2014;32:896-902.

213. Gu Z, Eils R, Schlesner M. Complex heatmaps reveal patterns and correlations in multidimensional genomic data.

214. Love MI, Huber W, Anders S. Moderated estimation of fold change and dispersion for RNA-seq data with DESeq2. *Genome Biology* 2014;15:550.

215. Blighe K, Rana S, Lewis M. EnhancedVolcano: Publication-ready volcano plots with enhanced colouring and labeling. *R package version* 2019;1.

216. Subramanian A, Tamayo P, Mootha VK, et al. Gene set enrichment analysis: a knowledge-based approach for interpreting genome-wide expression profiles. *Proceedings of the National Academy of Sciences* 2005;102:15545-15550.

217. Mootha VK, Lindgren CM, Eriksson K-F, et al. PGC-1α-responsive genes involved in oxidative phosphorylation are coordinately downregulated in human diabetes. *Nature Genetics* 2003;34:267-273.

218. Liberzon A, Subramanian A, Pinchback R, et al. Molecular signatures database (MSigDB) 3.0. *Bioinformatics* 2011;27:1739-1740.

219. Liberzon A, Birger C, Thorvaldsdóttir H, et al. The Molecular Signatures Database (MSigDB) hallmark gene set collection.

220. O'Leary NA, Wright MW, Brister JR, et al. Reference sequence (RefSeq) database at NCBI: current status, taxonomic expansion, and functional annotation.

221. Sun L, Lin Y, Wang G, et al. Correlation of zinc finger protein 2, a prognostic biomarker, with immune infiltrates in liver cancer. *Bioscience Reports* 2021;41.

222. Moon EK, Carpenito C, Sun J, et al. Expression of a Functional CCR2 Receptor Enhances Tumor Localization and Tumor Eradication by Retargeted Human T cells Expressing a Mesothelin-Specific Chimeric Antibody Receptor. *Clinical Cancer Research* 2011;17:4719-4730.

223. Ziogas AC, Gavalas NG, Tsiatas M, et al. VEGF directly suppresses activation of T cells from ovarian cancer patients and healthy individuals via VEGF receptor Type 2. *International journal of cancer* 2012;130:857-864.

224. Ammons DT, Guth A, Rozental AJ, et al. Reprogramming the Canine Glioma Microenvironment with Tumor Vaccination plus Oral Losartan and Propranolol Induces Objective Responses. *Cancer research communications* 2022;2:1657-1667.

225. Kleinerman ES, Jia SF, Griffin J, et al. Phase II study of liposomal muramyl tripeptide in osteosarcoma: the cytokine cascade and monocyte activation following administration. *Journal of Clinical Oncology* 1992;10:1310-1316.

226. Kager L, Pötschger U Fau - Bielack S, Bielack S. Review of mifamurtide in the treatment of patients with osteosarcoma.

227. MacDonald C, Ministero S, Pandey M, et al. Comparing thermal stress reduction strategies that influence MDSC accumulation in tumor bearing mice. *Cellular Immunology* 2021;361:104285.

228. Goodyear AW, Kumar A, Dow S, et al. Optimization of murine small intestine leukocyte isolation for global immune phenotype analysis. *Journal of Immunological Methods* 2014;405:97-108.

229. Chow L, Soontararak S, Wheat W, et al. Canine polarized macrophages express distinct functional and transcriptomic profiles. *Frontiers in Veterinary Science* 2022;9.

230. Croy B, Chapeau C. Evaluation of the pregnancy immunotrophism hypothesis by assessment of the reproductive performance of young adult mice of genotype scid/scid. bg/bg. *Reproduction* 1990;88:231-239.

231. Bonapace L, Coissieux M-M, Wyckoff J, et al. Cessation of CCL2 inhibition accelerates breast cancer metastasis by promoting angiogenesis. *Nature* 2014;515:130-133.

232. Ishikawa F, Yasukawa M Fau - Lyons B, Lyons B Fau - Yoshida S, et al. Development of functional human blood and immune systems in NOD/SCID/IL2 receptor {gamma} chain(null) mice.

233. Shibata S, Asano T Fau - Ogura A, Ogura A Fau - Hashimoto N, et al. SCID-bg mice as xenograft recipients.

234. Chekmasova AA, Rao TD, Nikhamin Y, et al. Successful Eradication of Established Peritoneal Ovarian Tumors in SCID-Beige Mice following Adoptive Transfer of T Cells Genetically Targeted to the MUC16 Antigen. *Clinical Cancer Research* 2010;16:3594-3606.

235. Klampatsa A, Achkova DY, Davies DM, et al. Intracavitary 'T4 immunotherapy' of malignant mesothelioma using pan-ErbB re-targeted CAR T-cells. *Cancer Letters* 2017;393:52-59.

236. Mohammadpour H, MacDonald CR, Qiao G, et al. β2 adrenergic receptor–mediated signaling regulates the immunosuppressive potential of myeloid-derived suppressor cells. *The Journal of clinical investigation* 2019;129:5537-5552.

237. Huang Q, Liang X, Ren T, et al. The role of tumor-associated macrophages in osteosarcoma progression – therapeutic implications. *Cellular Oncology* 2021;44:525-539.

238. Zhao Y, Zhang B, Zhang Q, et al. Tumor-associated macrophages in osteosarcoma.

239. Ito M, Hiramatsu H, Kobayashi K, et al. NOD/SCID/γcnull mouse: an excellent recipient mouse model for engraftment of human cells. *Blood* 2002;100:3175-3182.

240. Wrobel LJ, Le Gal FA. Inhibition of Human Melanoma Growth by a Non-Cardioselective β-Blocker. *Journal of Investigative Dermatology* 2015;135:525-531.

241. Beth K C, Matthew J A. A Clinically Relevant Mouse Model of Canine Osteosarcoma with Spontaneous Metastasis. *In Vivo* 2013;27:599.

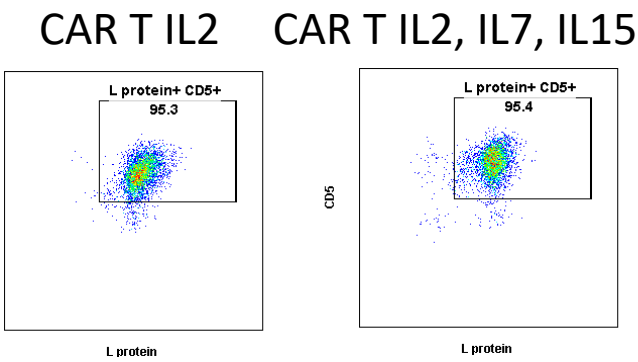

Supplemental fig 1. expression of CAR of canine B7-H3 CAR T cells post freeze thaw cycle at day 14 cultured in either IL-2 or IL-2, IL-7 and IL-15

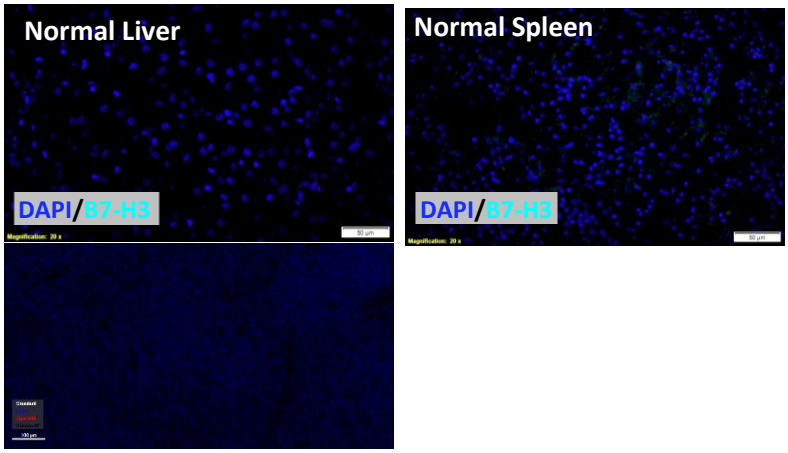

Supplemental fig 2. expression of B7-H3 on frozen normal canine tissues liver, spleen, and lymph node

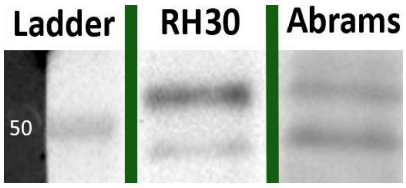

Supplemental fig 3. Human B7H3 monoclonal antibody binding to human rhabdosarcoma cell line (RH30) and canine OS cell line (Abrams) B7H3 protein by western blot at size 55kDA

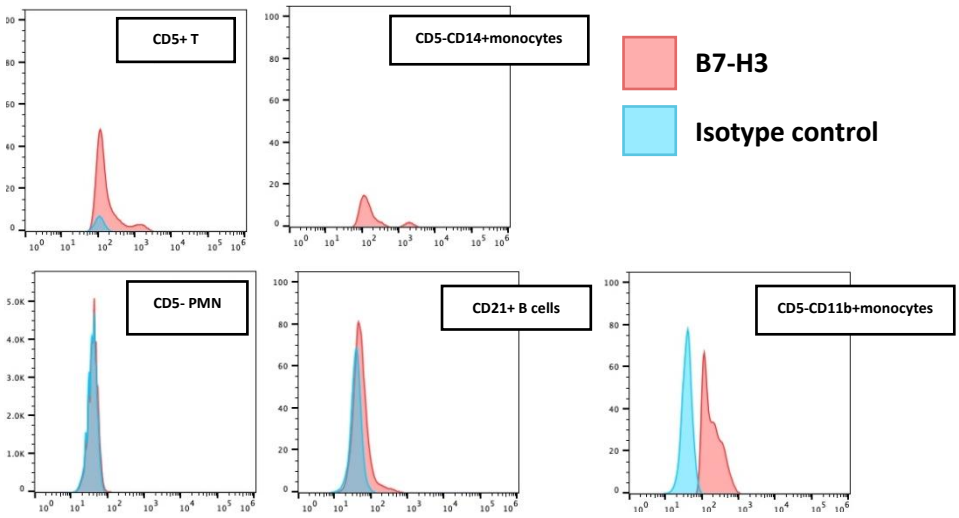

Supplemental fig 4. B7H3 expression on healthy dog PBMC by flow cytometry

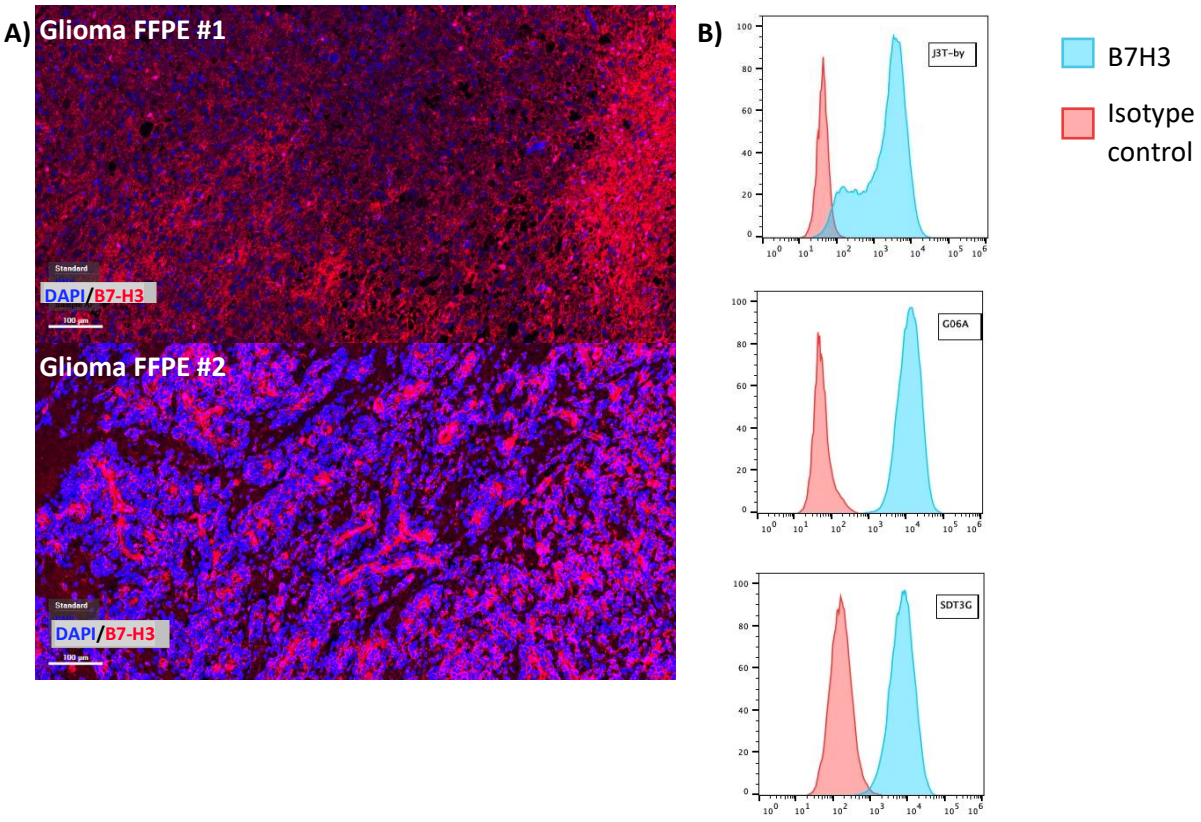

Supplemental fig 5. B7H3 is overexpressed in canine Glioma **A)** expression of B7H3 on formalin fixed paraffin embedded (FFPE) primary glioma tissues**. B)** Expression of B7H3 on canine glioma cell lines by flow cytometry.

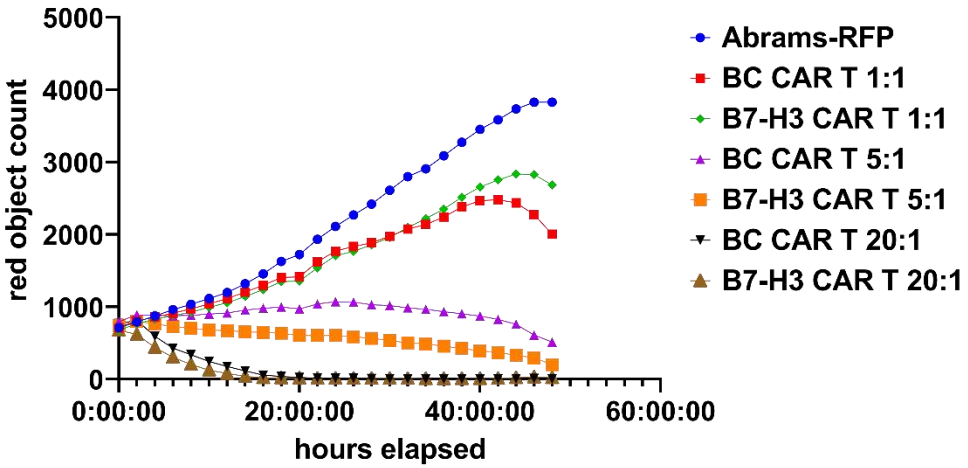

Supplemental fig 6. *in vitro* killing of canine OS cell line Abrams RFP by donor matched B7-H3-CXCR2 CAR T cells (BC CART) or B7-H CAR T cells at effector: target (E:T) ratios 1:1, 5:1, and 20:1 over 48 hours

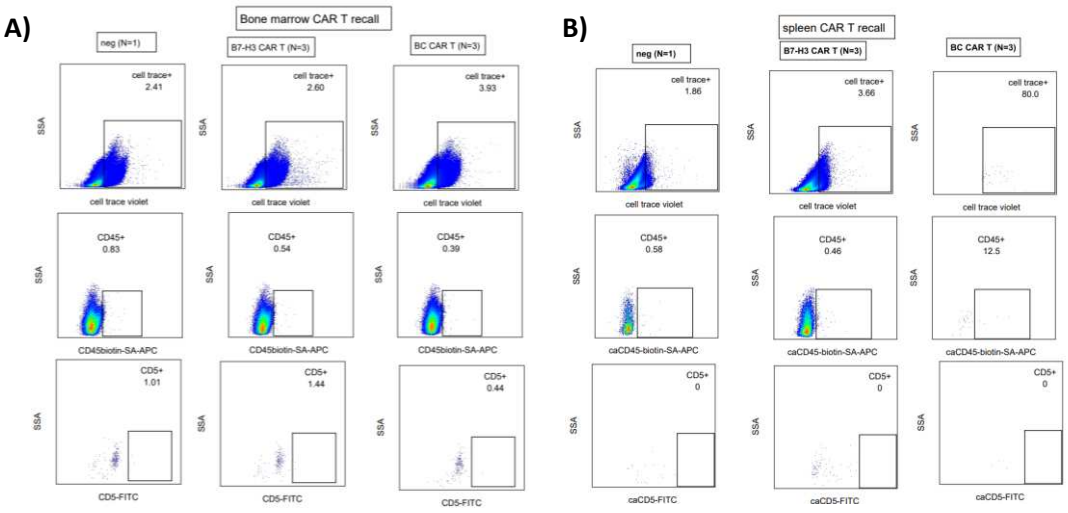

Supplemental fig 7. A) Bone marrow analyzed by flow cytometry for cell trace violet positive canine T cells and anti-canine CD45+ and CD5+ cells. **B)** spleen analyzed flow cytometry for cell trace violet positive canine T cells and anti-canine CD45+ and CD5+ cells.

Supplementary table 1. Significantly DEGs for B7-H3-CXCR2 CAR T cells vs B7-H3 CAR T cells Log_2FC >1.5 or <1.5 and adj. P<0.05

gene id	base mean	log2foldchange	p value	padj
CXCR2	10.6870	7.5104	1.46E-04	0.6299
ENSCAFG00000047315	12.4930	6.8192	5.90E-04	0.8912
RLBP1	11.9909	5.1344	6.10E-04	0.8912
ACTL8	4.8498	4.6079	3.62E-02	0.9999
MMP17	7.2424	4.1804	3.99E-02	0.9999
EFHB	7.8822	4.1241	3.41E-02	0.9999
ENSCAFG00000014051	15.9989	3.8372	9.32E-03	0.9999
ENSCAFG00000014612	7.8035	3.6306	3.36E-02	0.9999
PLA2G7	76.3356	3.5570	5.97E-03	0.9999
ENSCAFG00000005575	11.1439	2.9896	4.97E-02	0.9999
GFRA2	17.9798	2.9247	1.48E-02	0.9999
PTPRN2	7.3409	2.7704	4.93E-02	0.9999
GDA	15.4856	2.6477	5.13E-03	0.9999
DLX2	16.9119	2.5832	1.06E-02	0.9999
NTRK1	99.8161	2.0285	1.78E-03	0.9999
GLIS2	20.5008	1.9151	2.64E-02	0.9999
PTCH2	39.3890	1.8615	1.69E-02	0.9999
CAPN14	749.9637	1.7472	4.39E-02	0.9999
CHRNB2	21.1335	1.7022	2.85E-02	0.9999
IL15RA	24.7058	1.6797	6.92E-03	0.9999
GPC1	22.1510	1.6015	2.70E-02	0.9999
CALD1	50.7546	1.5494	6.40E-03	0.9999
SGK3	25.6423	1.5285	1.60E-02	0.9999
CP	31.4522	1.4722	2.58E-02	0.9999
ZIC2	79.4080	1.4264	3.81E-02	0.9999
LIF	357.2276	1.4168	2.49E-02	0.9999
C6H1orf194	26.8596	1.3924	2.52E-02	0.9999
ENSCAFG00000044395	25.5945	1.3487	4.47E-02	0.9999
CD109	76.1158	1.3177	4.58E-02	0.9999
ENSCAFG00000014312	135.4530	1.3080	2.88E-04	0.6299
HMOX1	181.2080	1.2934	3.34E-02	0.9999
CCL17	834.8082	1.2764	4.66E-03	0.9999
YAP1	42.4799	1.2680	3.70E-02	0.9999
IL13	882.3258	1.2296	1.92E-02	0.9999
RRAD	96.6581	1.2004	2.69E-02	0.9999
GNAQ	43.1719	1.1607	2.40E-02	0.9999
ENSCAFG00000035151	55.2521	1.1560	2.08E-02	0.9999
SCOC	284.1762	1.0147	3.90E-03	0.9999
IL17F	8037.8357	0.9730	2.13E-03	0.9999
CPNE6	576.1956	0.9035	2.10E-02	0.9999
ENSCAFG00000041232	753.8732	0.9035	9.69E-03	0.9999
OSM	633.0896	0.9015	3.48E-02	0.9999
PERP	626.4291	0.8853	3.29E-02	0.9999
SPHK1	91.2433	0.8818	3.20E-02	0.9999
CLUAP1	62.7892	0.8723	4.17E-02	0.9999
BATF3	1615.4839	0.8710	2.92E-02	0.9999
NPL	190.4110	0.8632	2.42E-02	0.9999
ENSCAFG00000041792	174.3478	0.8348	2.06E-02	0.9999
RASSF4	169.6539	0.8203	1.94E-02	0.9999
CAVIN3	265.6809	0.8175	3.73E-02	0.9999
KHDRBS3	305.3681	0.7884	4.61E-02	0.9999
LCLAT1	84.0942	0.7343	4.94E-02	0.9999
METTL27	176.3992	0.7164	2.48E-02	0.9999
CCDC86	461.9690	0.6726	3.55E-02	0.9999
CD86	327.0606	0.6654	3.90E-02	0.9999

LGALS3	5502.1484	0.6552	1.39E-02	0.9999
DMD	314.2898	0.6403	3.84E-02	0.9999
MTSS1	315.0857	0.6268	2.59E-02	0.9999
TREX2	172.7674	0.6166	2.75E-02	0.9999
ENSCAFG00000018271	178.4788	0.6094	4.05E-02	0.9999
KRT27	916.2100	0.5969	2.77E-02	0.9999
MT-ND2	40526.3405	0.5965	5.66E-04	0.8912
PTRH1	283.7905	0.5917	3.07E-02	0.9999
LIMA1	246.6932	0.5897	3.63E-02	0.9999
EGR2	1250.7801	-0.5919	3.29E-02	0.9999
NAPRT	500.4570	-0.6036	4.84E-02	0.9999
HLF	553.0267	-0.6050	3.80E-02	0.9999
CGRRF1	210.7461	-0.6075	1.91E-02	0.9999
ENSCAFG00000048188	119.7805	-0.6141	4.43E-02	0.9999
NRL	146.7214	-0.6193	3.92E-02	0.9999
GPR55	2298.8368	-0.6205	4.73E-02	0.9999
MANBA	381.4649	-0.6362	8.72E-03	0.9999
ARHGAP31	558.1042	-0.6401	1.18E-03	0.9999
ENSCAFG00000029414	391.7792	-0.6493	5.06E-03	0.9999
TNFSF8	462.2670	-0.6591	4.05E-02	0.9999
RORA	737.2386	-0.6676	4.51E-02	0.9999
LAX1	279.4937	-0.6830	3.80E-02	0.9999
BNIP3	397.7784	-0.6967	4.35E-02	0.9999
AFDN	379.1531	-0.6976	1.15E-02	0.9999
KLF5	183.8437	-0.6982	7.64E-03	0.9999
SCMH1	145.4325	-0.7097	2.15E-02	0.9999
KIFC3	155.3617	-0.7374	3.08E-02	0.9999
GPR83	397.2120	-0.7452	1.10E-04	0.6299
PDE3B	12171.7183	-0.7526	4.33E-02	0.9999
GNG7	118.4601	-0.7616	2.39E-02	0.9999
EIF5A2	202.7180	-0.7880	4.57E-03	0.9999
CCR9	312.4860	-0.7917	4.03E-02	0.9999
KLRG1	552.9139	-0.7963	2.91E-02	0.9999
PPM1H	620.2862	-0.7989	2.61E-03	0.9999
STON2	207.3961	-0.8043	9.64E-03	0.9999
FGL2	4865.6679	-0.8088	1.96E-02	0.9999
GALNT17	221.1843	-0.8238	1.23E-02	0.9999
CDH23	321.8810	-0.8250	1.33E-02	0.9999
ENSCAFG00000010596	158.7728	-0.8283	2.18E-03	0.9999
CRTAM	237.4817	-0.8478	3.32E-02	0.9999
LAT2	302.6236	-0.8636	3.29E-02	0.9999
ENSCAFG00000043059	89.8335	-0.8658	1.47E-02	0.9999
ITIH5	137.2614	-0.8679	2.57E-02	0.9999
ZC3H12C	192.6676	-0.9070	6.77E-03	0.9999
SCN2A	112.2906	-0.9528	4.15E-02	0.9999
CELF4	126.6702	-0.9767	3.41E-03	0.9999
CCDC146	103.6998	-0.9823	1.71E-02	0.9999
CCR2	1172.4622	-0.9901	2.85E-04	0.6299
PRDM8	81.7706	-1.0089	3.60E-02	0.9999
IL1R1	529.7001	-1.0491	1.75E-02	0.9999
ENOX2	69.2840	-1.0595	1.80E-02	0.9999
DNAH2	112.9119	-1.1184	1.99E-02	0.9999
ATP1A3	246.6571	-1.1331	2.74E-02	0.9999
CCRL2	143.6730	-1.1700	4.23E-03	0.9999
PLXNA4	202.2780	-1.1708	1.11E-02	0.9999
TULP3	55.8952	-1.1733	4.37E-02	0.9999
CCL1	917.6947	-1.1835	6.27E-03	0.9999
FAM189A2	196.4633	-1.2900	2.06E-03	0.9999
ADRB1	137.2051	-1.4278	5.21E-03	0.9999
ITGB3	134.0566	-1.4537	4.81E-03	0.9999

NR4A2	183.7382	-1.4779	2.34E-02	0.9999
ATP9A	58.4311	-1.4981	2.36E-02	0.9999
PTPRM	18.7740	-1.5845	4.49E-02	0.9999
PTK7	31.4221	-1.6434	1.59E-02	0.9999
ENSCAFG00000001949	27.6780	-1.6451	4.80E-02	0.9999
ADGRE1	25.2636	-1.6459	4.87E-02	0.9999
KDR	384.3585	-1.7055	2.90E-03	0.9999
ENSCAFG00000045028	34.0085	-1.7411	1.35E-02	0.9999
COL8A2	126.5807	-1.7590	2.15E-02	0.9999
MBOAT2	20.5834	-1.7906	3.86E-02	0.9999
ENSCAFG00000031239	85.7884	-1.8393	3.91E-02	0.9999
TMEM37	19.7321	-1.8928	4.76E-02	0.9999
PTAFR	28.5598	-2.0276	1.87E-03	0.9999
ENSCAFG00000046670	19.7404	-2.0348	4.84E-02	0.9999
SPRY2	29.2840	-2.0620	3.55E-02	0.9999
NTRK2	56.1350	-2.2013	7.83E-04	0.9999
PAK6	12.6527	-2.2256	4.66E-02	0.9999
HAPLN3	221.8006	-2.2777	3.12E-05	0.4096
PTPRN	10.8600	-2.3897	2.10E-02	0.9999
SASH1	10.3548	-2.6477	4.09E-02	0.9999
RFLNB	12.1342	-2.7105	2.02E-02	0.9999
ENSCAFG00000047444	12.1461	-2.7446	4.37E-02	0.9999
PLS3	89.6386	-2.8365	8.40E-04	0.9999
GPR82	27.3417	-2.8864	3.96E-02	0.9999
MCTP1	8.7521	-3.0411	1.38E-02	0.9999
IGDCC3	17.3798	-3.1145	2.21E-02	0.9999
H2AC13	11.1175	-3.2331	4.03E-02	0.9999
SNAI2	11.8444	-3.2606	4.00E-03	0.9999
XKRX	9.6093	-3.2771	7.86E-03	0.9999
INSYN1	7.4349	-3.4056	4.67E-02	0.9999
MSRB3	25.9947	-3.4071	2.04E-04	0.6299
COL9A3	11.2842	-3.4502	2.69E-02	0.9999
RNASE10	18.9151	-3.5463	2.14E-02	0.9999
ENSCAFG00000048350	6.1147	-3.8204	2.65E-02	0.9999
NDUFA4L2	6.5185	-3.9885	2.41E-02	0.9999
ENSCAFG00000040827	8.1046	-4.0262	4.43E-02	0.9999
MLLT11	6.6485	-4.1000	4.22E-02	0.9999
ENSCAFG00000042771	7.9595	-4.2328	1.14E-02	0.9999
ENSCAFG00000042971	6.9384	-4.6282	2.73E-02	0.9999

Supplementary table 2. Top 100 upregulated gene sets in B7-H3-CXCR2 CAR T cells that are significant at FDR <25%

NAME	NES	NOM p-val	FDR q-val
HALLMARK_MYC_TARGETS_V1	2.674732	0	0
GOBP_RIBOSOME_BIOGENESIS	2.627747	0	0
GOBP_RIBOSOMAL_LARGE_SUBUNIT_BIOGENESIS	2.479399	0	0
HALLMARK_MYC_TARGETS_V2	2.464651	0	0
GOBP_RIBONUCLEOPROTEIN_COMPLEX_BIOGENESIS	2.449432	0	0
GOBP_RRNA_PROCESSING	2.423047	0	0
REACTOME_RRNA_MODIFICATION_IN_THE_NUCLEUS_AND_CYTOSOL	2.410248	0	0
WP_OVERVIEW_OF_PROINFLAMMATORY_AND_PROFIBROTIC_MEDIATORS	2.351442	0	0
REACTOME_RRNA_PROCESSING	2.33324	0	0
REACTOME_MITOCHONDRIAL_TRANSLATION	2.3229	0	1.06E-04
GOBP_RRNA_METABOLIC_PROCESS	2.317315	0	9.65E-05
GOBP_NCRNA_PROCESSING	2.288344	0	4.26E-04
REACTOME_RESPIRATORY_ELECTRON_TRANSPORT_ATP_SYNTHESIS_BY_CHEMIOSMOTIC_COUPLING_AND_HEAT_PRODUCTION_BY_UNCOUPLING_PROTEINS	2.279003	0	5.49E-04
REACTOME_SYNTHESIS_OF_DNA	2.252796	0	0.00116975
GOMF_RNA_POLYMERASE_ACTIVITY	2.245556	0	0.00129803
GOBP_MITOCHONDRIAL_TRANSLATION	2.242321	0	0.0012808
REACTOME_SWITCHING_OF_ORIGINS_TO_A_POST_REPLICATIVE_STATE	2.212124	0	0.00186117
WP_IMMUNE_INFILTRATION_IN_PANCREATIC_CANCER	2.203809	0	0.00204148
REACTOME_RESPIRATORY_ELECTRON_TRANSPORT	2.201844	0	0.00198829
REACTOME_MITOCHONDRIAL_PROTEIN_IMPORT	2.199672	0	0.00194001
REACTOME_ORC1_REMOVAL_FROM_CHROMATIN	2.194412	0	0.00189586
KEGG_SPLICEOSOME	2.185034	0	0.00213995
REACTOME_MRNA_SPLICING	2.182499	0	0.00213621
GOBP_MITOCHONDRIAL_RESPIRATORY_CHAIN_COMPLEX_ASSEMBLY	2.174619	0	0.00226355
REACTOME_PROCESSING_OF_CAPPED_INTRON_CONTAINING_PRE_MRNA	2.164445	0	0.0028363
REACTOME_THE_ROLE_OF_GTSE1_IN_G2_M_PROGRESSION_AFTER_G2_CHECKPOINT	2.163907	0	0.00272721
GOBP_MATURATION_OF_SSU_RRNA	2.160127	0	0.00270237
GOBP_RIBOSOMAL_SMALL_SUBUNIT_BIOGENESIS	2.150301	0	0.00316077
REACTOME_APC_C_MEDIATED_DEGRADATION_OF_CELL_CYCLE_PROTEINS	2.150202	0	0.00305178
GOBP_MITOCHONDRIAL_GENE_EXPRESSION	2.148221	0	0.00298337

GOBP_MATURATION_OF_LSU_RRNA	2.144639	0	0.00302024
GOBP_ESTABLISHMENT_OF_PROTEIN_LOCALIZATION_TO_MITOCHONDRIAL_MEMBRANE	2.119884	0	0.00401515
REACTOME_TRNA_PROCESSING	2.111049	0	0.00463974
REACTOME_DNA_REPLICATION	2.097458	0	0.00559329
GOBP_RIBOSOME_ASSEMBLY	2.080793	0	0.00677881
GOBP_SPLICEOSOMAL_SNRNP_ASSEMBLY	2.078853	0	0.00667758
REACTOME_DECTIN_1_MEDIATED_NONCANONICAL_NF_KB_SIGNALING	2.078574	0	0.00658038
KEGG_PROTEASOME	2.078552	0	0.00640721
REACTOME_CROSS_PRESENTATION_OF_SOLUBLE_EXOGENOUS_ANTIGENS_ENDOSOMES	2.069435	0	0.00710975
PID_MYC_ACTIV_PATHWAY	2.063962	0	0.00754983
GOBP_RIBOSOMAL_LARGE_SUBUNIT_ASSEMBLY	2.06062	0.004672897	0.00764094
GOBP_CELL_DIFFERENTIATION_INVOLVED_IN_KIDNEY_DEVELOPMENT	2.054898	0	0.00809391
GOBP_RESPIRATORY_ELECTRON_TRANSPORT_CHAIN	2.049791	0	0.00845669
GOBP_ANTIMICROBIAL_HUMORAL_RESPONSE	2.048848	0	0.00838027
REACTOME_DNA_REPLICATION_PRE_INITIATION	2.043988	0	0.00871873
KEGG_RNA_POLYMERASE	2.037082	0	0.00928782
REACTOME_APC_C_CDH1_MEDIATED_DEGRADATION_OF_CDC20_AND_OTHER_APC_C_CDH1_TARGETED_PROTEINS_IN_LATE_MITOSIS_EARLY_G1	2.031213	0	0.00983556
GOBP_EPITHELIAL_CELL_DIFFERENTIATION_INVOLVED_IN_KIDNEY_DEVELOPMENT	2.023062	0	0.010573
GOMF_SNORNA_BINDING	2.021464	0	0.01067313
WP_MITOCHONDRIAL_COMPLEX_I_ASSEMBLY_MODEL_OXPHOS_SYSTEM	2.014373	0	0.01128252
WP_GPCRS_CLASS_A_RHODOPSINLIKE	-2.16032	0	0.01282772
GOMF_G_PROTEIN_COUPLED_RECEPTOR_ACTIVITY	-2.12493	0	0.01475028
GOMF_STEROL_BINDING	-2.11512	0	0.01245006
KEGG_COMPLEMENT_AND_COAGULATION_CASCADES	-2.10789	0	0.01179527
WP_CHOLESTEROL_METABOLISM_WITH_BLOCH_AND_KANDUTSCHRUSSELL_PATHWAYS	-2.10534	0	0.00983369
GOMF_PEPTIDE_RECEPTOR_ACTIVITY	-2.09423	0	0.00982778
REACTOME_INTEGRIN_CELL_SURFACE_INTERACTIONS	-2.05953	0	0.01474076
GOBP_RESPONSE_TO_AMPHETAMINE	-2.0486	0	0.01498626
GOBP_CD8_POSITIVE_ALPHA_BETA_T_CELL_ACTIVATION	-2.04342	0	0.01452137
GOBP_POSITIVE_REGULATION_OF_CYTOSOLIC_CALCIUM_ION_CONCENTRATION	-2.03822	0	0.01434393
REACTOME_CLASS_A_1_RHODOPSIN_LIKE_RECEPTORS	-2.02764	0	0.01642844
GOBP_REGULATION_OF_PROTEIN_MATURATION	-2.02666	0	0.01538757
GOBP_REGULATION_OF_ADENYLATE_CYCLASE_ACTIVITY	-2.02233	0	0.01534047

GOBP_HOMOPHILIC_CELL_ADHESION_VIA_PLASMA_MEMBRANE_ADHESION_MOLECULES	-2.01769	0	0.01550682
GOMF_MOLECULAR_TRANSDUCER_ACTIVITY	-2.01715	0	0.01453885
REACTOME_GPCR_LIGAND_BINDING	-2.01172	0	0.01560505
GOBP_CELL_JUNCTION_DISASSEMBLY	-2.00395	0	0.01780961
GOMF_STEROID_BINDING	-2.00321	0	0.01703951
GOBP_REGULATION_OF_T_HELPER_1_TYPE_IMMUNE_RESPONSE	-1.97705	0	0.02464737
GOBP_POSITIVE_REGULATION_OF_NATURAL_KILLER_CELL_MEDIATED_IMMUNITY	-1.9723	0	0.0258253
GOBP_POSITIVE_REGULATION_OF_RHO_PROTEIN_SIGNAL_TRANSDUCTION	-1.96718	0	0.02660827
GOMF_CHOLESTEROL_BINDING	-1.96631	0	0.0257116
REACTOME_G_ALPHA_S_SIGNALLING_EVENTS	-1.94879	0	0.03203754
GOBP_LIPOPOLYSACCHARIDE_MEDIATED_SIGNALING_PATHWAY	-1.94574	0	0.03180996
GOBP_GAMMA_DELTA_T_CELL_ACTIVATION	-1.93541	0.003478261	0.0352559
GOBP_ALPHA_BETA_T_CELL_ACTIVATION	-1.93278	0	0.0350333
GOBP_T_HELPER_1_CELL_DIFFERENTIATION	-1.93022	0.005181347	0.03537461
GOBP_T_CELL_CYTOKINE_PRODUCTION	-1.92298	0	0.0380481
GOBP_NEGATIVE_REGULATION_OF_CARDIAC_MUSCLE_TISSUE_GROWTH	-1.91441	0	0.04049586
WP_EXTRAFOLLICULAR_AND_FOLLICULAR_B_CELL_ACTIVATION_BY_SARSCOV2	-1.91354	0	0.0394708
WP_PEPTIDE_GPCRS	-1.90886	0	0.04085913
GOBP_STEROL_BIOSYNTHETIC_PROCESS	-1.89989	0	0.04490069
GOBP_POSITIVE_REGULATION_OF_NATURAL_KILLER_CELL_MEDIATED_CYTOTOXICITY	-1.89479	0.001754386	0.04718122
GOBP_REGULATION_OF_LIPOPOLYSACCHARIDE_MEDIATED_SIGNALING_PATHWAY	-1.89103	0.003278689	0.0477603
REACTOME_CHOLESTEROL_BIOSYNTHESIS	-1.88227	0	0.0524369
GOMF_PROTEASE_BINDING	-1.88154	0	0.05149979
GOBP_POSITIVE_REGULATION_OF_CYTOKINE_PRODUCTION_INVOLVED_IN_IMMUNE_RESPONSE	-1.88008	0	0.05119795
GOBP_POSITIVE_REGULATION_OF_BMP_SIGNALING_PATHWAY	-1.87961	0	0.05011045
GOBP_NEGATIVE_REGULATION_OF_ORGAN_GROWTH	-1.87915	0	0.04912832
BIOCARTA_NO1_PATHWAY	-1.87517	0.003558719	0.05053488
WP_PHOSPHODIESTERASES_IN_NEURONAL_FUNCTION	-1.87407	0	0.05016571
GOBP_ADENYLATE_CYCLASE_MODULATING_G_PROTEIN_COUPLED_RECEPTOR_SIGNALING_PATHWAY	-1.86721	0.001492537	0.05407683
GOBP_CELLULAR_EXTRAVASATION	-1.86553	0.001620746	0.05403071
GOBP_T_CELL_DIFFERENTIATION	-1.8595	0	0.05725186
GOBP_POSITIVE_REGULATION_OF_MITOCHONDRIAL_FISSION	-1.85485	0	0.05956779

GOBP_REGULATION_OF_RESPONSE_TO_REACTIVE_OXYGEN_SPECIES	-1.85134	0	0.06133072
GOBP_RESPONSE_TO_THYROID_HORMONE	-1.85013	0	0.06086356
GOMF_IMMUNE_RECEPTOR_ACTIVITY	-1.84796	0	0.06135755
GOBP_CELL_CELL_ADHESION_VIA_PLASMA_MEMBRANE_ADHESION_MOLECULES	-1.84664	0	0.0611283
WP_CHOLESTEROL_METABOLISM	-1.8465	0.001560062	0.05998461
REACTOME_SIGNALING_BY_GPCR	-1.84383	0	0.0607519

Supplemental fig. 8 Canine B7H3-CXCR2 CAR T cell SOP

Background

Adoptive cell therapy with chimeric antigen receptor (CAR) T cells directed against CD19- and CD22 has demonstrated unprecedented outcomes in patients with chemotherapy-refractory lymphoid malignancies[1,2]. However, this approach is met with significant hurdles in its application to solid cancers[3,4]. One challenge has been the identification of surface targets on solid cancers whose expression is limited in normal tissues. Recent studies in numerous adult- and pediatric tumors, including osteosarcoma (OS), have identified the checkpoint molecule B7-H3 to be a restricted tumor antigen, with limited expression by normal tissues other than antigen presenting cells[5-7]. Accordingly, clinical trials targeting this receptor with antibodies are being conducted and to date, show tolerability and no significant toxicity[8,9].

Osteosarcoma is a common and devastating disease in both dogs and humans. Upon diagnosis, the majority of dogs require amputation and chemotherapy. Despite this, most relapse within a year of diagnosis. In humans, OS is the most common bone tumor of adolescents and young adults (AYA)[10,11]. Pediatric and AYA patients with metastatic OS at diagnosis or who relapse after frontline therapy have an extraordinarily poor prognosis, with only a 20-30% survival at 5-years[12]. Despite concerted attempts, these outcomes have not changed in >25 years.

Due to similarities in genetics, biologic behavior and treatment responses, canine OS is considered the best model of pediatric and AYA OS[13]. We have used this model to investigate new immunotherapies[14] and some of these have been translated into human trials (NCT03900793)[15]. In preliminary studies, we have determined that canine OS overexpresses B7-H3, whereas normal dog tissues (heart, liver, brain, kidney and spleen) are negative for B7-H3 expression. Moreover, we demonstrate that human and canine T cells expressing a human B7-H3 CAR construct recognize canine OS targets, as reflected by activation, cytokine secretion and direct tumor cell killing. Therefore, we propose to assess the safety and effectiveness of B7-H3 targeted CAR T cells in dogs with macroscopic pulmonary OS metastases.

Despite the promise of CAR T cell therapy, the immune suppressive tumor microenvironment (TME) represents a major impediment to cellular therapies. Myeloid cells, including tumor associated macrophages (TAMs) and myeloid derived suppressor cells (MDSCs) are major components of the immune suppressive TME, where they suppress T cell mediated tumor immunity. To reverse this attenuation of T cell function, we have used a repurposed CCR2 antagonist (losartan) and the beta-adrenergic antagonist propranolol to block monocyte and MDSC recruitment to the TME in rodent models[14] and in ongoing clinical studies in dogs with OS metastases. Impressive results in the dog trial

(clinical tumor response in 5 of 5 dogs treated with the losartan/propranolol combination together with a TKI drug (toceranib) indicate high activity in the setting of advanced lung OS metastases.

Inclusion/exclusion criteria

- Dogs eligible for inclusion in the study will have undergone previous amputation for primary OS, followed by accepted adjuvant chemotherapy with either carboplatin or doxorubicin 30 days or greater prior to enrollment.
- Dogs eligible will have subsequently developed measurable metastases to the lungs that do not exceed a lung burden in the clinician's judgement where the animal would not survive an additional 30 days.
- Dogs with metastatic lesions on sites other than the lung will be excluded.
- Study eligible dogs must be > 20 kg in body weight and be free of other significant medical conditions including renal insufficiency and are not receiving immune modulatory drug therapy.
- Dogs that have received prior immunotherapy for OS (e.g., tumor vaccines, cytokine therapy, adoptive T cell therapy) are also not eligible for inclusion.

Dosing of lymphodepleting chemotherapy

Cyclophosphamide 50kg/m2 PO Days -6, -5, -4, -3 (4 days consecutively, stop 2 days before CAR T cell infusion)

Dosing of drugs

Dogs will receive losartan (10mg/kg BID) and propranolol (0.5mg/kg BID) starting at Day –14 to precondition the tumor. Propranolol dosing will increase to 1 mg/kg BID after two weeks. Losartan will be stopped on Day 1, day 0 and day 1 and resume losartan treatment on day 2. Propranolol will continue the whole trial.

Dosing of cells

There will be 3 CAR T cell doses evaluated (5 X 10^5 CAR T cells/kg, 1 X 10^6 CAR T cells/kg, and 2.5 X 10^6 CAR T cells/kg). These doses have been chosen based on safety of a similar CAR construct (without the CXCR2 component) in dogs (ref) as well as CD19 CAR T cell studies in dogs with B cell lymphoma (ref). Enrollment to the next higher dose cohort will not commence until at least 1 month of follow-up without significant AEs for the previous cohort. The decision to escalate to the next dose cohort will be based on lack of severe (grade III or IV) AEs in the previous cohort. If noted, the first cohort will be expanded to n=6 dogs.

Rate of infusion of the cells

CAR T cells will be infused as a slow IV injection via peripheral vein at 10mL, 20mL or 30mL volume pf sterile PBS for the 5 X 10^5 CAR T cells/kg, 1 X 10^6 CAR T cells/kg, and 2.0 X 10^6 CAR T cells/kg cohorts

respectively and infused at a rate of 2mL per minute for all patients. Dogs will be monitored for heart rate, blood pressure and respiratory rate during and for 10 minutes after infusion.

Post-Infusion Monitoring Study dogs will remain in the oncology clinic for 3hr post infusion to observe for any immediate treatment related AEs. Owners will be sent home with an information pamphlet for at home monitoring post infusion (see appendix). Dogs will return to Flint animal cancer center 72hours post infusion. The trial will include only a single CAR T cell treatment for each study animal.

Follow-up visits (when and what is done)

- D-14 dogs get chest rads and base line blood draw for plasma cytokines, flow qRT-PCR and CBC, Chem, CRP
- Dogs will receive follow-up appointments at 24 hours post infusion, 72 hours, D7 and D14 for collection of 10 mL of blood in EDTA to evaluate plasma cytokine levels by multiplex and to identify peripheral circulating CAR T cells by flow cytometry and qRT-PCR. Dogs will receive follow-up chest radiographs on pretreatment day 14, day 30 and to evaluate metastatic tumor burden. Dogs will also receive a physical exam at the time of each follow up measuring temperatures, respiratory rate, renal function by urinalysis, complete blood count and chemistry and mental status.
- Separate blood draw for CBC, Chem, CRP pretreatment, 72hr, D7, D14 (D30)

Visit/ follow up	collection	purpose
D-14	Chest rad, 2x 5mL blood in EDTA Physical exam	Clinical: Monitor metastatic disease burden, CBC, Chem, CRP Research: plasma cytokines, baseline CAR T detection (flow and PCR),
D0	2x5mL blood in EDTA Keep central line in for 3 hrs post infusion and monitoring every 10 min for the first 30min, and in 15 min intervals following	Clinical: CBC, Chem, CRP. Research: plasma cytokines, CAR T detection (flow and PCR)
D1 (24hrs)	2x5mL blood in EDTA Physical exam	Clinical: CBC, Chem, CRP. Research: plasma cytokines, CAR T detection (flow and PCR)
D3 (72Hrs)	2x5mL blood in EDTA Physical exam	Clinical: CBC, Chem, CRP. Research: plasma cytokines, CAR T detection (flow and PCR)
D7	2x5mL blood in EDTA Physical exam	Clinical: CBC, Chem, CRP. Research: plasma cytokines, CAR T detection (flow and PCR)
D14	Chest rad, 2x 5mL blood in EDTA	Clinical: Monitor metastatic disease burden, CBC, Chem, CRP

	Physical exam	Research: plasma cytokines, baseline CAR T detection (flow and PCR),
D30	Chest rad Physical exam	Clinical: Monitor metastatic disease burden

Collection of adverse events (definitions), etc.

Adverse events will be classified as grade I-V. In the event of any grade V AEs, cell product associated infection or any AE related to CAR T cell treatment that results in hospitalization the trial will be stopped. In the event of a grade II AE the trial will pause dose escalation and expand the current dose cohort to n=6 and re-evaluate dose limiting toxicities. Grade IV AEs will indicate a step down in dose and expansion of the cohort below.

Grade I mild lethargy, hyporexia will receive supportive therapy and monitoring.

Grade II GI signs, vomiting diarrhea will receive supportive therapy and monitoring.

Grade III mild Cytokine release syndrome not requiring steroids. Fever, hypotension requiring fluid support, pulmonary signs requiring supplemental oxygen.

Grade IV severe CRS fever, hypotension requiring fluid support, tachypnea or pulmonary signs requiring supplemental O2, elevated IL6, IL2 TNF, treatment with fluids and steroids.

Grade V death

CAR T cell generation to infusion Timeline

Day –14 Wednesday Dogs start on losartan (10mg/kg BID) and propranolol (0.5mg/kg BID starting)

Day -12 Friday – Draw 50mL of blood from dog -> EDTA tubes= Activate with canine antiCD3/antiCD28 beads at 3:1 with IL21 (30 ng/ml), IL2 (100 IU/ml), IL7 (5 ng/ml), and IL15 (5 ng/ml).

Day -9 Monday-Tuesday- Transduce cells

Day -7 Wednesday – Remove beads and put in fresh culture media with IL2 (100 IU/ml), IL7 (5 ng/ml), and IL15 (5 ng/ml). Dogs increase the dose of propranolol to 1.0mg/kg BID PO.

Day -6, Thursday - take a sample of supernatant send to CSU D lab for aerobic culture and mycoplasma testing. Dogs start Cyclophosphamide 50mg/m^2 PO daily

Day -5, -4, -3 Friday-Sunday Dogs continue Cyclophosphamide 50mg/m^2 PO daily

Day –2, Monday Dogs go off cyclophosphamide

Day –1 Tuesday Dogs go off losartan

Day 0 Wednesday AM count and flow CAR T product, wash 1x sterile PBS, count and resuspend in 10 mL for the first cohort, 20mL for the second and 30mL sterile PBS to calculated CAR T cell dose. Freeze any extra CAR T cells. Dogs get 10mL blood drawn for baseline multiplex. CAR T cell infusion with infusion

pump at a rate of 2mL per minute. Monitor for the next 24 hrs. Increase propranolol dosing to 1.0mg/kg BID

Day 1 Take 10 mL blood in EDTA for multiplex, qRT-PCR, and flow cytometry, monitor with physical exam for AEs. Take 10mL of blood for CBC, Chem and CRP. Dogs go home

Day 2 dogs go back on losartan (10mg/kg BID)

Day 3 dogs come back in as outpatient for follow up, take blood for multiplex (plasma) Flow cytometry (L protein CXCR2, CD5, L/D stain, run 1.0e6 events) qRT-PCR copies of CAR DNA, physical exam

Day 7 follow up physical exam and blood draw (15 mL for multiplex, qRT-PCR and flow cytometry)

CAR T cell manufacturing

293GP Transient Retroviral Vector Production

Materials:

1. Lipofectamine 2000 from Invitrogen
2. 293GP Cell Line
3. Opti-MEM media (Invitrogen)
4. T75 and T175 flasks
5. RD114 Envelope Plasmid
6. Vector Plasmid

Prior to making retroviral supernatants:

1. Thaw 293GP cells and establish culture (1 vial --> 1 T75 plate)
2. Split after 2 days – each T75 into 3 T175 flasks
3. Use trypsin when splitting cells. Pipette up and down before neutralizing trypsin with media containing serum, to break up the clumps.
4. Healthy 293GPs are important for production of good retroviral supernatants. These cells should appear stellate and should not be coming off of the plastic when healthy.
5. 293GPs should be ready for virus four days after split from T75 to T175 flasks. Cells should be around 70-80% confluent.

Day 1

1. Warm Opti-MEM to room temperature and DMEM to 37°C
2. Per plate, prepare transfection mixes in non-polystyrene tubes
3. **Mix A:**
4. 3.4mL Opti-MEM

5. 20.25µg Vector plasmid
6. 10.125µg RD114 (Env) plasmid
7. **Mix B:**
8. 3.4mL Opti-MEM
9. 100µL Lipofectamine 2000
10. Incubate A and B separately for 10 minutes at RT
11. Mix A and B together gently and incubate for 30min at RT
12. Replace the media in the flasks during the 30 min incubation with 22.5mL of fresh DMEM (no antibiotics)
13. Add 6.75mL lipid/DNA complex dropwise to cells. Swirl flask gently to mix.
14. Incubate at 37°C for 24 hours.

Day 2

1. Replace media with 22.5mL of fresh DMEM. Discard old media into bleach.
2. Incubate at 37°C for an additional 24 hours.

Day 3

- Harvest viral supernatant (48-hour viral supernatant) into a 50 ml tube through a 70uM filter.
- Replace 22.5mL of media and incubate at 37°C for 24 hours.
- Aliquot ~ 12 mL of viral supernatant in 15 mL conical tubes. (Enough for 1 X 6 well plate).
- Snap freeze on dry ice and store at -80°C.

Day 4

- Harvest viral supernatant (72-hour viral supernatant) into a 50 ml tube through a 70uM filter.
- Aliquot ~ 12 mL of viral supernatant in 15 mL conical tubes.
- Snap freeze on dry ice and store at -80°C.
- Throw away flasks after rinsing with bleach.

Human T-Cell Transduction Protocol Using CD3/CD28 Beads and Expansion

Materials:

- 50 ml conical tubes
- Lymphoprep

- Non-tissue culture coated 6 well plates (BD 351146)
- Retronectin (Takara TAK-T100B)
- Dynabeads M-450 tosylactivated
- Dog functional anti CD3 antibody clone (MCA1774GA)
- Dog functional anti CD28 antibody clone (5B8)
- Human recombinant IL2, IL7, IL15 and IL21
- Canine T cell media (CTCM): DMEM media no sodium pyruvate (500 ml) + 10% sterile filtered FBS (50 ml), 55uM BME, 10mM HEPES, 1% pen/strep, 1% L glut, 1%essential amino acid, 1% bicarbonate solution
- Retroviral supernatants (Stored @ -80°C)
- PBS + 2% BSA blocking buffer (10g BSA per 500mL, sterile filter)

Day –12: (Friday) T Cell Stimulation with CD3/CD28 Beads:

50 ml of canine blood will be collected from study dog and placed in EDTA tubes. Jessica will pick up blood from CSU on ice and transport back to CU Anschutz. At CU, the blood will be separated using lymphoprep.

1. The canine blood will be washed with PBS up to 80 ml. Two 50 ml tubes will have 10 ml of lymphoprep in the bottom and 40 ml of canine blood/PBS mix will be pipetted slowly on top of lymphoprep. The tubes will then be centrifuged at 2000 rpm, 20 degrees Celsius for 20 minutes with the brake off.
2. The buffy coat will be obtained using a sterile pipette and transferred to a new 50 ml tube. This will be brought up to 50 ml with PBS and an aliquot will be taken for counting. The cells will be centrifuged at 1500 rpm for 5 minutes. The cells will be resuspended at 2.0e6/mL and plated 4ml per well in a 6 well plate for 90 min at 37 degrees to adhere monocytes. Non-adherent peripheral blood lymphocytes (PBL) will be washed off after the 90 min incubation and the PBLs will be resuspended at 1.0e6/mL in CTCM and transferred to a new upright flask.
3. Canine CD3/28 beads will be washed with PBS and added to the cells at a 3:1 beads to cells ratio. Cytokines will also be added as follows: IL21 (30 ng/ml), IL2 (100 IU/ml), IL7 (5 ng/ml), and IL15 (5 ng/ml). The flask will be placed in the incubator at 37 degrees, 10% CO2 for 3 days.

Day –9 (Monday or can be done on day –10): Prepare Retronectin Plates and Day 1 transduction:

- Determine number of plates you need based on number of T cells (need 3E6 cells per plate or 500K per well). For each plate, mix 600ul of retronectin in 12 wells of sterile PBS.
- Vortex the solution and then pipette 2 mL (24 µg/mL) into each well @ RT for 2 hours or overnight in cold room (covered with foil since it is light sensitive).

- After 2 hours or next day, remove retronectin solution from wells and transfer to new plates (2 ml per well) for next day transduction. Cover new plates with foil and place in 4 degrees overnight.
    - Block with 2mL per well of PBS + 2% BSA @ room temperature for 30 minutes.
    - While blocking, set the settings on the centrifuge to get it warming up to 32°C. (This may take a while so plan accordingly – 3050 rpm).
    - Thaw retroviral supernatants (stored in -80°C) in 37°C water bath. (Do not get the tops of tubes wet). Immediately put on ice once thawed. Note: Virus will begin to adhere to tube once thawed so make sure centrifuge and other components are prepared prior to reaching this step.
    - Remove the PBS + 2% BSA from each of your retronectin coated plates and add 2mL of viral supernatant to the appropriate wells.
- Centrifuge 2.5 hours at 3050 x RPM @ 32°.
- Near the end of centrifuge time, count T cells to be transduced and suspend them in CTCM media with IL2 (100 IU/ml), IL7 (5 ng/ml), and IL15 (5 ng/ml) at a final concentration of 250K per ml.
- Remove the retroviral supernatant from each well into bleach, using ONE PIPET for each CAR condition.
- Add 2 ml of T-cell suspension (500K) to each well.
- Put plates in 37°C incubator under 10% CO_2.

<u>Day –8 (Tuesday): CAR Transduction Day 2 of 2:</u>

- Repeat steps 3-4 using the second set of Retronectin coated plate you made on prior day.
- After centrifugation, remove supernatant and discard into bleach.
- Working one well at a time, transfer the cells from the Day 1 plate to the corresponding well on the new, Day 2 plate. Be sure to resuspend the cells before transferring.
- To resuspend: pipette up and down with a P-1000 pipette set at 1mL and squirt the entire surface of the well to gently resuspend the cells that are slightly adherent.
- Add 2 mL of warm, fresh CTCM media with IL2 (100 IU/ml), IL7 (5 ng/ml), and IL15 (5 ng/ml) to each well for a total of 4 ml/well.
- Put plates in 37°C incubator under 10% CO_2.

<u>Day –7 (Wednesday): Rescue Cells from Virus:</u>

- Harvest cells from wells by pipetting up and down with a 5mL pipette and squirt the entire surface of the well so as to gently resuspend the cells that are slightly adherent to the plastic. Transfer the cells to a 50mL conical tube. (Rinse the well with CTCM media and add the rinse to the conical tube).

- Count cells.
- Remove beads by allowing them to sit in magnetic field for a few minutes, removing the cell suspension to a fresh conical tube. Repeat once more.
- Centrifuge at 1500 RPM for 5 minutes.
- Suspend cells in CTCM media with IL2 (100 IU/ml), IL7 (5 ng/ml), and IL15 (5 ng/ml) and transfer to 6 well Grex plate at 1-2E6 cells per well (35 ml per well).
- Put Grex plate in 37°C incubator under 10% CO_2.
- Refresh media and cytokines [IL2 (100 IU/ml), IL7 (5 ng/ml), and IL15 (5 ng/ml)] every 4 days. As cells are settled on the bottom, replace media by removing 20 ml from top and replacing with fresh media.

Day –6 (Thursday): FACS for transduction efficiency and collection of supernatants for culture (overnight Fedex to CSU on ice)

Day –3 (Sunday): Change media in Grex plate

Remove 20 ml from top and replace with fresh media (+ cytokines).

Day 0 (Wednesday): Transfer of CAR T cells to CSU for injection into dogs

The morning of Day 0, T cells will be prepared by resuspending them in CTCM at 1E6/ml in 50 ml tubes. CSU will pick them up and transported upright at room temperature.